Discovery and Characterization of Genes Responsible for Inherited Hearing Loss

Ryan James Carlson

A dissertation

submitted in partial fulfillment of the

requirements for the degree of

Doctor of Philosophy

University of Washington

2022

Reading Committee:

Mary-Claire King, Chair

Jay Rubinstein

David Perkel

Program Authorized to Offer Degree:

Genome Sciences

University of Washington

ABSTRACT

Discovery and Characterization of Genes Responsible for Inherited Hearing Loss

Ryan James Carlson

Chair of Supervisory Committee:

Mary-Claire King

Department of Genome Sciences

Hearing loss is the most common sensory dysfunction in humans, affecting 1 in 400 newborns and an estimated 27 million adults in the United States. Current treatments, such as hearing aids and cochlear implants, increase functional hearing but do not achieve complete restoration and do not address the underlying cause of hearing loss. Remaining hearing loss can substantially impact quality of life on personal, cultural, and social levels. As modern public health measures have successfully reduced rates of prenatal infection and acoustic trauma, a growing proportion of hearing loss is genetic in origin (>50%). More than 120 genes critical to mammalian hearing have been identified so far through studies based on mouse models and informative human families. Improved understanding of hearing loss genes and their resulting phenotypes will lead to better clinical care for patients with hearing impairment, yield valuable information for genetic counseling efforts, increase our understanding of the fundamental mechanisms of hearing, and provide crucial information for the development of novel therapies for hearing loss.

In pursuit of these goals, I utilized massively parallel sequencing methods to identify the causes of hearing loss in individuals across various backgrounds and countries of origin. In a large cohort of pediatric hearing loss patients from the United States, I used a custom targeted sequencing panel to identify mutations in known hearing loss genes. After combining these genomic findings with longitudinal phenotypic information obtained from each participant's audiologic care, I present informative audioprofiles for over 40 genes, quantify hearing loss progression in key genes, and identify differences in cochlear implant success based on causative gene. In multiplex families from the Middle East and US without a causative gene identified by this method, I applied whole exome and whole genome sequencing to discover other interesting candidate hearing loss genes. First, I found two different mutations in *NOG* in two separate families (one from Israel and the other from the US) with conductive hearing loss and features of *NOG*-symphalangism spectrum disorder (*NOG*-SSD) and characterized the effects of these mutations experimentally. Next, in a Palestinian family with congenital nonsyndromic profound hearing loss, I identified homozygous damaging mutations in *ALDOC* which encodes a protein involved in fructose metabolism (aldolase C). I showed that this mutation leads to severely decreased enzymatic activity in a custom *in vitro* assay, but that the mutation does not recreate hearing loss in CRISPR/Cas9 edited mouse line. Lastly, in another Palestinian family with congenital nonsyndromic profound hearing loss, I evaluated the effects of a first-codon missense mutation in *GOSR2*. This mutation caused decreased, but not absent, translation that was sufficient to avoid the severe epileptic phenotype associated with other pathogenic mutations in this gene.

These findings emphasize the importance of utilizing modern genetic sequencing methods to better characterize phenotypic differences between different causative hearing loss genes and to identify additional genes involved in the biochemical processes of human hearing.

TABLE OF CONTENTS

LIST OF FIGURES

LIST OF TABLES

ACKNOWLEDGEMENTS

To begin, I would like to thank my mentor, Mary-Claire King. Over the course of my PhD training, her boundless curiosity and passion for science has been a constant source of motivation. Her ability to dissect scientific theories and experimental datasets has taught me the importance of slowing down to fully appreciate the fundamental science behind the headlines. Thanks also to Jay Rubinstein, who has provided me with a link to the clinical world throughout my PhD work and served as an astounding role model as a physician scientist. Together, Mary-Claire and Jay have been absolutely crucial to the success of my work, and their guidance has been pivotal to my growth as a researcher and future clinician.

I would also like to give tremendous thanks to my colleagues in the King Lab who have taught me experimental techniques, provided guidance and support, and become close friends over the last few years: Aaron Seo, Amal Abu Rayyan, Anna Sunshine, Hannah Kortbawi, Jessica Mandell, Ming Lee, Sarah Baxter, Sarah Pierce, Silvia Casadei, Suleyman Gulsuner, Tom Walsh, and Yagiz Anasiz. Thank you for lending your expertise and encouragement, and thank you also for making the King lab an outstanding place of work.

As often happens in scientific research, the projects described in this dissertation required the assistance and specialized knowledge of individuals outside of my lab and area of expertise. I would like to specifically thank those that went out of their way to assist in these experiments, as they would surely have been impossible otherwise. This includes Ed Rubel, Jenny Stone, Robin Gibson, Rochelle Berg, Sergei Doulatov, Van Redila, and Xioaping Wu.

My PhD work has also taken me across the world to visit various international collaborators. Thanks to all who welcomed me with extraordinary hospitality and friendship: Danielle Gelber, Hanan Abid Alghni, Helen Berman, Karen Avraham, Lama Khalaily, Lara Kamal, Moien Kanaan, Mor Bordeynik-Cohen, Prathamesh Nadar Ponniah, Shahar Taiber, Tal Koffler-Brill, Yael Noy,

and Zippi Brownstein. Special thanks to the Abu Rayyan family, Abdallah, Majed, Mohammad, and Mutaz, and to the Palestinian people for accepting me into their homes and country.

Work involving human genetics would never be possible without the support of those participating. Thank you to all the individuals and families who participated in this research for their generosity and invaluable contribution to science.

A truly substantial amount of work was required to identify and recruit individuals with hearing loss for my research. This would not have been possible without the support of the otolaryngology and audiology clinics at Seattle Children's Hospital and UWMC. Thank you specifically to David Horn, Henry Ou, Kathy Sie, Kerri Corkrum, Lara Clark, Lisa Mancl, Shawn Beck, and Sheridan Frank.

I would also like to thank the rest of my advisory committee, Christine Quietsch and David Perkel, for their incredibly useful advice that helped guide these projects to completion.

Perhaps the most deserved and most substantial thank you goes to my partner, Nicole Mattson, for her relentless support and optimism. Your remarkable ability to find limitless joy and laughter is incredible, infectious, and inspiring. Thank you for paving the way through medical training, and for embodying the compassionate clinician that I hope someday to be.

Finally, I would like to thank my parents for their long history of support for my academic and professional goals. Thank you for your unending encouragement and for providing me the freedom to choose my own path. And thank you to my brothers, David and Trevor, for your continuous support and friendship. Thanks also to my second family, Rob, Karin, and Connor Mattson, and to my closest friends for their companionship throughout my extended time in Seattle: Adrian Monstad, Anna Le, Anthony Recidoro, Carlos Enciso, Cass Sunga, Chelsea Chaviers, Comron Ganji, Danielle Bojorquez, Darrin Moy, Lindzey Faust, Michael Watling, Skylar Madsen, and Tori Recidoro.

CHAPTER 1. Introduction

Hearing impairment is the most common sensory dysfunction, affecting 1 of 400 newborns and more than half of the US population by the age of 80[1,2]. Early-onset severe or profound hearing loss can lead to dramatic impairment in speech acquisition, communication, and literacy. Environmental factors, such as ototoxic drugs, infection, and acoustic trauma all contribute to the prevalence of hearing loss, but the majority of early-onset hearing loss (>50% in the U.S.) is genetic in origin[3–5]. To date, 124 genes have been implicated in nonsyndromic hereditary hearing loss, and many other genes are responsible for syndromes that include hearing impairment[6]. Much of our current knowledge about auditory transduction and inner ear structure has been learned from studying these genes and their functions.

Despite a rapidly expanding understanding of the genetic causes of hearing loss, many patients do not receive genetic testing in routine clinical care. This is primarily due to a reluctance of insurance providers and a perceived lack of importance to treatment course. Further, if a patient's hearing loss is due to a rarely-encountered gene, often little gene-specific prognostic information is available regarding severity, age of onset, or progression. The primary treatment options for hearing loss are hearing aids and cochlear implants, and currently their implementation is dependent mainly on hearing loss severity and speech discrimination ability[7]. While for many individuals with hearing loss, cochlear implants (CI) dramatically increase speech perception and improve quality of life, for some recipients, CIs do not perform well[8]. Some of this variability in CI outcomes is likely caused by underlying genetic variation[9].

To better understand the features of hearing loss due to different mutations and different genes, and to assess differences in cochlear implant outcomes, I designed a study that combines targeted panel sequencing with longitudinal audiological and speech perception evaluations. By combining these data, I was able to develop gene-specific audioprofiles, quantify progression of

hearing loss due to a number of key genes, and explain some variability in CI outcomes based on genotype. The results of this work are presented in Chapter 2.

Although many nonsyndromic and syndromic hearing loss genes have been identified, interpreting their specific mutations remains a significant challenge. This problem is constant throughout human genetics, in which the effects of missense, noncoding, splicing, and some copy number variants are difficult to predict without functional characterization. In Chapter 3, I outline my efforts to identify and characterize two novel mutations in *NOG*, a gene whose mutation is known to cause a syndrome including stapes ankylosis (conductive hearing loss) as its most common feature. I also describe a key surgical consideration in the care of these patients[10].

While a large number of genes have been implicated in human hearing loss over the last 30 years[6], some families with inherited hearing loss are still unsolved by sequencing of known hearing loss genes. Our lab's approach to discovering and characterizing new hearing loss genes is to work with our international partners to ascertain informative families, identify candidate genes with genomics tools, and characterize these mutations and genes with *in vitro* experiments and *in vivo* models[11–17]. However, gene discovery work rarely leads in an expected direction, and often yields unexpected findings in diverse fields of biology and biochemistry. In chapters 4 and 5, I describe my application of this gene discovery strategy to two genes identified by whole exome sequencing in families with autosomal recessive, nonsyndromic, congenital, profound, and bilateral sensorineural hearing loss. The first, *ALDOC*, encodes aldolase C, a glycolytic enzyme most highly expressed in brain, including in the sensory epithelium of the inner ear (Chapter 4). In Chapter 5, I evaluate the translational effects of a first codon mutation in *GOSR2*, a gene integral to ER-Golgi trafficking.

CHAPTER 2. Genetic and phenotypic heterogeneity of childhood-onset hearing loss and implications for success of cochlear implants

2.1 - ABSTRACT

Background: Hearing loss is the most common human sensory disorder. In the US, most childhood-onset hearing loss is genetic and highly heterogeneous with more than 120 genes and thousands of different alleles known to cause the condition. Cochlear implants are the management of choice for many children with hearing loss, and their success may be associated with the cause of an individual's hearing loss. In a large cohort based in a single clinic, we evaluated the genetic causes of hearing loss and how these causes might contribute to cochlear implant success.

Methods: Participants were 449 children with bilateral sensorineural hearing loss from 407 different families. All children were treated at Seattle Children's Hospital or the University of Washington between 2019 and 2021. Genomic DNA was evaluated by targeted sequencing of 191 genes and by structural variant analysis. Longitudinal audiologic testing was used to evaluate severity and progression of hearing loss, and longitudinal speech perception testing was used to evaluate cochlear implant success.

Results: A genetic cause of hearing loss was found for 53% (216/407) of families, with causal mutations in 49 different genes. Audioprofiles revealed gene-dependent variation in severity, progression, and affected frequencies. Hearing loss was progressive for children with hearing loss due to mutations in *MYO6, OTOA, SLC26A4*, *TMPRRS3,* or to severe loss-of-function mutations in *GJB2.* Cochlear implant success was high overall, with 89% of implanted patients scoring at least 60% on adult-level speech perception tests. Even so, level of success varied significantly by genotype (ANCOVA $P < 0.0001$). Adjusting for age at implant and interval since implant, speech perception was most successful for children with hearing loss due to *ESRRB,*

MITF, or *TMPRRS3* and less successful for children with hearing loss due to *GPSM2, PAX3, SLC26A4*, or *OTOF*.

Conclusions: Cochlear implants benefitted children with hearing loss regardless of cause, but level of speech perception after implant varied by causal gene. Management of childhood-onset hearing loss can benefit from cochlear implantation undertaken in the context of genetic diagnosis.

2.2 - INTRODUCTION

Hearing impairment is the most common sensory dysfunction, affecting 1 of 400 newborns and more than half of the US population by the age of 80[1]. Environmental factors, such as ototoxic drugs, infection, and acoustic trauma all contribute to the prevalence of hearing loss, but most pediatric hearing loss is genetic in origin[3,4]. To date, 124 genes have been implicated in non-syndromic hereditary hearing loss, and many others are involved in syndromes that include hearing impairment[6]. This genetic heterogeneity is reflected in the diversity observed in hearing loss phenotypes: mutations in different genes lead to hearing loss of varying severity, involvement of different frequencies, and extent of progression over time[18]. Because genetic testing for hearing loss is relatively recent, phenotypic information for many rare or recessive hearing loss genes is limited and available primarily from case reports and small family studies. Collection of both genetic diagnoses and longitudinal phenotype data from more individuals with hearing loss will allow providers to more accurately predict hearing loss severity and progression and to better manage treatment.

At present, there are no therapeutic options to reverse hearing loss. Patients with hearing impairment are typically treated with amplification (hearing aids) or cochlear implants (CI). At present, choice of approach depends primarily on an individual's level of speech discrimination[7]. Cochlear implants have led to substantial improvement in hearing thresholds, speech

understanding, and quality of life for hundreds of thousands of individuals[19]. While the majority of patients experience dramatic improvement with their CI, a significant portion do not, and approximately 7% will eventually become non-users[8]. Few clinical predictors of speech recognition outcomes have been identified to date[20–23]. Given the genetic heterogeneity of childhood-onset hearing loss, it is possible that variability in CI outcomes can be partially explained by underlying genetic variation[24,25]. Previous studies have confirmed that the majority of hearing loss in pediatric cochlear implant patients is genetic in origin[9,26], and that the group of cochlear implant patients with high speech performance is enriched for those with genetic causes[9].

This study has several goals. (1) We evaluate the yield of genetic diagnoses from gene-panel sequencing (with additional structural variant analysis) for a clinic-based cohort of children with bilateral sensorineural hearing loss. (2) We integrate longitudinal audiologic data with genetic diagnoses to understand pediatric audioprofiles based on gene, and within gene, on type of mutation. (3) For children with cochlear implants, we integrate results of post-cochlear implant speech perception tests with genetic diagnoses to evaluate effect of the cause of hearing loss on cochlear implant success.

2.3 - METHODS

Participants

A total of 443 families were approached for participation in this study and 36 declined to participate. Ultimately, 449 participants from 407 families were recruited from the otolaryngology and audiology clinics at Seattle Children's Hospital (SCH) and the pediatric audiology clinic at the University of Washington (UW; Table 2.1). The criterion for enrollment was onset younger than age 18y of bilateral hearing loss with a sensorineural component, defined as testing at 30dB or

poorer in at least 3 different testing frequencies in at least one ear in at least one testing session (Fig. 2.1A). Participants could be any age at enrollment (Fig. 2.1B).

The study was approved by the human subjects review boards of SCH and UW (STUDY00001526). Written informed consent was obtained from participants 18y and older, written assent from children 7-17y with parental consent, and written parental consent for children younger than 7y. Saliva samples were collected for DNA extraction from probands, affected siblings, and one or both parents using the OGR-500 saliva sampling kit (DNA Genotek). Phenotypic and demographic information was collected at enrollment and later confirmed from the electronic medical record (EMR).

Genetic testing

Genomic DNA was extracted using prep-IT-L2P reagent (DNA Genotek) and tested by hybridization to a custom gene panel containing 191 known and candidate genes for hearing loss, updated from previous publications[27]. All genes included in the panel are indicated in Appendix A. Sequencing data was analyzed using our in-house bioinformatics pipeline, as previously described[5].

To identify copy number variants (CNVs) in *STRC* and *OTOA*, which are located in genomic regions with segmental duplications, copy number analysis was carried out using TaqMan CNV qPCR (Thermo). For *STRC*, genomic DNA was tested using two probes: Probe 1 = Hs04444756 (Thermo), overlapping intron 36 and exon 37; and Probe 2 = custom[28] (Thermo), in intron 23. For *OTOA*, DNA was tested using Hs00068385 (Thermo), overlapping intron 5 and exon 6.

VCF (variant call format) files were generated including annotations for genomic position, genic location, population allele frequency (from gnomAD[29]), predicted function, and previously reported

clinical significance (ClinVar; https://www.ncbi.nlm.nih.gov/clinvar/). We independently interpreted all variants using the guidelines of the American College of Medical Genetics and Genomics[30]. Mutations were interpreted as potentially damaging if they were truncating, were predicted to lead to a loss of transcript, completely deleted a critical gene, or were missense with a predicted negative functional effect. All previously unreported mutations predicted to be damaging were submitted to ClinVar.

Audiograms

Audiologic and speech perception testing was performed during normal clinical care. Records from SCH were downloaded from the hospital's audiological database (AudBase; http://www.audbase.com/), and testing from UW was obtained from the EMR. Analysis was based on pure tone thresholds (air and bone). Bone conduction thresholds were substituted for air conduction for tests of individuals with middle ear involvement, with all other analyses based on air conduction thresholds. Both ears for each individual were included. For analyses involving pure-tone averages (PTA), thresholds at 500, 1000, 2000, 4000Hz were used.

Speech perception testing

Speech perception data for AzBio[31], Pediatric AzBio[32], HINT-C[33], PBK[34], and CNC[35] tests were obtained from audiology notes in the EMR. Raw scores (% correct) were used to determine associations of independent variables to scores for each test. To compare results across tests, z-scores were calculated for each test using that test's sample mean and standard deviation.

Statistics

Analyses were carried out by regression, analysis of variance, or analysis of covariance, as appropriate. All P-values were 2-tailed and adjusted for multiple comparisons.

2.4 - RESULTS

GENETIC CAUSES OF HEARING LOSS IN THE COHORT

Overview: Of the 407 families tested, a genetic cause of hearing loss was identified for 53% (216/407) (Fig. 2.2A). Viral, iatrogenic, or environmental causes accounted for hearing loss in 6% of families (27/407), although this proportion is likely an underestimate because environmental exposures were not evaluated for many participants. Among the 216 families with genetic diagnoses, 241 different causal mutations were identified in 49 different genes (Fig. 2.2B), with nearly all families carrying a pathogenic mutation(s) in only one gene. (The exception was family RC387, with mutations in both *GJB2* and *MYO6*, shown in Fig 2.4) The most commonly implicated genes were *GJB2* (69 families, 32%), *STRC* (27 families, 13%), *SLC26A4* (15 families, 7%), *MYO15A* (7 families, 3%), and *TMPRSS3* (7 families, 3%).

Yield of genetic testing was significantly greater for families in which multiple affected individuals were tested (34 of 37 families solved, 92%) compared to those with probands only (179 of 369 families solved, 49%; P = 4.7E-7, Fig. 2.2C). Of the 241 different pathogenic mutations in the 216 solved families, 45% (109/241) of variants had not been previously reported (Fig. 2.2D). Given that the ancestries of families in our cohort are typical of American families studied for hearing loss, the proportion of previously unreported mutations is quite high, reflecting the allelic heterogeneity of the phenotype.

Copy number variants are known to contribute a major fraction of mutations in hearing loss[36], and this was also true in our cohort. Full-gene deletions were identified through a combination of short-read sequencing and qPCR, and were causal mutations in 25 of 27 families with *STRC*-related hearing loss, in 4 of 5 families with *OTOA*-related hearing loss, and in 1 of 4 families with *MITF*-

related hearing loss. Pathogenic CNVs involving less than a complete gene included deletion of a splice junction region of *ADGRV1* and deletion of a noncoding enhancer region of *GJB2*.

To determine if the *STRC* deletions in this cohort arose from independent genomic events or from a few founder mutations, we evaluated haplotypes with microsatellite markers flanking *STRC:* D15S778 at chr15:43,834,857, and D15S783 at chr15:44,244,161 (hg19/GRCH37). In the 23 families harboring at least one *STRC* deletion, 16 different haplotypes were identified, suggesting that the deletion has occurred multiple times, and that *STRC* lies at a genomic hotspot, an observation consistent with the many segmental duplications and deletions in its genomic neighborhood.

Genotype and sensitivity of newborn hearing screening. Of the 449 children in the cohort, 347 (77%) had been tested by newborn hearing screening, with 214 (62%) referred in both ears, 17 (5%) referred in one ear only, and 115 (33%) passed in both ears (Table 2.2). Sensitivity of newborn hearing screening varied by gene, as children with mild, progressive, or later-onset hearing loss were frequently referred after infancy (Fig. 2.3A). Specifically, newborn hearing screening failed to detect hearing loss in 39% of children with mutations in *STRC*, in 70% of children with mutations in *TMPRSS3*, and in 33% of children with mutations in *SLC26A4*. Among children with mutations in *GJB2*, for which hearing loss severity depends on genotype with truncating mutations more severe than most missense mutations[37,38], newborn hearing screening failed to detect hearing loss in 36% of children with hearing loss due to *GJB2* missense mutations versus less than 10% of children with one or more *GJB2* truncating mutations.

Genotype and cochlear malformations. Of the 449 children in the cohort, 227 (51%) had undergone imaging of their inner ears by either CT or MRI, with cochlear malformations found in 59 (26% of those with imaging; Table 2.2). Prevalence of cochlear malformation varied by gene,

with enlarged vestibular aqueduct and/or Mondini deformity identified in 16 of 17 children evaluated by imaging and with hearing loss due to SLC26A4[39,40] (and 5 children with only one *SLC26A4* mutation identified by our panel) and absence of semicircular canals in 6 of 7 children evaluated by imaging and with hearing loss due to *SOX10* or *CHD7*[41,42] (Fig 3B).

Prior genetic testing and CMV testing. Of the 449 children in the cohort, 169 (38%) had received some form of genetic testing prior to our study, varying from single gene testing (usually of *GJB2*) to the OtoSCOPE gene panel (https://morl.lab.uiowa.edu/clinical-diagnostic-services) to whole exome sequencing, with 85 of these children receiving a genetic diagnosis prior to our study (Table 2.2, Fig. 2.3C). We carried out sequencing without knowledge of any prior genetic diagnoses. For all children with prior genetic diagnoses, our results were technically concordant with prior results, but we disagreed with the clinical interpretation of variants for 6 children (all of which were variants of unknown significance that we believed to be benign or likely benign). Furthermore, for 31 children with negative results on prior genetic testing, we identified causal mutations in genes not included in the prior tests. Many of these (19) were tested for damaging variants in *GJB2* without any further testing. For 4 individuals, previous hearing loss gene panels were negative because the panel did not cover their causative gene. Testing for congenital cytogmegalovirus (cCMV) by newborn bloodspot qPCR was carried out at various clinical centers for 201 children, with 11 children (5.5%) testing positive. We did not carry out CMV testing for this project.

Audioprofiles of hearing loss due to each gene. Audiograms of individuals with hearing loss due to the same gene (or genotype) were binned by age to create an age-dependent audioprofile for each gene (Fig. 2.5). The audioprofiles confirmed previously reported severity and patterns of hearing loss attributable to individual genes. In particular, mutations in *CDH23*, *MYO15A,* and *SOX10* caused stable severe-to-profound hearing loss across all frequencies, whereas mutations

in *DMXL2*, *MYO6*, and *STRC* caused stable milder hearing loss across all frequencies. Hearing loss due to *CLDN9, ESPN, GZF1, OTOG, SLC26A4, SYNE4,* and *TMPRSS3* predominantly affected high frequencies; hearing loss due to *COL4A5* predominantly affected lower frequencies; and hearing loss due to *EDNRB, MYO6, MYO7A*, or *OTOA* presented with a U-shaped or "cookie-bite" audiogram, all stable with age.

Progressive hearing loss. Based on the audioprofiles, hearing losses due to mutations in *CEACAM16*, *GZF1, SLC26A4*, or *TMPRSS3* clearly progressed with age. To evaluate changes in hearing loss by age for each gene, four-tone pure tone averages (PTA) were calculated for each audiologic test, binned by gene, and plotted against the participant's age at test (Fig. 2.6). Only genes with audiological data for 3 or more individuals were assessed. To reduce bias due to loss to follow-up after cochlear implantation, only ears that never received cochlear implants were included in this analysis. Thus, PTA values were higher than average for the genotype, but accurately represented progression over time.

As expected based on previous reports[38,43–46], genes that showed significant worsening of hearing by age were *GJB2* (truncating mutations), *MYO6, OTOA, SLC26A4,* and *TMPRSS3* (Table 2.3). Between birth and age 18y, *TMPRSS3* showed the steepest progression, with PTA increasing by 3.69 dB/year. Rates of progression for other genes were 1.86 dB/year for *SLC26A4*, 1.41 dB/year for truncating mutations in *GJB2*, 1.30 dB/year for *MYO6*, and 1.15 dB/year for *OTOA* ($P < 0.0001$ for slope of PTA versus age for each gene).

Variation in hearing loss depending on genotype within gene. For hearing loss due to *GJB2*, variation in severity depending on specific genotype has been described[37,38], with truncating mutations leading to more severe hearing loss than missense mutations. A similar pattern was seen in our cohort, with audiograms for each genotype completely separate from each other (Fig.

2.7A). Comparison of PTA at first audiogram by *GJB2* genotype also reflects this difference (Fig. 2.7B).

Mutations in *TMPRSS3* cause both DFNB8 and DFNB10[47,48]. DFNB10 typically describes severe hearing loss of congenital or early-childhood onset, and DFNB8 presents as a later-onset, progressive hearing loss preferentially affecting high frequencies. Our study cohort included ten children with hearing loss due to mutations in *TMPRSS3*. (Fig. 2.8). Two children were compound heterozygous for frameshift mutations (fs/fs), presented with congenital severe hearing loss, and received bilateral cochlear implants before age 3y. Five children with both a frameshift and a missense mutation (fs/miss), and three children with two missense mutations (miss/miss) received unilateral cochlear implants at older ages.

To better understand severity and progression of hearing loss due to different *TMPRSS3* genotypes, hearing thresholds were plotted by age and genotypes for un-implanted ears (Fig. 2.8). A significant increase in hearing thresholds with age was observed at all frequencies for fs/miss genotypes and at 500Hz and 8000Hz for miss/miss genotypes (Table 2.4). As expected, hearing thresholds increased most dramatically at frequencies with the most residual hearing, such as 500Hz (fs/miss: 6.43 dB/year, miss/miss: 3.55 dB/year) and 1000Hz (fs/miss: 6.17 dB/year, miss/miss 3.31 dB/year). Interestingly, at lower frequencies, the rate of hearing decline was significantly steeper for children with fs/miss genotypes compared to those with miss/miss genotypes (P=0.0006; Table 2.5). These data suggest that *TMPRSS3* hearing loss phenotypes exist on a spectrum, with truncating (frameshift) mutations leading, in a dose-dependent manner, to more severe and rapidly progressive hearing loss.

For some patients with *TMPRSS3* mutations, hearing is partially preserved after cochlear implantation[49] (Fig. 2.9 and Fig. 2.10) These results varied among the 6 individuals with cochlear

implants and mutations in *TMPRSS3*. Hearing levels at 500Hz were compared between implanted vs un-implanted ears in unilaterally implanted individuals. Individuals I, V, and VII show a steep decline in hearing post-implantation although its timing was variable. Post-implant hearing levels were much more stable in individuals III and IV, and the trajectory was unclear for individual II. There was no clear distinguishable factor (including genotype or implant model) between individuals who experienced post-implant hearing decline versus those who did not.

GENOTYPE AND SUCCESS OF COCHLEAR IMPLANT IN THE COHORT

Overview: Of the 449 participants, 251 (56%) were treated with amplification in the form of hearing aids (Fig. 2.11A), while 168 (38% of all participants) had received either unilateral or bilateral cochlear implants (Table 2.6). A minority of children (32, 7%) mostly very young children and those with mild forms of hearing loss, did not use amplification or cochlear implants. The distribution of age at first implant was heavily skewed towards implantation early in life (Fig. 2.11B). Of the 168 children with cochlear implants, 107 (64%) had a genetic diagnosis of their hearing loss based on our gene panel, which is more than for the cohort as a whole. For 17 children with implants (10%), hearing loss was due to a confirmed non-genetic cause. For 44 children with implants (26%) hearing loss was of unknown origin.

Cochlear implant success. Cochlear implants reliably improve audiologic hearing thresholds to normal levels, and therefore speech perception is a more successful metric of cochlear implant success than hearing thresholds measured by audiogram. We evaluated data from five speech perception tests: AzBio, Pediatric AzBio, HINT-C, PBK, and CNC. The first three (AzBio, Pediatric-AzBio, HINT-C) are sentence-based, and others are composed of lists of monosyllabic words (CNC) or phonetically-balanced word pairs (PBK). These tests are appropriate for patients of varying age, as the Pediatric AzBio, HINT-C, and PBK tests are designed specifically for use in a pediatric population, and AzBio and CNC are adult level tests.

We first evaluated association of non-genetic influences with speech perception among implant patients, without including patients' genotype in the analysis (Table 2.7). Age at implantation was inversely correlated with speech perception as measured by Pediatric AzBio in quiet (slope -0.194, P = 0.0005), CNC phonemes (slope -0.046, P = 0.003), and CNC words (slope -0.064, P = 0.005; Fig. 2.12A) and for all tests combined (slope -0.003, P<0.0001; Table 2.7). Interval between implantation and test was inversely correlated with speech perception as measured by HINT-C quiet (slope -0.157, P = 0.0002) and Pediatric AzBio in noise (slope -0.231, P = 0.0005) and positively correlated with speech perception as measured by AzBio in noise (+5 SNR; slope 0.055, P = 0.03; Fig. 2.12B). There was no significant correlation between time since implant and performance on the tests combined (Table 2.7). There was no significant correlation between the percent of currently active electrodes and speech perception with any specific test or the tests combined, likely because the number of active electrodes was universally high.

To assess overall success of cochlear implantation, we counted the number of participants with a score of at least 60% on their most successful AzBio or CNC adult-level test (Fig. 2.13A). By this measure, speech perception was successful for 89% (42 of 47) cochlear implant patients. Five individuals did not meet this benchmark: This includes one individual with a syndromic presentation of *GPSM2* hearing loss that likely impaired their testing ability. Another individual has *OTOF* hearing loss which has long been suspected to have lower CI performance due to expression of *OTOF* in the auditory ribbon synapse and its implication in auditory neuropathy spectrum disorder (ANSD). The final two children with relatively poor performance and a genetic cause for their hearing loss are individuals with *GJB2* hearing loss and no clear explanation for their performance.

Finally, we evaluated whether variability in speech perception after implant was associated with genotype. All children with implants were included in the analysis. Analysis of covariance (ANCOVA) included the causal gene as the independent variable, speech perception z-score as the outcome, and covariates age at implant, time since implant, and individual participant (as a block variable to adjust for variable numbers of tests per subject). Age at implant and individual ID had significant influences on speech performance (P = 1.97E-6 and P = 7.73E-11, respectively). Adjusting for these factors, genes associated with strongest speech perception were *TMPRSS3* (P < 0.0001; Table 2.8; Fig. 2.13B), and *ESRRB* and *MITF* (P < 0.0001); and genes associated with weakest speech perception were *SLC26A4* (P < 0.0001), *GPSM2* and *PAX3* (P < 0.0001), and *OTOF* (P = 0.015). No significant differences were observed among specific genotypes for those with hearing loss due to *GJB2* or *TMPRSS3* mutations (Fig. 2.13C).

2.5 - DISCUSSION

As genes implicated in human hearing continue to be discovered, the efficacy of genetic testing continues to improve. Even in a diverse population such as the United States, targeted gene panel sequencing has consistently had a high yield of genetic diagnoses among individuals with pre-lingual hearing loss, regardless of family history[4,50]. Yield is highly dependent on the sequencing technology used. Our finding that 45% of mutations responsible for hearing loss in our participants had not previously been reported on ClinVar reinforces the allelic heterogeneity of hearing loss and the critical role of complete sequencing of genes for hearing loss in order to obtain an accurate genetic diagnosis.

Newborn hearing screening detected hearing loss in 67% of the children meeting our inclusion criteria. If this testing were coupled with evaluation by our targeted gene panel, 83% of children with hearing loss would have been identified. Other, less expensive, technologies such as SNP

tests that target specific common pathogenic mutations[51] would miss a large portion of these individuals.

While genetic diagnosis is often pursued as part of clinical workup for children with hearing loss, results of genetic testing are frequently not used as effectively as they could be. The primary treatments for hearing loss, hearing aids and cochlear implants, are implemented often based only on remaining level of speech discrimination[7]. In order for the benefits of genetic testing in pediatric hearing loss to be fully realized, genetic diagnoses should be integrated with current severity in order to assess the future hearing of the child. The audioprofiles presented in this study represent a contribution to that endeavor. Our cohort included adequate numbers of participants with hearing loss due to *GJB2, MYO15A, OTOG, SLC26A4, SOX10, STRC,* and *TMPRSS3* to confidently describe their hearing phenotypes across affected frequencies and with age. For hearing loss due to other genes, we present audiological data for a small number of individuals at high resolution so that they may be combined with other studies to create a clear genotype audioprofile as a whole. Our analysis of hearing loss progression with age identified significant hearing decline in those with *GJB2* (truncating mutations), *MYO6, OTOA, SLC26A4*, and *TMPRSS3* genotypes and provided quantification of the rate. The addition of more individuals and data points to this type of analysis could identify more subtle trends in progression in other genes. Our results, along with existing phenotypic information, enable one to consider treatment decisions such as earlier implantation for progressive-hearing-loss genes with confirmed high levels of implant success.

For two genes, *GJB2* and *TMPRSS3*, we outline phenotypic differences depending on genotype. In both cases, missense mutations result in a less severe phenotype than do truncation mutations. This effect is apparent in both the severity and progression of hearing loss. The delay in progression of hearing loss among individuals with milder phenotypes presents the possibility that

homozygosity or compound heterozygosity for mild mutations, or heterozygosity for mutations of severe effect when homozygous, may contribute to hearing loss at later ages. Heterozygosity for a frameshift in *TMPRSS3* has been suggested as a potential cause of early-onset age-related hearing loss[52]. Further study of this class of mutations among persons with age-related hearing loss will reveal if this hypothesis is broadly applicable. If so, the current understanding of a relatively uniform phenotype for each gene will need to be revised, and interpretations of phenotypic severity for different variants should be communicated to care providers as part of genetic testing.

The development of cochlear implants has led to a dramatic improvement in hearing thresholds, speech perception, and quality of life in those with severe hearing impairment. This is especially true in pediatric patients, and was apparent in our cohort, of which 89% of participants ultimately scored >60% on adult level post-implant speech perception tests. Genetic heterogeneity is a likely culprit in explaining the remaining variability in success. Previous studies have suggested that implant success may be related to tissue specific expression of the causative gene[24,25]. In our cohort, too few individuals carried mutations in genes primarily expressed outside of the inner ear (*AIFM1, DIAPH3, DFNB59, MT-RNR1, OPA1*) to evaluate this claim. After adjusting for age at implant, time between implant and test, and individual, our analysis identified significantly better speech perception post-implant among individuals with hearing loss due to *TMPRSS3, ESRRB, MITF* and poorer speech perception post-implant among individuals with hearing loss due to *SLC26A4, OTOF, GPSM2*, or *PAX3*. While the level of this variation is not substantial enough to preclude implantation for any patient who meets the necessary criteria, it still provides valuable information for care. Poor predicted implant success could lead to emphasis on other communication methods or a delay to implantation in the setting of residual hearing. In contrast, increased confidence of success may suggest early implantation to maximize benefit from early adaptation.

One clear example of this information's relevance is for patients with *TMPRSS3* hearing loss. Studies of cochlear implantation in adults with *TMPRSS3* mutations have described an unclear pattern of success[24,46,48,53,54]. Similarly, evidence of CI outcomes in children with *TMPRSS3*-hearing loss is limited to a report of 3 individuals who demonstrated variable levels of post-implant speech perception[49]. The decision to pursue implantation in these patients is of particular importance because their hearing loss primarily affects mid to high frequencies with poor amplification by hearing aids. Due to variable progression, many *TMPRSS3* patients with milder phenotypes do not meet FDA cochlear implant candidacy criteria at the time of genetic diagnosis. Our cohort includes the largest reported pediatric cohort of implanted *TMPRSS3* patients to date. Their post-implant speech perception testing indicates that implantation was universally successful, and patients achieved one of the highest post-implant speech performance scores of any genotype. These findings suggest that best clinical practices for pediatric *TMPRSS3*-hearing loss patients should include early genetic diagnosis and early cochlear implantation, and suggest revision to FDA candidacy procedures for those with a *TMPRSS3* diagnosis.

2.6 – FIGURES

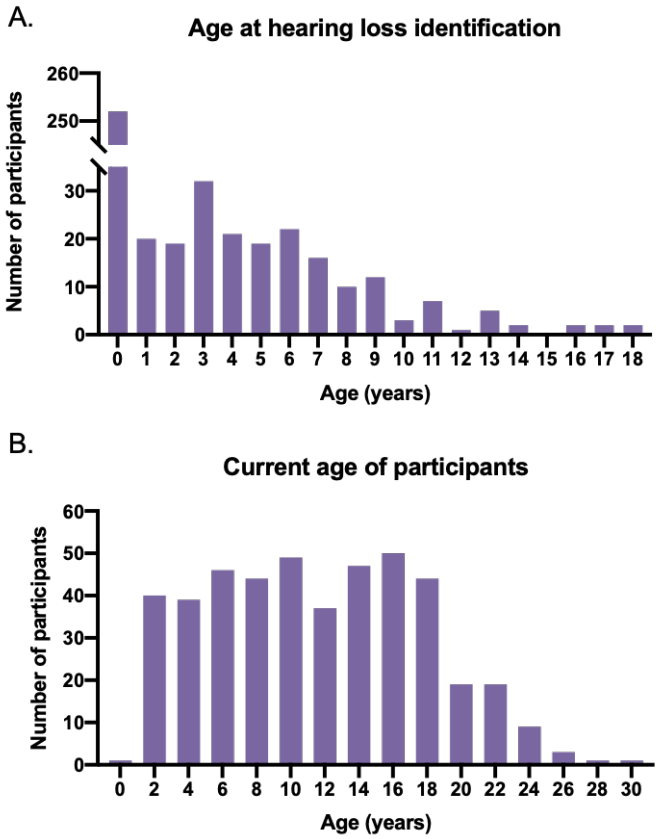

Figure 2.1: Ages at diagnosis of hearing loss
A. Age at first identification of hearing loss, defined as age at first failed screening or diagnostic test.
B. Age of enrollment of all participants of in the study.

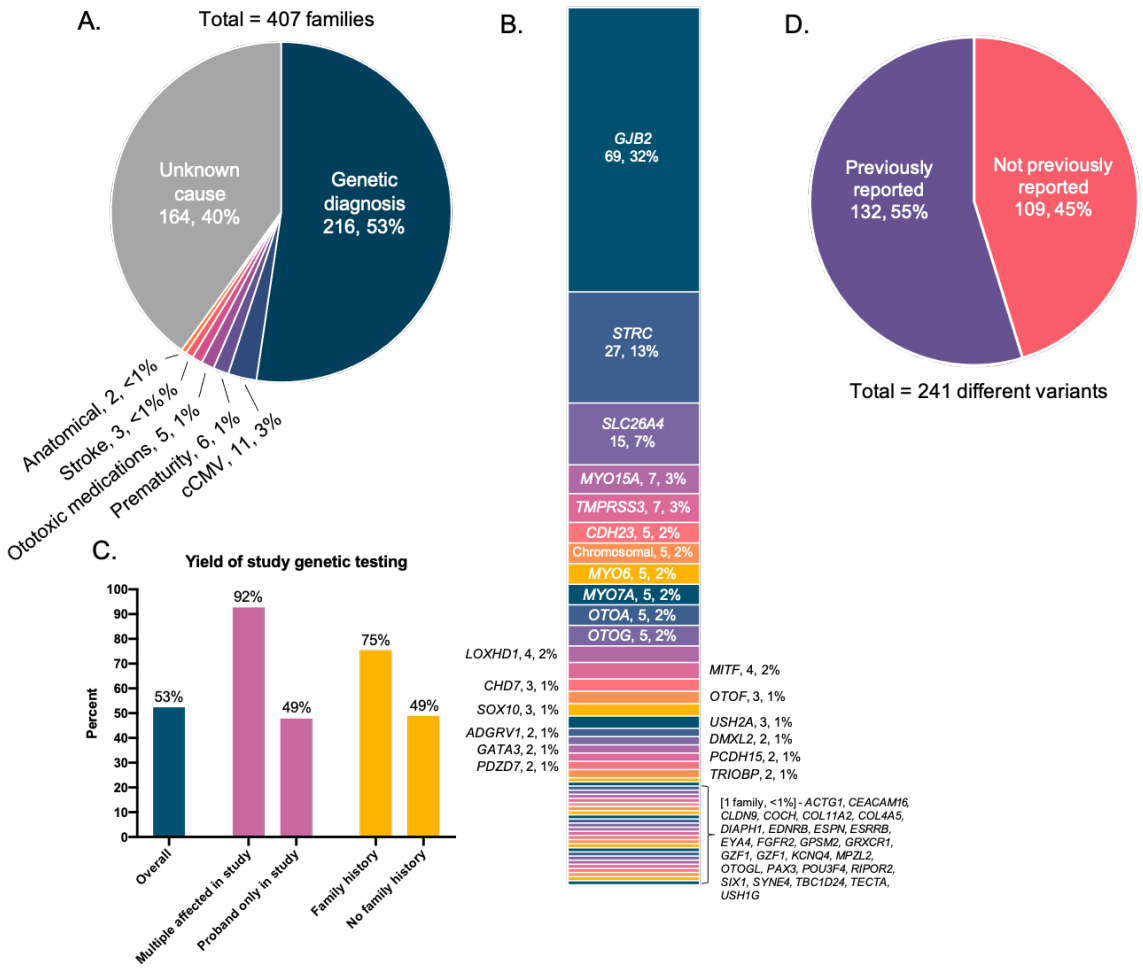

Figure 2.2: Genetic diagnoses
A. Causes of hearing loss for all 407 families based on sequencing with our gene panel.
B. Genes responsible for hearing loss for the 216 families with genetic diagnoses.
C. Yield of gene panel testing by family history.
D. Proportions of damaging mutations, previously vs. not previously reported.

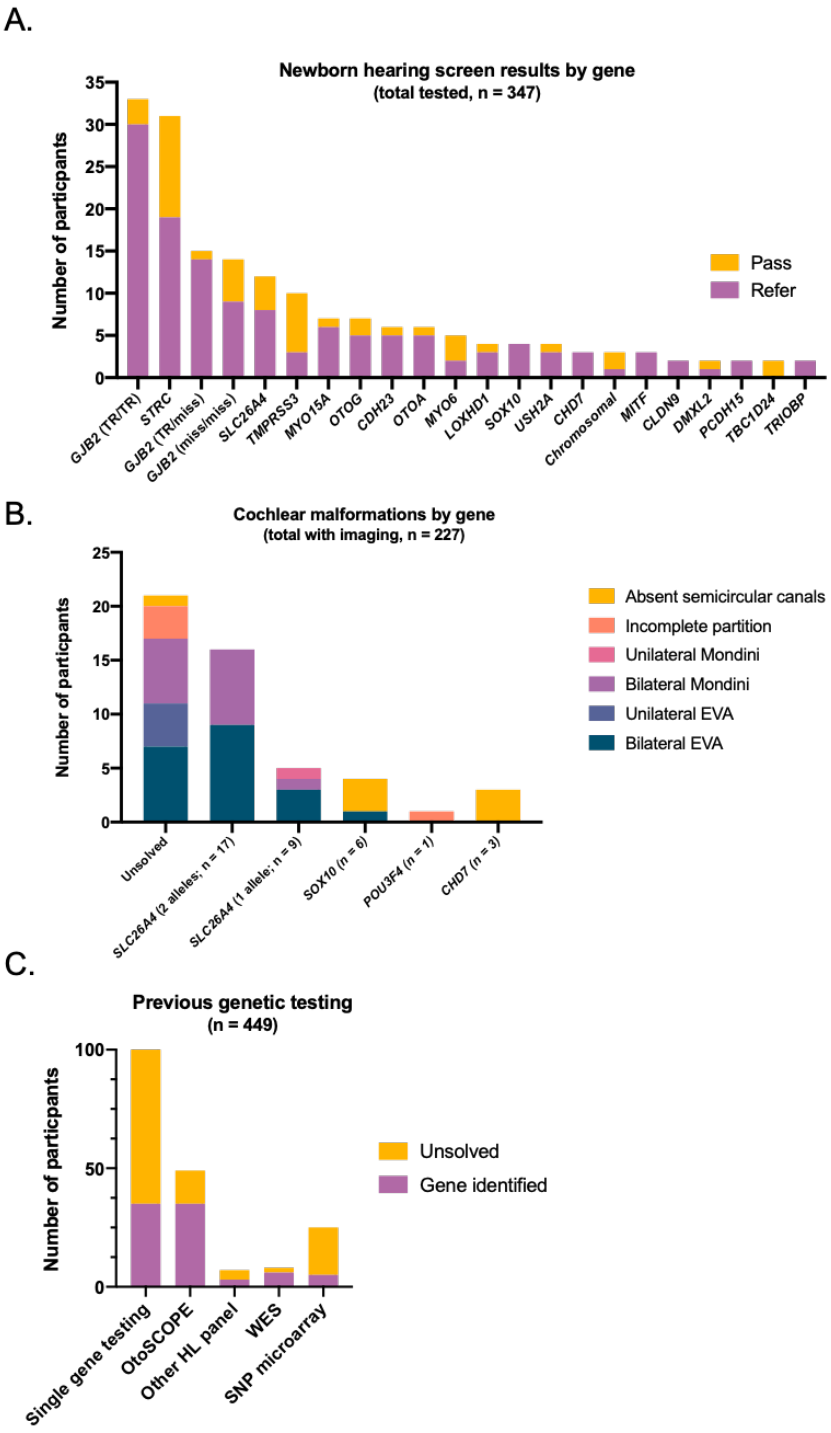

Figure 2.3: Previous clinical studies

A. Results of newborn hearing screen for study participants, by gene ultimately found to be causative.

B. Presence of cochlear malformations in study participants, by causative gene. Only participants with imaging are depicted. Overall number of participants with each genotype are given on x-axis.

C. Genetic testing carried out prior to study enrollment as part of clinical care.

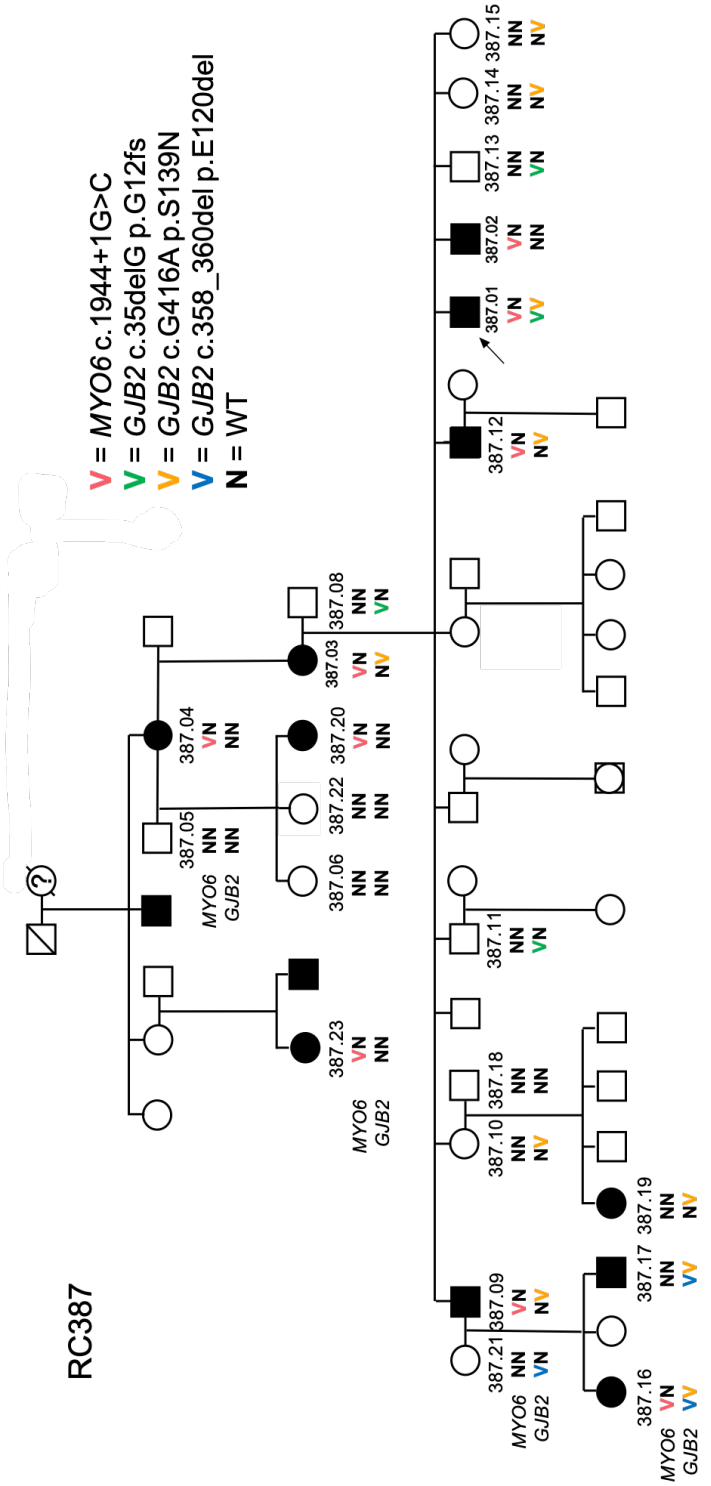

Figure 2.4: Pedigree of Family RC387
Affected individuals have prelingual moderate to severe hearing loss due to mutations in *MYO6, GJB2,* or both.

Figure 2.5: Audioprofiles of individuals with hearing loss, by causative gene.
All tests were unaided, and bone conduction was substituted for air conductions for tests with middle ear involvement. Results for each ear are included separately. For each panel, n indicates number of participants with available audiologic data. “TR” denotes truncating mutations. Error bars depict SEM. Several genes indicate progressive hearing loss. See figure 2.6 for additional details.

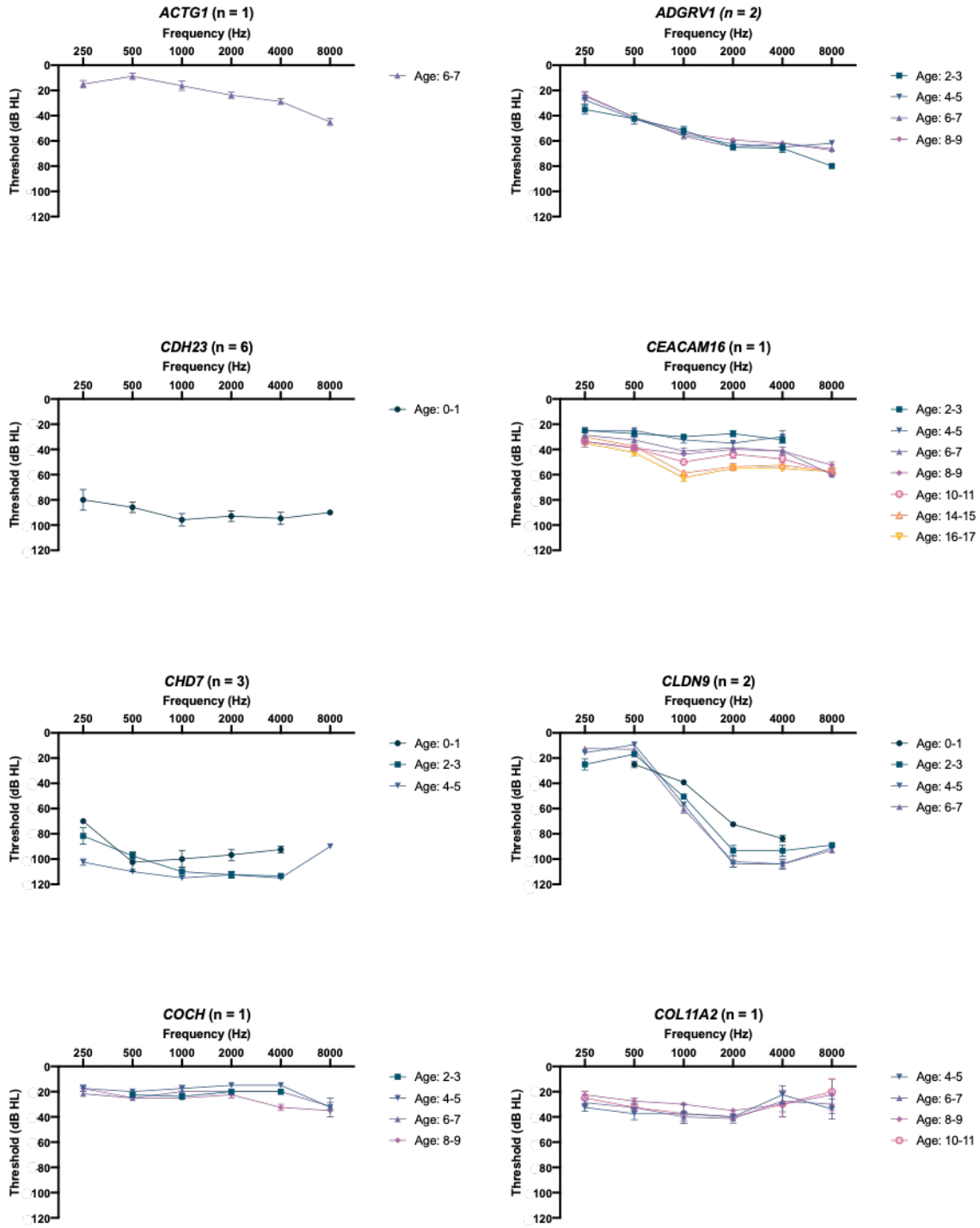

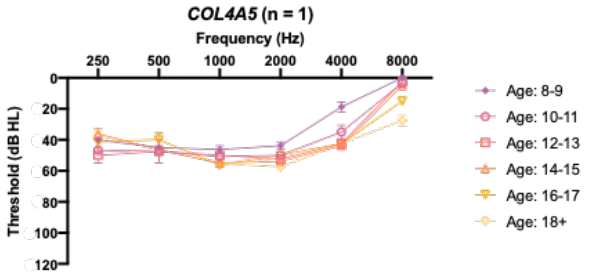
COL4A5 (n = 1)
Frequency (Hz)
250
500
1000
2000
4000
8000
Threshold (dB HL)
0
20
40
60
80
100
120
Age: 8-9
Age: 10-11
Age: 12-13
Age: 14-15
Age: 16-17
Age: 18+

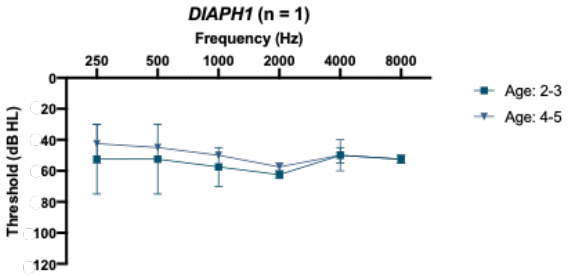
DIAPH1 (n = 1)
Frequency (Hz)
250
500
1000
2000
4000
8000
Threshold (dB HL)
0
20
40
60
80
100
120
Age: 2-3
Age: 4-5

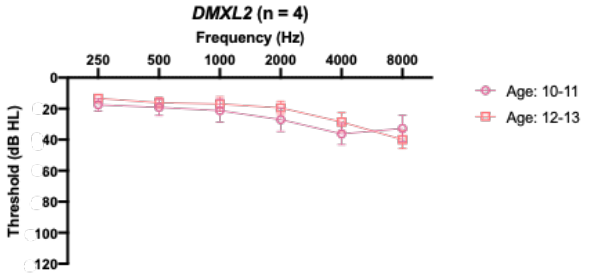
DMXL2 (n = 4)
Frequency (Hz)
250
500
1000
2000
4000
8000
Threshold (dB HL)
0
20
40
60
80
100
120
Age: 10-11
Age: 12-13

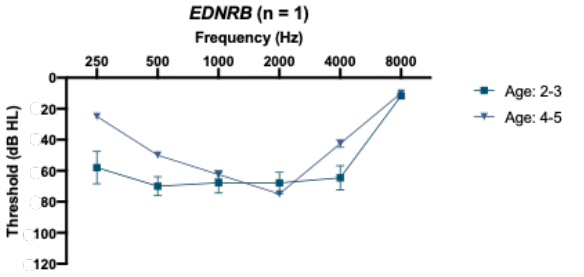
EDNRB (n = 1)
Frequency (Hz)
250
500
1000
2000
4000
8000
Threshold (dB HL)
0
20
40
60
80
100
120
Age: 2-3
Age: 4-5

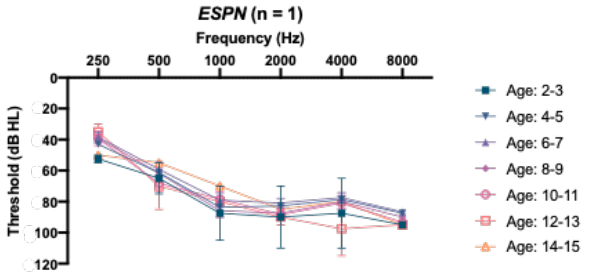
ESPN (n = 1)
Frequency (Hz)
250
500
1000
2000
4000
8000
Threshold (dB HL)
0
20
40
60
80
100
120
Age: 2-3
Age: 4-5
Age: 6-7
Age: 8-9
Age: 10-11
Age: 12-13
Age: 14-15

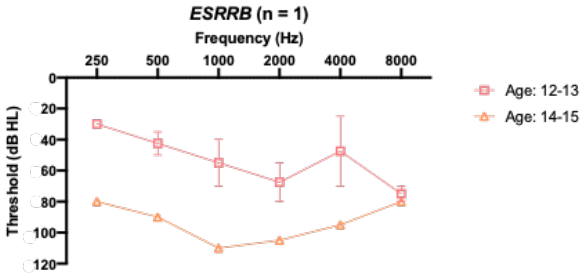
ESRRB (n = 1)
Frequency (Hz)
250
500
1000
2000
4000
8000
Threshold (dB HL)
0
20
40
60
80
100
120
Age: 12-13
Age: 14-15

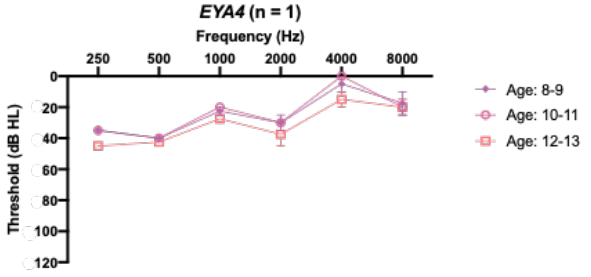
EYA4 (n = 1)
Frequency (Hz)
250
500
1000
2000
4000
8000
Threshold (dB HL)
0
20
40
60
80
100
120
Age: 8-9
Age: 10-11
Age: 12-13

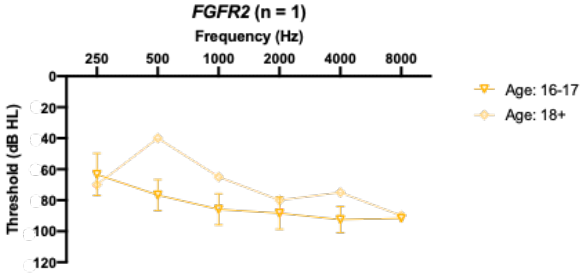
FGFR2 (n = 1)
Frequency (Hz)
250
500
1000
2000
4000
8000
Threshold (dB HL)
0
20
40
60
80
100
120
Age: 16-17
Age: 18+

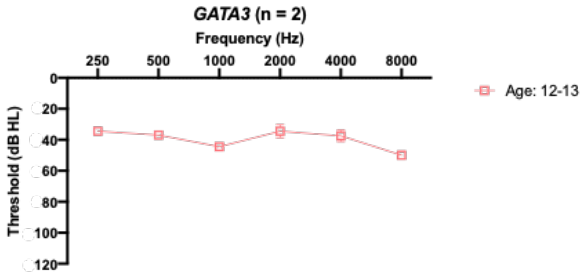
GATA3 (n = 2)
Frequency (Hz)
250
500
1000
2000
4000
8000
Threshold (dB HL)
0
20
40
60
80
100
120
Age: 12-13

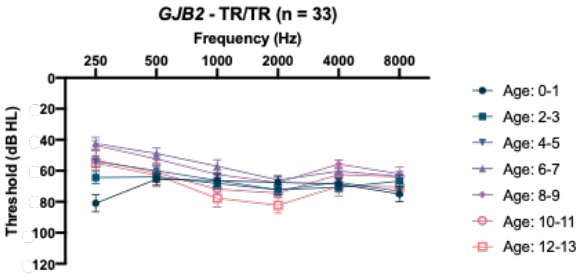
GJB2 - TR/TR (n = 33)
Frequency (Hz)
250
500
1000
2000
4000
8000
Threshold (dB HL)
0
20
40
60
80
100
120
Age: 0-1
Age: 2-3
Age: 4-5
Age: 6-7
Age: 8-9
Age: 10-11
Age: 12-13

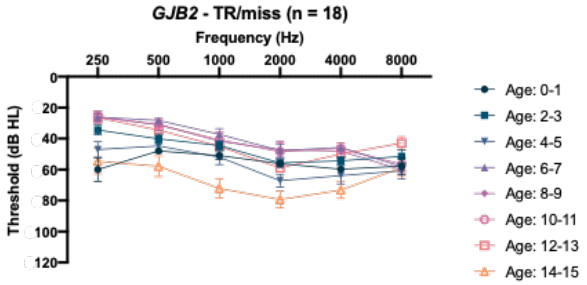
GJB2 - TR/miss (n = 18)
Frequency (Hz)
250
500
1000
2000
4000
8000
Threshold (dB HL)
0
20
40
60
80
100
120
Age: 0-1
Age: 2-3
Age: 4-5
Age: 6-7
Age: 8-9
Age: 10-11
Age: 12-13
Age: 14-15

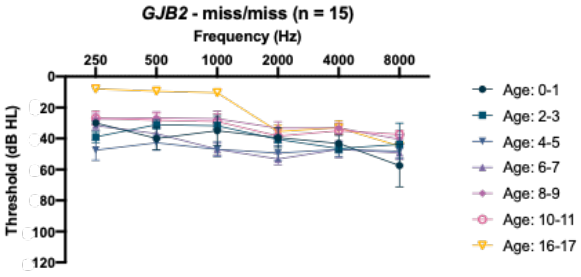
GJB2 - miss/miss (n = 15)
Frequency (Hz)
250
500
1000
2000
4000
8000
Threshold (dB HL)
0
20
40
60
80
100
120
Age: 0-1
Age: 2-3
Age: 4-5
Age: 6-7
Age: 8-9
Age: 10-11
Age: 16-17

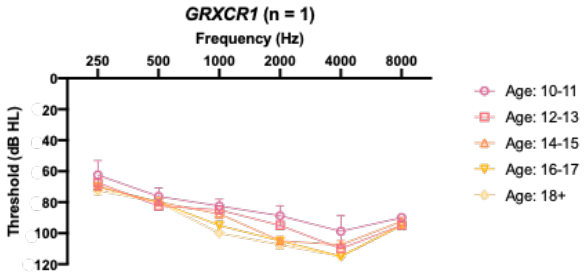
GRXCR1 (n = 1)
Frequency (Hz)
250
500
1000
2000
4000
8000
Threshold (dB HL)
0
20
40
60
80
100
120
Age: 10-11
Age: 12-13
Age: 14-15
Age: 16-17
Age: 18+

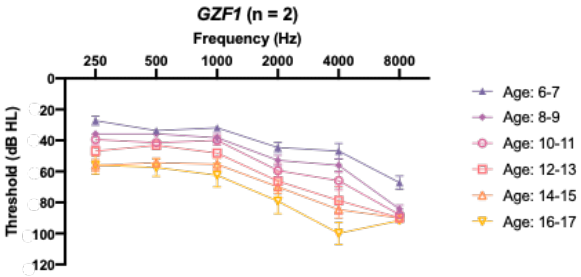
GZF1 (n = 2)
Frequency (Hz)
250
500
1000
2000
4000
8000
Threshold (dB HL)
0
20
40
60
80
100
120
Age: 6-7
Age: 8-9
Age: 10-11
Age: 12-13
Age: 14-15
Age: 16-17

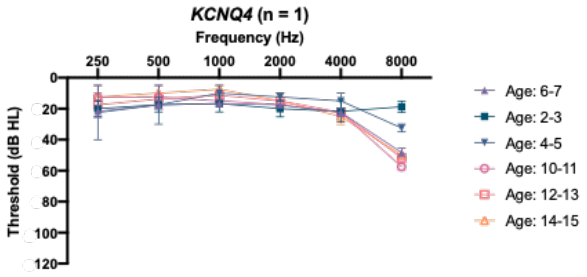
KCNQ4 (n = 1)
Frequency (Hz)
250
500
1000
2000
4000
8000
Threshold (dB HL)
0
20
40
60
80
100
120
Age: 6-7
Age: 2-3
Age: 4-5
Age: 10-11
Age: 12-13
Age: 14-15

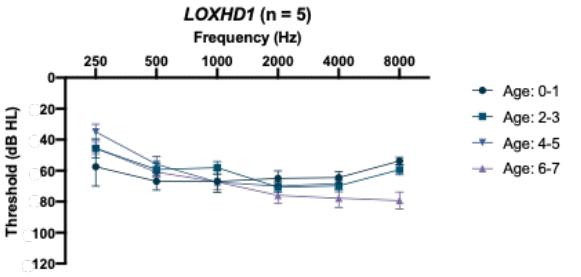
LOXHD1 (n = 5)
Frequency (Hz)
250
500
1000
2000
4000
8000
Threshold (dB HL)
0
20
40
60
80
100
120
Age: 0-1
Age: 2-3
Age: 4-5
Age: 6-7

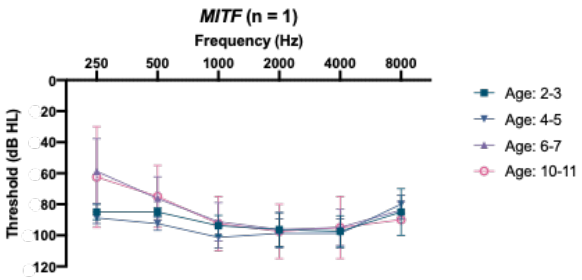
MITF (n = 1)
Frequency (Hz)
250
500
1000
2000
4000
8000
Threshold (dB HL)
0
20
40
60
80
100
120
Age: 2-3
Age: 4-5
Age: 6-7
Age: 10-11

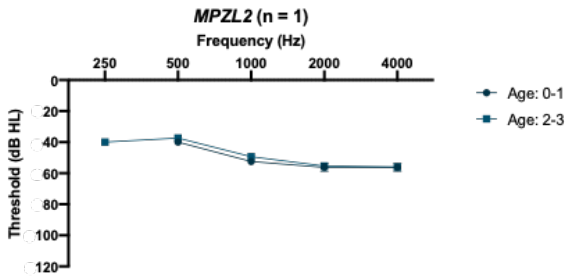
MPZL2 (n = 1)
Frequency (Hz)
250
500
1000
2000
4000
Threshold (dB HL)
0
20
40
60
80
100
120
Age: 0-1
Age: 2-3

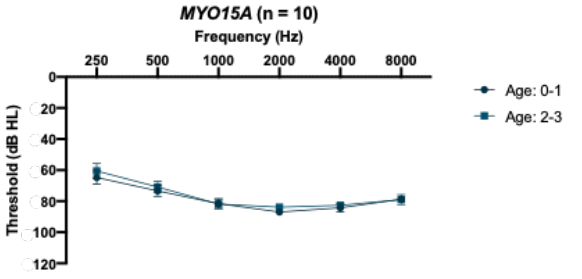
MYO15A (n = 10)
Frequency (Hz)
250
500
1000
2000
4000
8000
Threshold (dB HL)
0
20
40
60
80
100
120
Age: 0-1
Age: 2-3

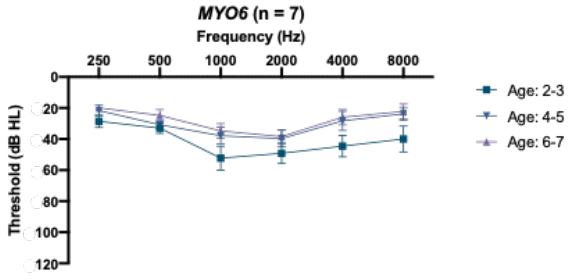
MYO6 (n = 7)
Frequency (Hz)
250
500
1000
2000
4000
8000
Threshold (dB HL)
0
20
40
60
80
100
120
Age: 2-3
Age: 4-5
Age: 6-7

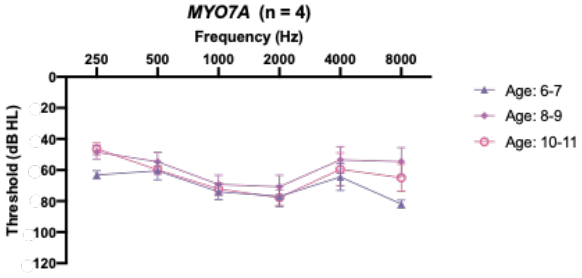
MYO7A (n = 4)
Frequency (Hz)
250
500
1000
2000
4000
8000
Threshold (dB HL)
0
20
40
60
80
100
120
Age: 6-7
Age: 8-9
Age: 10-11

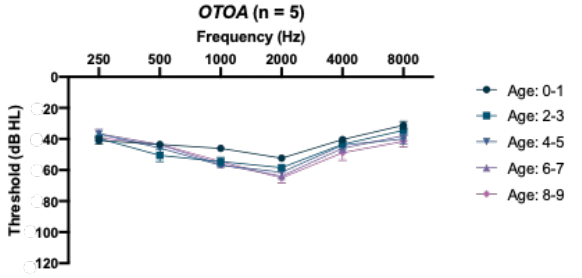
OTOA (n = 5)
Frequency (Hz)
250
500
1000
2000
4000
8000
Threshold (dB HL)
0
20
40
60
80
100
120
Age: 0-1
Age: 2-3
Age: 4-5
Age: 6-7
Age: 8-9

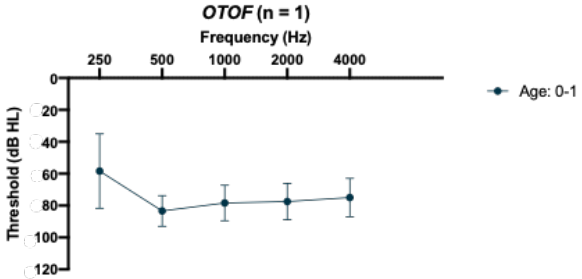
OTOF (n = 1)
Frequency (Hz)
250
500
1000
2000
4000
Threshold (dB HL)
0
20
40
60
80
100
120
Age: 0-1

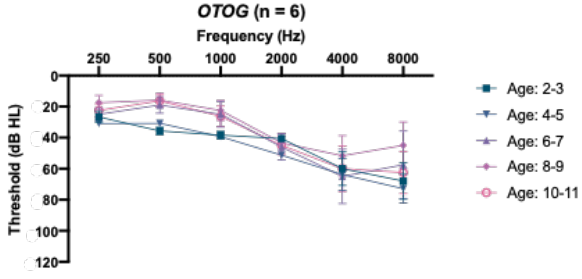
OTOG (n = 6)
Frequency (Hz)
250
500
1000
2000
4000
8000
Threshold (dB HL)
0
20
40
60
80
100
120
Age: 2-3
Age: 4-5
Age: 6-7
Age: 8-9
Age: 10-11

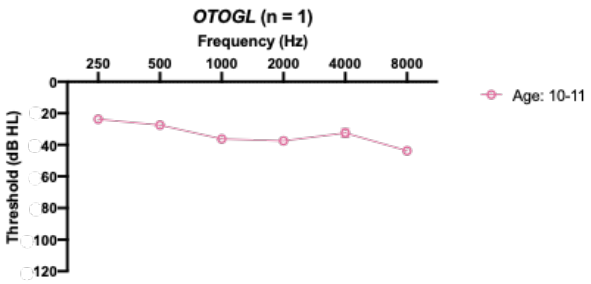
OTOGL (n = 1)
Frequency (Hz)
250
500
1000
2000
4000
8000
Threshold (dB HL)
0
20
40
60
80
100
120
Age: 10-11

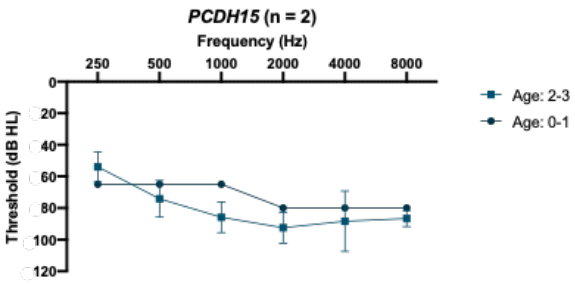
PCDH15 (n = 2)
Frequency (Hz)
250
500
1000
2000
4000
8000
Threshold (dB HL)
0
20
40
60
80
100
120
Age: 2-3
Age: 0-1

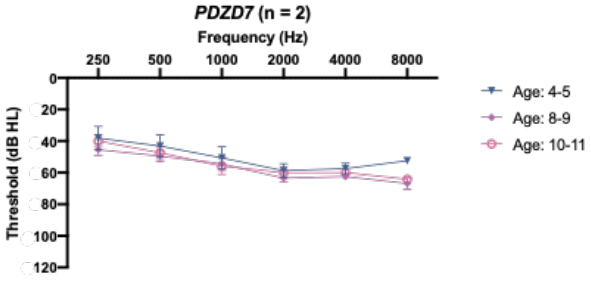
PDZD7 (n = 2)
Frequency (Hz)
250
500
1000
2000
4000
8000
Threshold (dB HL)
0
20
40
60
80
100
120
Age: 4-5
Age: 8-9
Age: 10-11

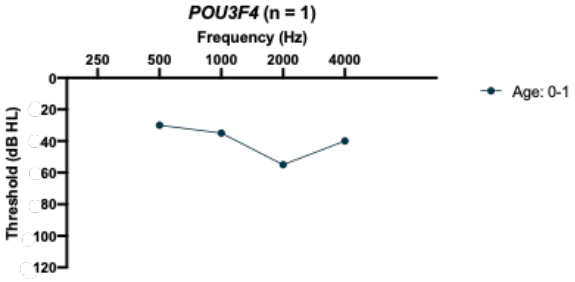
POU3F4 (n = 1)
Frequency (Hz)
250
500
1000
2000
4000
Threshold (dB HL)
0
20
40
60
80
100
120
Age: 0-1

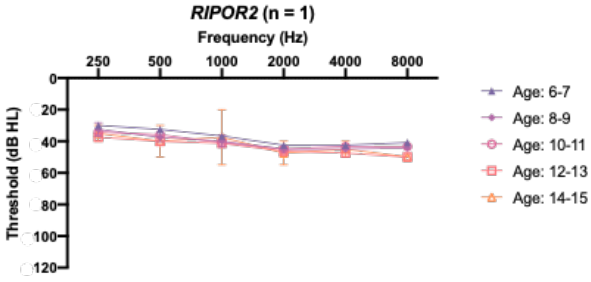
RIPOR2 (n = 1)
Frequency (Hz)
250
500
1000
2000
4000
8000
Threshold (dB HL)
0
20
40
60
80
100
120
Age: 6-7
Age: 8-9
Age: 10-11
Age: 12-13
Age: 14-15

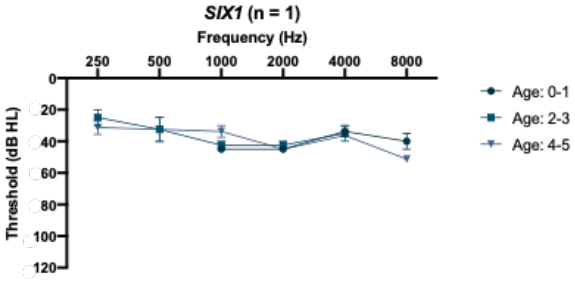
SIX1 (n = 1)
Frequency (Hz)
250
500
1000
2000
4000
8000
Threshold (dB HL)
0
20
40
60
80
100
120
Age: 0-1
Age: 2-3
Age: 4-5

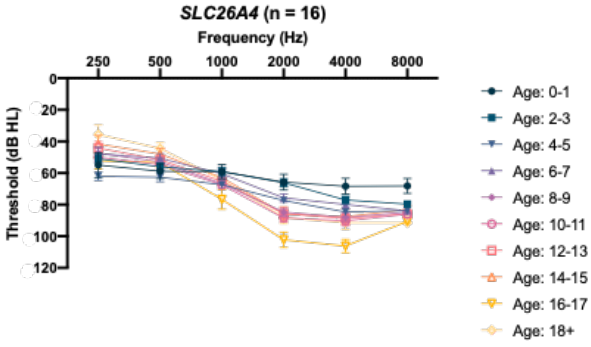
SLC26A4 (n = 16)
Frequency (Hz)
250
500
1000
2000
4000
8000
Threshold (dB HL)
0
20
40
60
80
100
120
Age: 0-1
Age: 2-3
Age: 4-5
Age: 6-7
Age: 8-9
Age: 10-11
Age: 12-13
Age: 14-15
Age: 16-17
Age: 18+

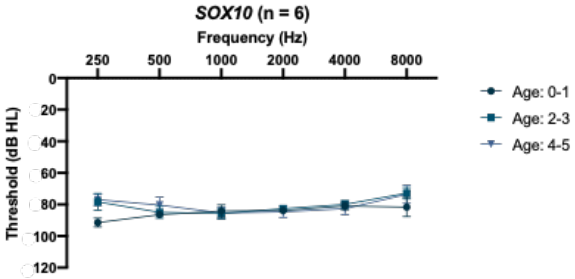
SOX10 (n = 6)
Frequency (Hz)
250
500
1000
2000
4000
8000
Threshold (dB HL)
0
20
40
60
80
100
120
Age: 0-1
Age: 2-3
Age: 4-5

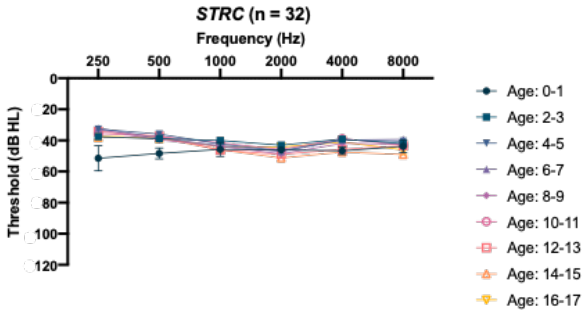
STRC (n = 32)
Frequency (Hz)
250
500
1000
2000
4000
8000
Threshold (dB HL)
0
20
40
60
80
100
120
Age: 0-1
Age: 2-3
Age: 4-5
Age: 6-7
Age: 8-9
Age: 10-11
Age: 12-13
Age: 14-15
Age: 16-17

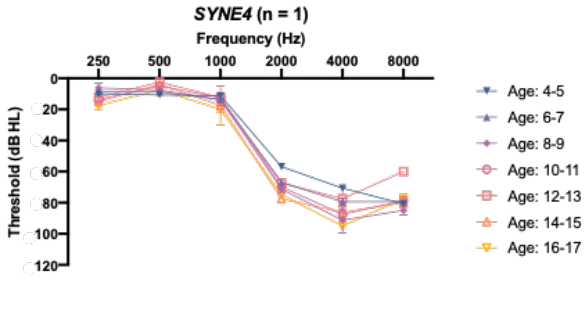
SYNE4 (n = 1)
Frequency (Hz)
250
500
1000
2000
4000
8000
Threshold (dB HL)
0
20
40
60
80
100
120
Age: 4-5
Age: 6-7
Age: 8-9
Age: 10-11
Age: 12-13
Age: 14-15
Age: 16-17

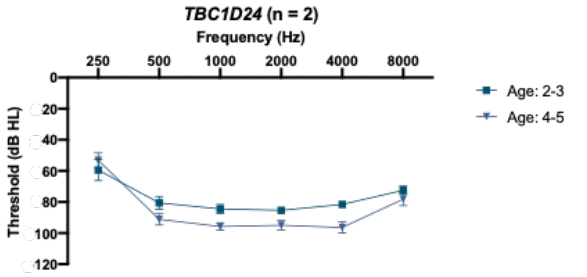
TBC1D24 (n = 2)
Frequency (Hz)
250
500
1000
2000
4000
8000
Threshold (dB HL)
0
20
40
60
80
100
120
Age: 2-3
Age: 4-5

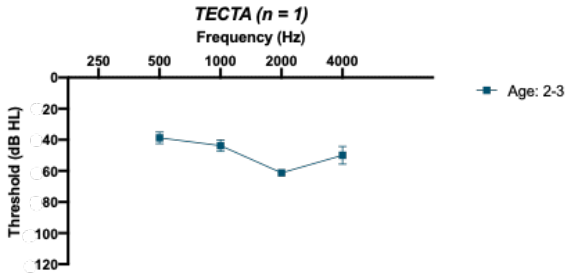
TECTA (n = 1)
Frequency (Hz)
250
500
1000
2000
4000
Threshold (dB HL)
0
20
40
60
80
100
120
Age: 2-3

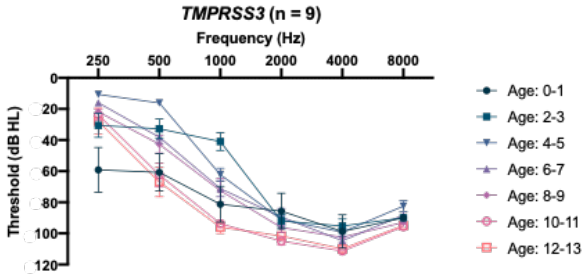
TMPRSS3 (n = 9)
Frequency (Hz)
250
500
1000
2000
4000
8000
Threshold (dB HL)
0
20
40
60
80
100
120
Age: 0-1
Age: 2-3
Age: 4-5
Age: 6-7
Age: 8-9
Age: 10-11
Age: 12-13

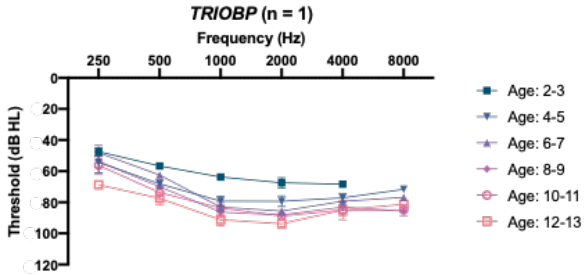
TRIOBP (n = 1)
Frequency (Hz)
250
500
1000
2000
4000
8000
Threshold (dB HL)
0
20
40
60
80
100
120
Age: 2-3
Age: 4-5
Age: 6-7
Age: 8-9
Age: 10-11
Age: 12-13

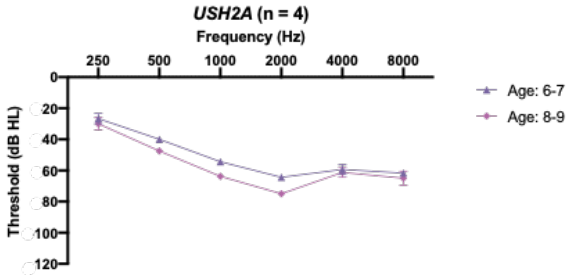
USH2A (n = 4)
Frequency (Hz)
250
500
1000
2000
4000
8000
Threshold (dB HL)
0
20
40
60
80
100
120
Age: 6-7
Age: 8-9

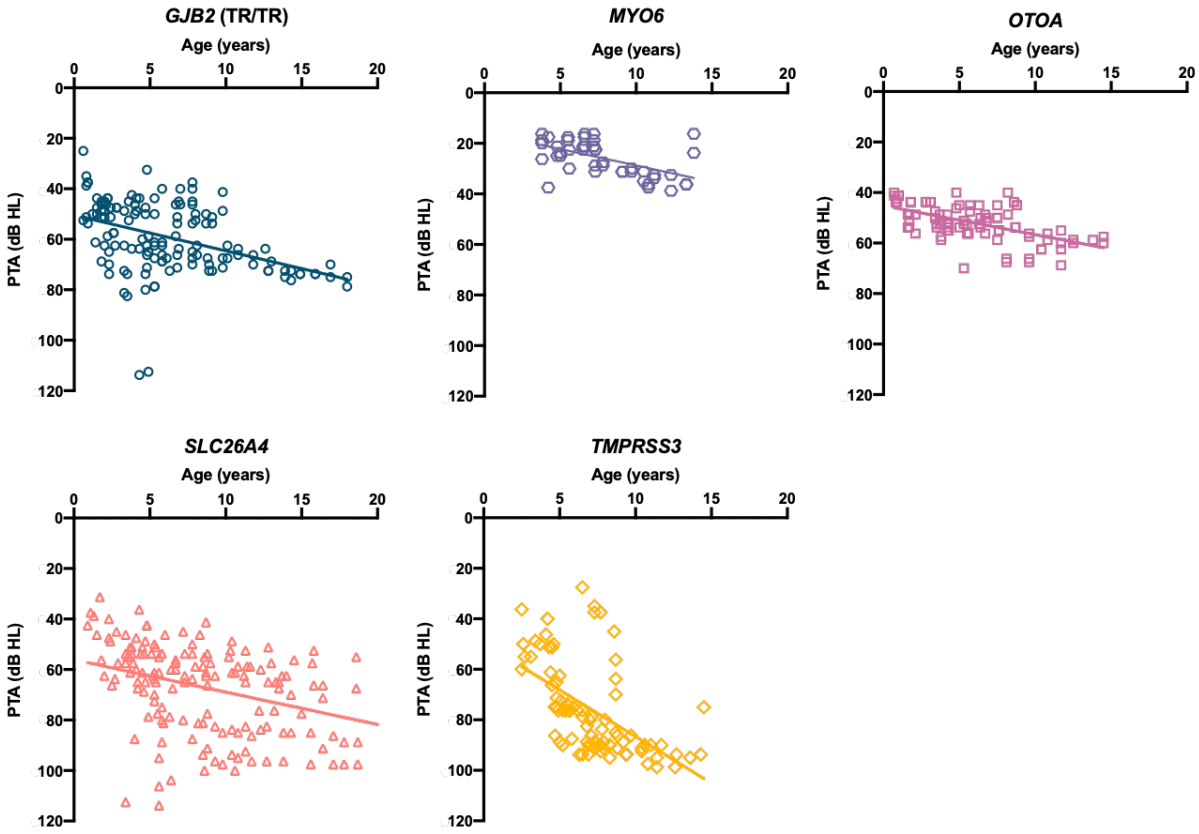

Figure 2.6: Progression of hearing loss by causative gene
Pure tone averages (PTA) across 500, 1000, 2000, 4000Hz are plotted by age at test. Only ears that never received cochlear implants are included. Significant progression in hearing loss was observed for individuals with mutations in *GJB2* (truncating mutations, TR), *OTOA*, *SLC26A4*, *TMPRSS3*, and *MYO6* (see Table 2.3).

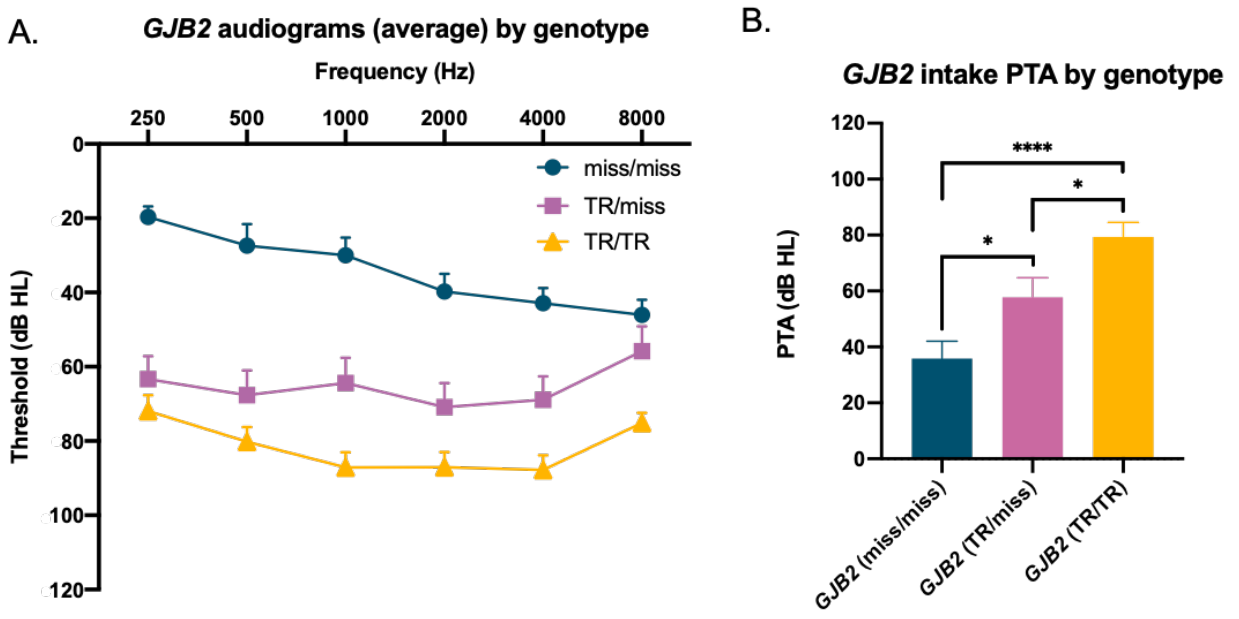

Figure 2.7: Hearing loss severity by type of mutation in *GJB2*
A. Average audiograms for individuals with two frameshift or nonsense (truncating, TR) mutations, one truncating and one missense mutation, or two missense mutations. Error bars depict SEM.
B. Four-tone PTA (500, 1000, 2000, 4000Hz) for individuals at first audiogram, separated by *GJB2* genotype. Error bars depict SEM.

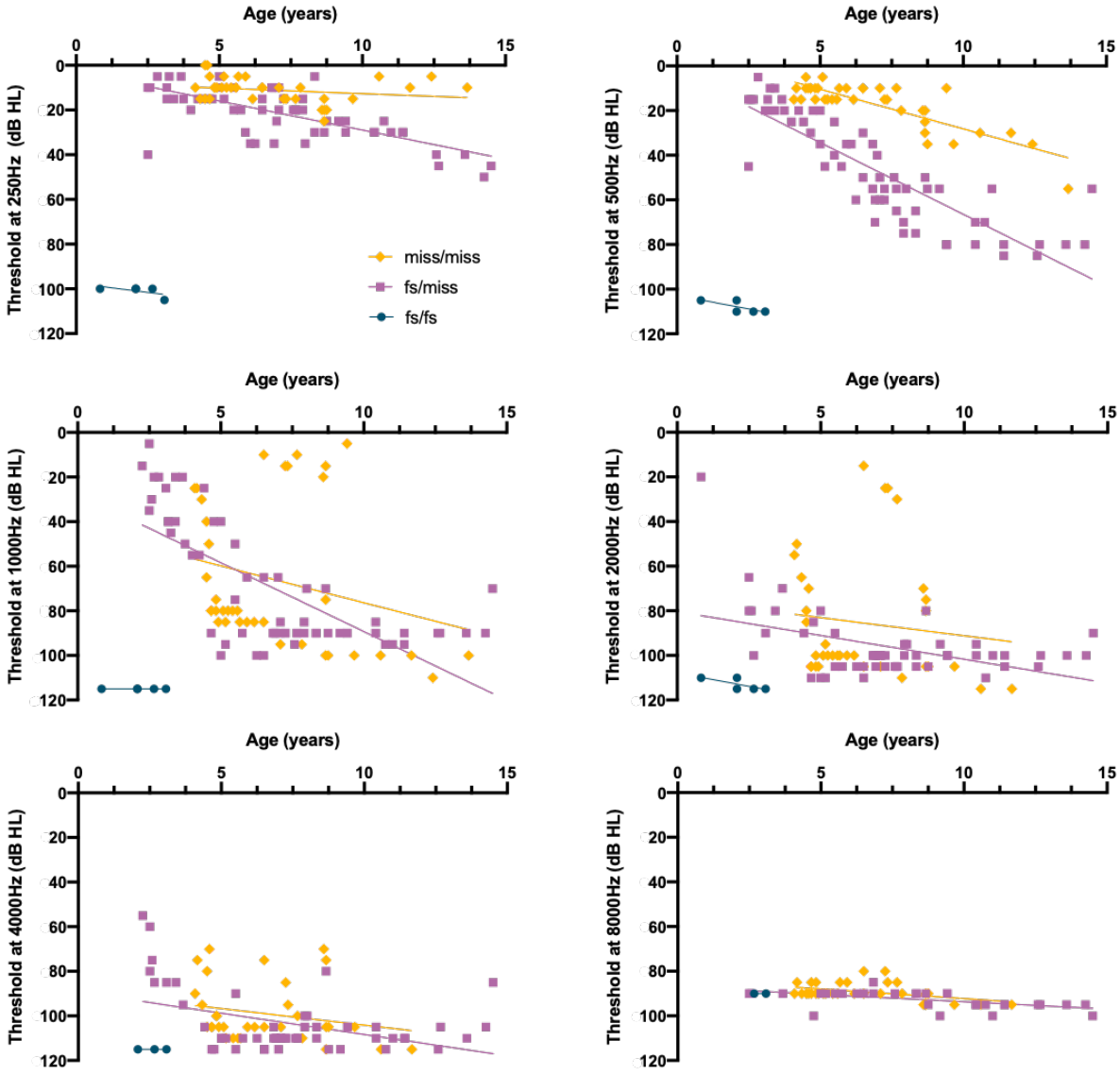

Figure 2.8: Progression of hearing loss by type of mutation in *TMPRSS3*
For fs/miss and miss/miss genotypes, only ears that never received cochlear implants are included. The fs/fs individuals received bilateral implantations at a young age and are included for comparison to other genotypes. The rate of progression (slope) was significantly different for fs/miss versus miss/miss genotypes at 250 and 500Hz (see Tables 2.4 and 2.5).

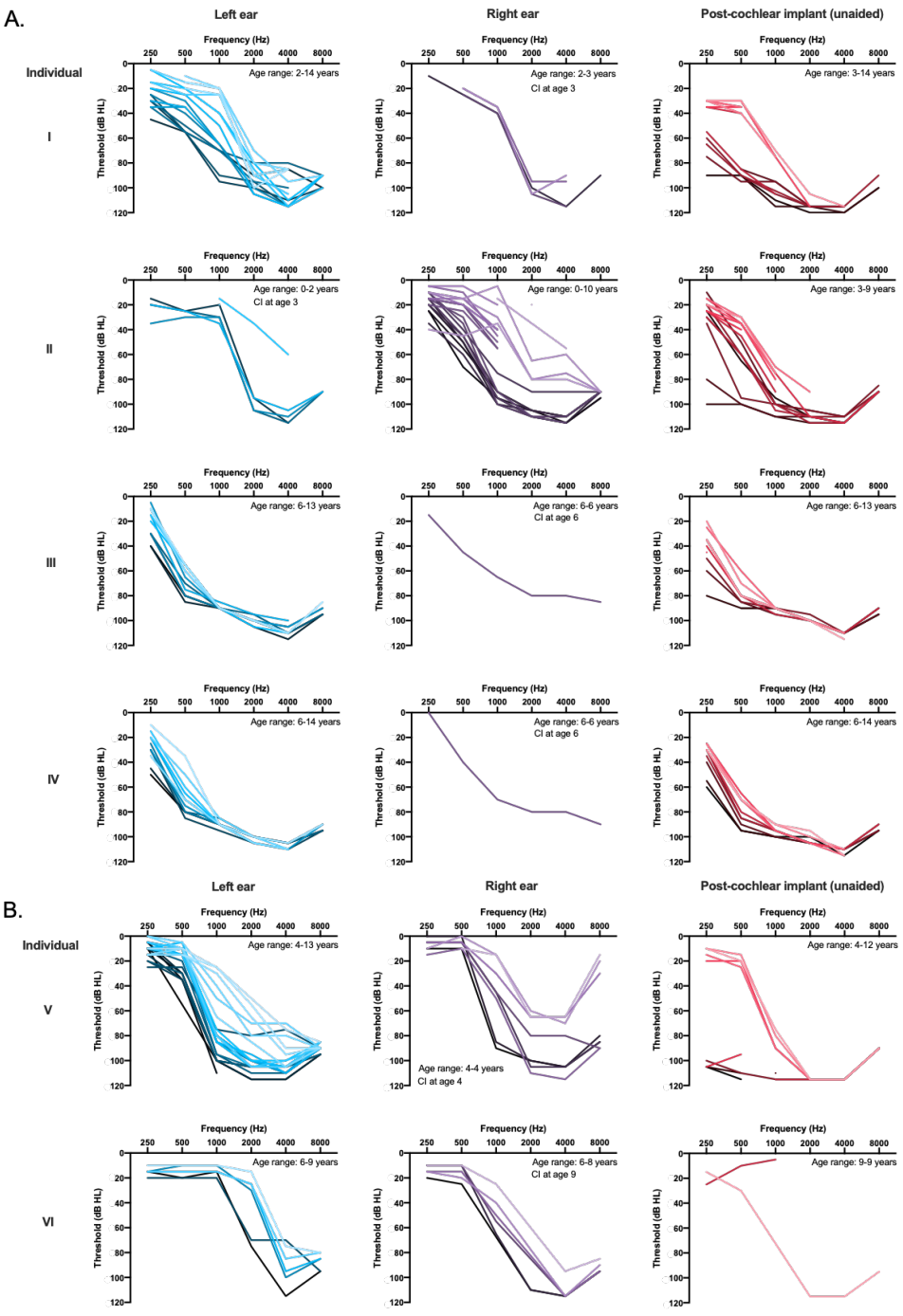

Figure 2.9: Progression of hearing loss in individuals with *TMPRSS3* mutations
A. For individuals with fs/miss genotypes, audiograms are plotted as overlaid traces, with colors darkening with age at test. Color grading is dependent on sequential order of test, but is not scaled by the age of the patient at each test point. From left to right, plots depict testing of each individual's left ear > right ear > and post-cochlear implant (unaided). Rows represent different individuals.
B. Similar plots showing audiogram traces for individuals with *TMPRSS3* miss/miss genotypes.

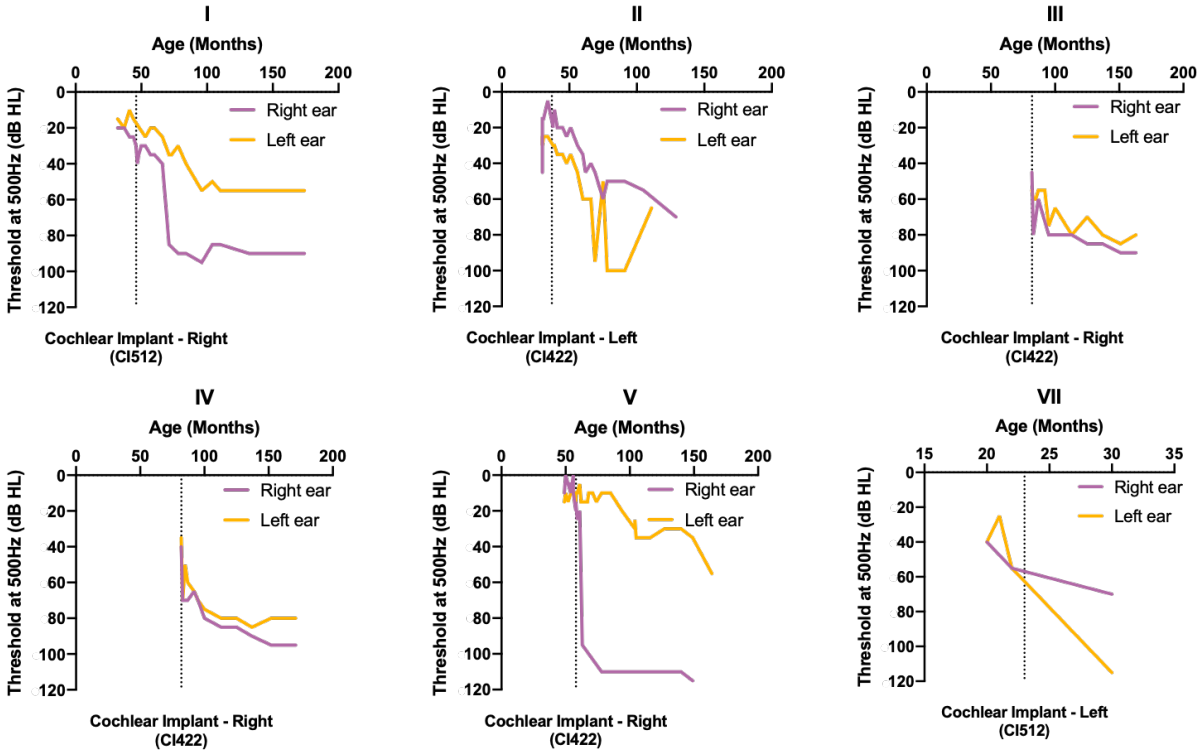

Figure 2.10: Change in hearing level in *TMPRSS3* participants following cochlear implantation Thresholds at 500Hz are depicted over time. Each plot represents one individual (numeral above plot) with both ears plotted. Vertical lines indicate time of implantation. Individuals V and VII have miss/miss genotype, all others are fs/miss.

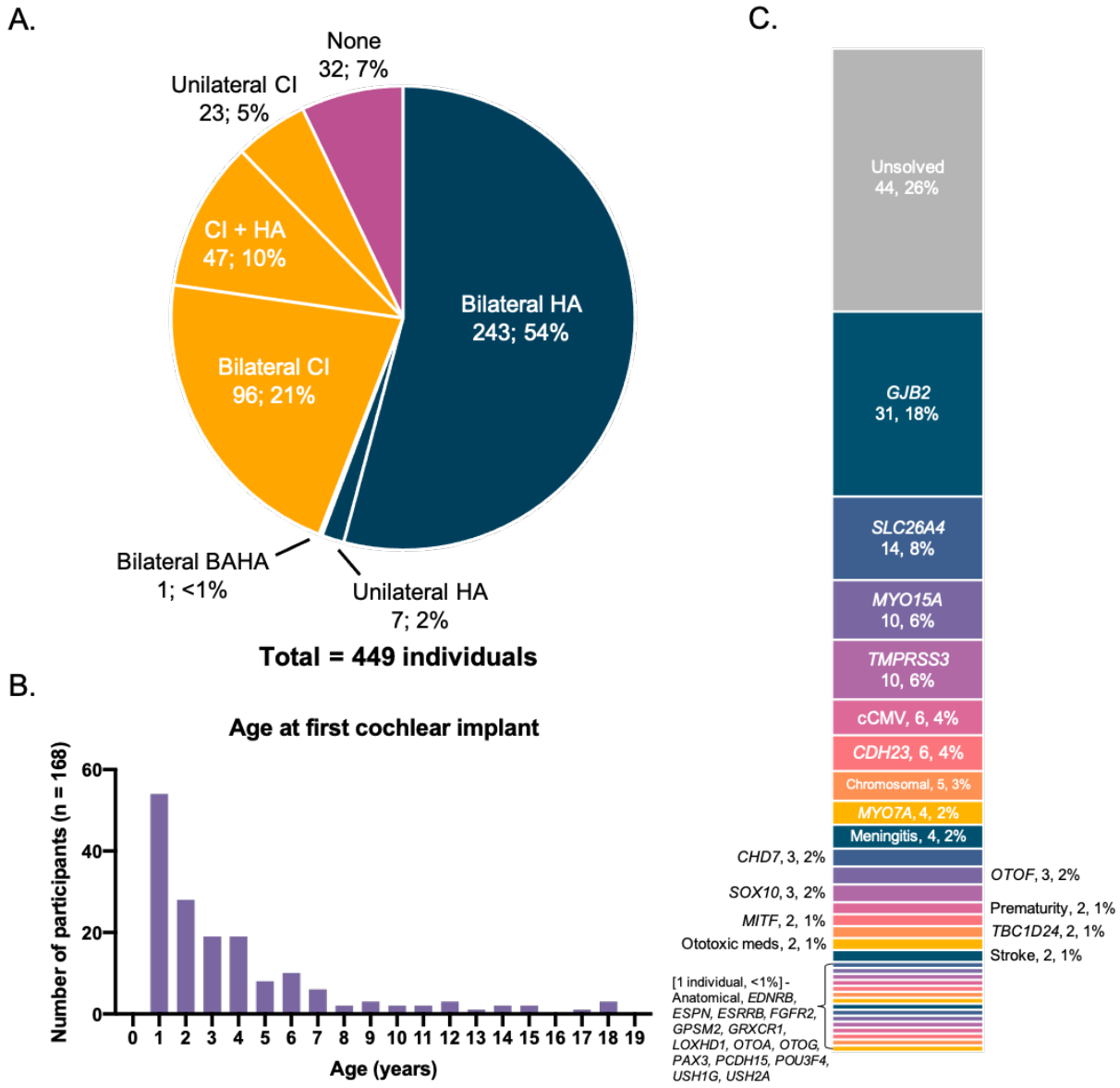

Figure 2.11: Implantation metrics
A. Hearing devices of study participants.
B. Age at first cochlear implant.
C. Causes of hearing loss among study participants with cochlear implants.

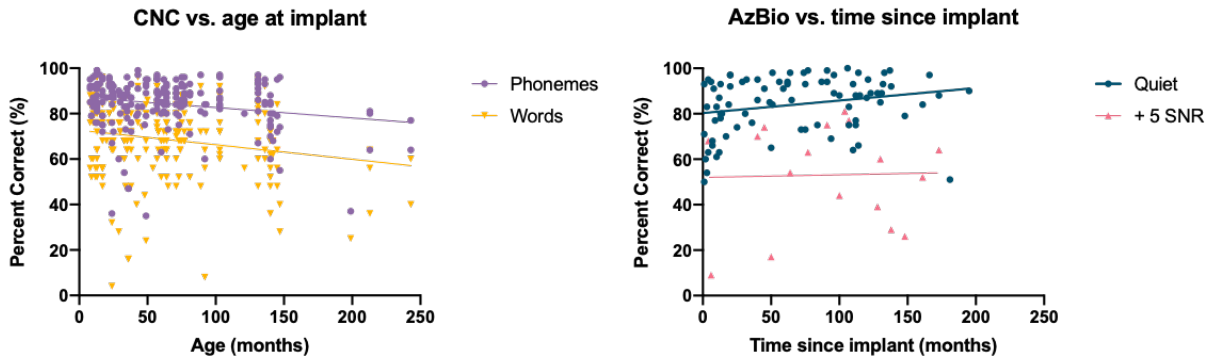

Figure 2.12: Examples of post-implant speech perception vs. age at cochlear implant and time since implant
A. Correlation of CNC scores and age at implant.
B. Correlation of AzBio scores and time since implant.

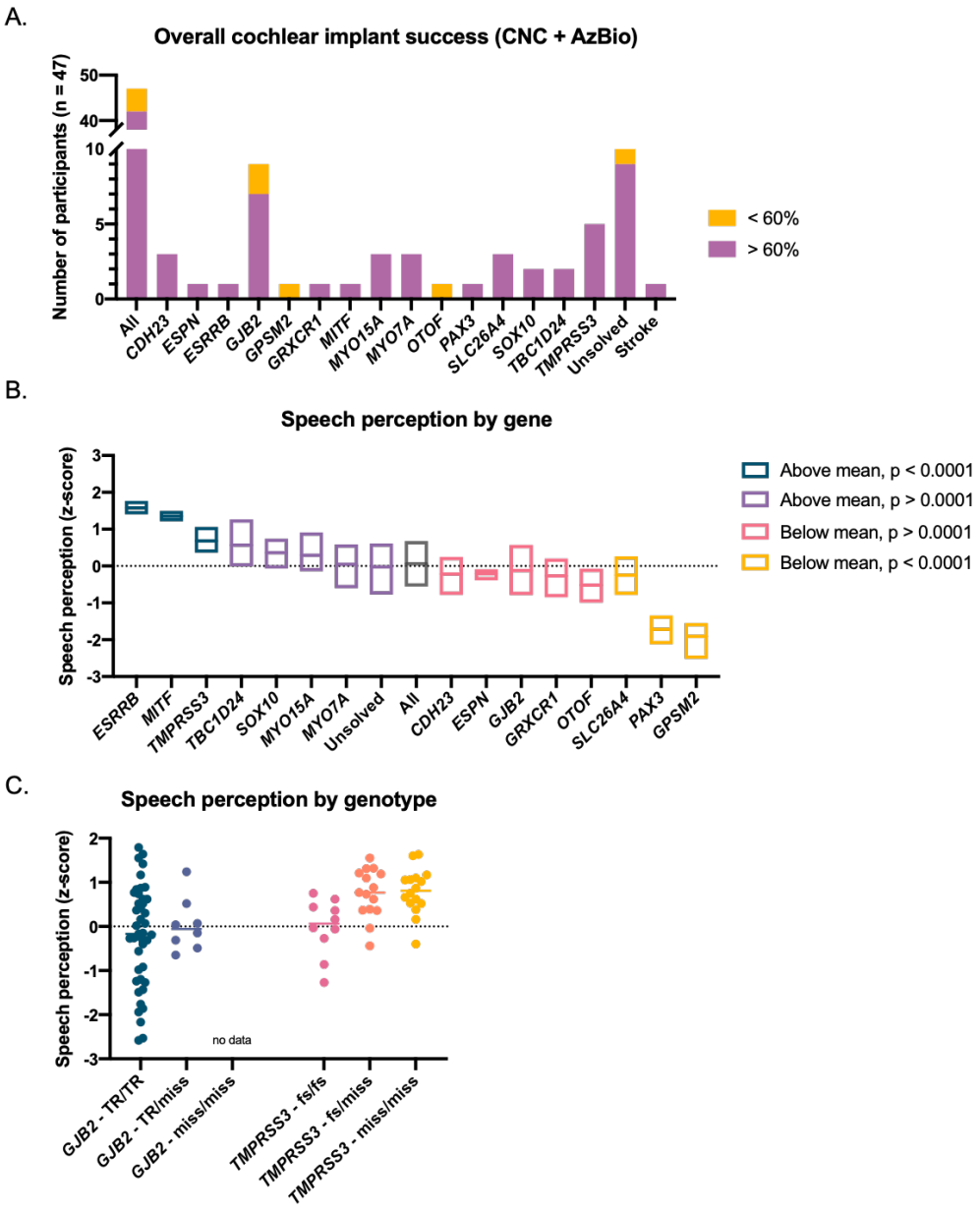

Figure 2.13: Differences in speech perception by gene and genotype
A. Proportion of participants achieving a maximum score >60% on either AzBio (Quiet) or CNC (Phonemes) test.
B. Differences in speech perception by gene. Scores for each test (HINT-C, Pediatric AzBio, AzBio, PBK, and CNC) were converted to z-scores by comparison to the mean for that test, and each participant's best score for each test was included. Horizontal lines in box plots represent 25%, 50%, and 75% percentiles. After adjusting for age at implantation and time between implantation and testing, scores for participants with mutations in *ESRRB*, *MITF*, or *TMPRSS3* were significantly higher than average ($P < 0.0001$) and for participants with mutations in *GPSM2*, *PAX3*, and *SLC26A4* were lower than average ($P < 0.001$) (Table 2.8).
C. Speech perception by genotype of *GJB2* and *TMPRSS3*. No significant differences were observed. TR denotes truncating mutations.

2.7 – TABLES

Table 2.1: Demographic information

Characteristic	Number	Percent
Total individuals in study	449	
Total families	407	
Seattle Children's Hospital	359	88.2
University of Washington	48	11.8
Sex		
Male	219	48.8
Female	229	51.0
Non-binary	1	0.2
Primary language		
English	361	80.4
American sign language (ASL)	34	7.6
Signed-exact English (SEE)	6	1.3
Spanish	28	6.2
Mandarin	6	1.3
Somali	3	0.7
Telugu	2	0.4
Cantonese	1	0.2
French	1	0.2
Korean	1	0.2
Punjabi	1	0.2
Swahili	1	0.2
Ukrainian	1	0.2
Family History		
Parent or sibling with hearing loss	122	30.0
Multiple affected siblings in study	38	9.3

Table 2.2: Previous clinical workup

Type of testing	Number	Percent	Number solved	Percent solved
Newborn hearing screen				
Total who received screening	347			
Pass in both ears	115	33.1		
Refer in one ear only	17	4.9		
Refer in both ears	214	61.7		
Imaging (CT/MRI)				
Total who received imaging	227			
Enlarged vestibular aqueduct	35	15.4		
Mondini deformity	14	6.2		
Incomplete partition	8	3.5		
Other	26	11.5		
Previous genetic testing				
GJB2	86	19.2	23	26.7
Other single gene test	21	4.7	12	57.1
OtoSCOPE	49	10.9	35	71.4
Other hearing loss gene panel	7	1.6	3	42.9
Whole exome sequencing	8	1.8	6	75
SNP microarray	25	5.6	5	20
Genetic diagnosis				
Previously diagnosed	85	18.9		
New diagnosis from this study	183	40.8		
CMV neonatal blood spot PCR				
Total tested	201			
Positive	11	5.4		
Negative	190	94.6		

Table 2.3: Change in hearing thresholds per year for children with mutations in progressive hearing loss genes

(PTA: Pure tone average of thresholds at 500, 1000, 2000, 4000 Hz)

Gene	ΔPTA (dB/year)	p-value
CHD7	-5.018	0.2009
DMXL2	-0.693	0.2248
GJB2	-0.517	0.0620
GJB2 – TR/TR	**1.407**	**<0.0001**
GJB2 – TR/miss	-0.457	0.0778
GJB2 – miss/miss	-0.502	0.3745
LOXHD1	-1.026	0.2229
MYO15A	0.254	0.6572
MYO6	**1.297**	**<0.0001**
MYO7A	0.180	0.7447
OTOA	**1.147**	**<0.0001**
OTOG	-1.100	0.0894
SLC26A4	**1.861**	**<0.0001**
SOX10	0.565	0.5569
STRC	0.186	0.1017
TMPRSS3	**3.691**	**<0.0001**

Table 2.4: *TMPRSS3* hearing thresholds over time

Genotype	Frequency (Hz)	Linear regression		
		Slope (dB/year)	R2	p-value
fs/fs	250	0.1350	0.3780	0.2698
	500	0.2001	0.5536	0.1493
	1000	n/a	n/a	n/a
	2000	0.2001	0.5536	0.1493
	4000	n/a	n/a	n/a
	8000	n/a	n/a	n/a
fs/miss	250	2.598	0.4939	**<0.0001**
	500	6.434	0.7339	**<0.0001**
	1000	6.170	0.5014	**<0.0001**
	2000	2.135	0.2107	**0.0005**
	4000	1.912	0.1838	**0.0014**
	8000	0.654	0.3529	**0.0002**
miss/miss	250	0.492	0.0477	0.2077
	500	3.547	0.6925	**<0.0001**
	1000	3.311	0.0611	0.1402
	2000	1.624	0.0134	0.5153
	4000	1.486	0.0491	0.2153
	8000	0.862	0.1923	**0.0107**

Table 2.5: Comparison of progression of hearing loss at each frequency for children with fs/miss vs miss/miss mutations in *TMPRSS3*

Frequency (Hz)	p-value
250	**0.0006**
500	**0.0006**
1000	0.1519
2000	0.7979
4000	0.7385
8000	0.5400

Table 2.6: Types of cochlear implants

Item	Number	Percent
Total implanted individuals	168	37.5
Total number of cochlear implants	270	
Brand/Model		
Advanced Bionics		
90K	1	0.37
90K Advantage	1	0.37
90K Mid Scala	12	4.44
90K Helix	2	0.74
HiRes 90k 1j	8	2.96
HiRes Ultra	5	1.85
Cochlear		
CI24M	1	0.37
CI24RCS	2	0.74
CI24RE (CA)	78	28.89
CI422	9	3.33
CI512	39	14.44
CI512 (CA)	10	3.70
CI522	5	1.85
CI532	1	0.37
CI612	64	23.70
CI622	10	3.70
Med El		
Combi40	1	0.37
Concert	3	1.11
Pulsar	1	0.37
Sonata	1	0.37
Synchrony	4	1.48
Synchrony Flex 28	4	1.48
Synchrony Form24	2	0.74

Table 2.7: Multiple regression of non-genetic factors on cochlear implant performance

Test	Condition	Age at implant (months)			Time since implant (months)			Active electrodes (%)		
		Slope	R^2	p-value	Slope	R^2	p-value	Slope	R^2	p-value
HINT-C	Quiet	0.037	0.005	0.5084	**-0.157**	**0.138**	**0.0002**	0.111	0.005	0.6684
	+5 SNR	0.054	0.012	0.5767	0.072	0.021	0.4614	-0.398	0.008	0.7886
Pediatric	Quiet	**-0.194**	**0.338**	**0.0005**	0.046	0.019	0.4576	-0.376	0.016	0.5481
AzBio	+5 SNR	**0.600**	**0.580**	**0.0104**	**-0.231**	**0.799**	**0.0005**	-2.999	0.539	0.0603
AzBio	Quiet	-0.047	0.045	0.0540	**0.055**	**0.054**	**0.0338**	0.607	0.100	0.0566
	+5 SNR	-0.042	0.011	0.6868	0.012	0.001	0.9177	0.855	0.046	0.4821
PBK	Phonemes	-0.027	0.004	0.3463	0.025	0.006	0.2344	0.025	0.001	0.8201
	Words	-0.033	0.002	0.4568	-0.002	1e-5	0.9615	-0.006	1e-9	0.9781
CNC	Phonemes	**-0.046**	**0.041**	**0.0026**	0.028	0.013	0.0963	0.983	0.053	0.0559
	Words	**-0.064**	**0.036**	**0.0047**	0.040	0.011	0.1152	1.404	0.044	0.0809
z-score	Combined	**-0.003**	**0.015**	**<0.0001**	0.001	0.002	0.1749	1e-4	2e-6	0.9791

Table 2.8: Effect of causal gene on speech perception post-implant, adjusted for age at implant, months between implant and test, and individual (-: not applicable; ns: not significant)

Effect	Number of children	Number of tests	Mean z-score	p-value
Age at CI	-	-	-	<0.0001
Months since CI	-	-	-	ns
CDH23	3	16	-0.26	ns
ESPN	1	3	-0.27	ns
ESRRB	1	3	1.59	<0.0001
GJB2	11	51	0.17	ns
GPSM2	1	5	-1.81	<0.0001
GRXCR1	1	5	-0.06	ns
MITF	1	2	1.36	<0.0001
MYO15A	5	18	0.27	ns
MYO7A	3	12	0.11	ns
OTOF	1	7	-0.53	0.015
PAX3	1	3	-1.75	<0.0001
SLC26A4	7	30	-0.28	<0.0001
SOX10	2	11	0.59	ns
TBC1D24	2	7	0.66	ns
TMPRSS3	9	41	0.40	<0.0001
Subject ID	-	-	-	<0.0001

CHAPTER 3. Genetic heterogeneity and core clinical features of *NOG*-related-symphalangism spectrum disorder

Note: This chapter is based on the following published paper.

Carlson, R.J., Quesnel, A., Wells, D., Brownstein, Z., Gilony, D., Gulsuner, S., Avraham, K. B., King, M. C., Walsh, T., Rubinstein, J. Genetic heterogeneity and core clinical features of *NOG*-related-symphalangism spectrum disorder. *Otol. Neurotol*. **42**, e1143-51 (2021)

3.1 - ABSTRACT

Objectives: To better distinguish *NOG*-related-symphalangism spectrum disorder (*NOG*-SSD) from chromosomal 17q22 microdeletion syndromes and to inform surgical considerations in stapes surgery for patients with *NOG*-SSD.

Background: Mutations in *NOG* cause a variety of skeletal syndromes that often include conductive hearing loss. Several microdeletions of chromosome 17q22 lead to severe syndromes with clinical characteristics that overlap *NOG*-SSD. Isolated deletion of *NOG* has not been described, and therefore the contribution of *NOG* deletion in these syndromes is unknown.

Methods: Two families with autosomal dominant *NOG*-SSD exhibited stapes ankylosis, facial dysmorphisms, and skeletal and joint anomalies. In each family, *NOG* was evaluated by genomic sequencing and candidate mutations confirmed as damaging by *in vitro* assays. Temporal bone histology of a patient with *NOG*-SSD was compared to temporal bones of 40 patients diagnosed with otosclerosis.

Results: Family 1 harbors a 555kb chromosomal deletion encompassing only *NOG* and *ANKFN1*. Family 2 harbors a missense mutation in *NOG* leading to absence of noggin protein. The incus-footplate distance of the temporal bone was significantly longer in a patient with *NOG*-SSD than in patients with otosclerosis.

Conclusion: The chromosomal microdeletion of family 1 led to a phenotype comparable to that due to a *NOG* point mutation and much milder than the phenotypes due to other chromosome 17q22 microdeletions. Severe clinical findings in other microdeletion cases are likely due to deletion of genes other than *NOG.* Based on temporal bone findings, we recommend that surgeons obtain longer stapes prosthetics prior to stapes surgery in individuals with *NOG*-SSD stapes ankylosis.

3.2 - INTRODUCTION

Noggin is a secreted regulator of bone morphogenic proteins that is vital for the development of limb bones and joints of all vertebrates. Mutations in the noggin-encoding gene *NOG* are associated with multiple autosomal dominant syndromes including proximal symphalangism (SYM1, OMIM 185800)[55], stapes ankylosis with broad thumbs and toes (SABTT, OMIM 184460)[56,57], multiple synostoses syndrome (SYNS1, OMIM 186500)[55], tarsal-carpal coalition syndrome (TCC, OMIM 186570)[58,59], and brachydactyly type B2 (BDB2, OMIM 611377)[60]. Shared signs of these disorders include conductive hearing loss, hyperopia, and digital anomalies. The overlapping features of these syndromes, and their variable expression even within families, has led to their grouping under the term *NOG*-related-symphalangism spectrum disorder *(NOG*-SSD)[61].

In our studies of families with inherited hearing loss, we discovered two novel mutations leading to *NOG*-SSD. In family 1, an Israeli kindred with a mild form of *NOG*-SSD, affected relatives are heterozygous for a 555kB microdeletion including only *NOG* and *ANKFN1,* the smallest 17q22 microdeletion described to date[62–68]. Examination of the clinical features of family 1 compared to other microdeletion cases could suggest which symptoms of *NOG*-SSD can be attributed to deletion of *NOG* versus other genes. In family 2, a child diagnosed with multiple synostoses syndrome (SYNS1) is heterozygous for *NOG* c.41T>C, p.L14P. Surgical reports from the two families together with previous literature suggest that exceptionally long stapes prostheses may be required during stapedectomy surgery for individuals with *NOG*-SSD. To test this possibility, we compared the incus-footplate distance in a temporal bone from an individual with *NOG*-SSD to this distance in 40 temporal bones with a diagnosis of otosclerosis.

3.3 - MATERIALS AND METHODS

The project was approved by the human subjects' committees of Seattle Children's Hospital and the University of Washington (IRB# STUDY00001526) and of Tel Aviv University, and by the Israel National Helsinki Committee. Written informed consent was obtained from adults and assent from children. All included pictures are shared with permission from the families.

Genomic analyses. DNA was extracted from whole blood. For sequencing using our deafness gene panel[5], protein-coding genes and microRNAs related to hearing loss were captured using the SureSelect Target Enrichment system (Agilent). Molecular barcodes were assigned and the samples were multiplexed and sequenced in a single flow-cell of the HiSeq 2500 (Illumina) with 100bp paired-end reads. Whole exome sequencing, alignment, and interpretation of variants were performed as previously described[69]. Rare CNVs in exome data were identified by Conifer 0.11. Once the *NOG* microdeletion was found, all relatives in the family were genotyped using Taqman probes (*NOG*: Hs0059770, *ANKFN1*: Hs05501071; Thermo) for qPCR run on an ABI 7900HT Sequence Detection System (AB Biosciences)[16]. Whole genome sequencing was completed through MedGenome (Foster City CA). Sequencing reads were aligned to hg19 with BWA-MEM (0.7.12-r1039), split-reads and discordant-reads extracted using SAMBLASTER (0.1.22) and BAM files sorted and indexed using Sambamba (0.6.7). Breakpoints of the genomic deletion were identified by using read-depth, split-reads and discordant-reads from BAM files using IGV (2.8.0).

Functional analyses. Plasmid pCMV6-XL5 containing the human *NOG* open reading frame (Origene) was mutagenized using the Q5 site-directed mutagenesis kit (NEB) to create plasmids containing *NOG* missense mutations. Sequences were verified by Sanger sequencing. HEK 293T cells were transfected with each plasmid, or empty pCMV6 as control, using the Lipofectamine 2000 transfection kit (Invitrogen). Cells were plated in phenol red-free DMEM with reduced FBS

(0.2%). After 48 hours, cells and media were collected separately. Cells were lysed and protein and mRNA were extracted. Media was concentrated 20x using Vivaspin 20 centrifugal concentrators (GE). Protein concentrations of lysate and media fractions were determined by Pierce BCA assay (Thermo). Identical quantities of protein for each sample were analyzed by western blot using a rabbit polyclonal anti-Noggin antibody (Abcam, ab16054). Lysate samples were normalized to a mouse monoclonal anti-actin antibody (Sigma, A2228). RT-qPCR of *NOG* was performed as described above to measure transcript levels and compare between conditions. For lactacystin experiments, 10μM of lactacystin (Sigma) in fresh media was added 10 hours prior to cell harvest.

Phenotypic analyses. The incus-stapes footplate distance was measured in human temporal bone specimens collected as part of the NIDCD National Human Temporal Bone Pathology Resource Registry and processed at the Massachusetts Eye and Ear Otopathology Laboratory. Temporal bones were prepared for histologic analysis via standard techniques including fixation in formalin, decalcification in EDTA, dehydration in alcohols, and embedment in celloidin. Specimens were sectioned into 20 μm thick slices horizontally relative to the lateral semicircular canal. Every tenth section was stained with hematoxylin and eosin and mounted on a glass slide. From each case, the most inferior slide that included the stapes footplate was selected. The incus-stapes footplate distance was measured between the medial surface of the distal long process of the incus and the stapes footplate, with the measurement line being perpendicular to the footplate. All measurements were performed using ImageJ software[70]. As otosclerosis is by far the most common reason for stapedectomy surgery, temporal bones from 40 patients with otosclerosis were used as controls. These measurements were used to establish normative data for the incus-stapes footplate distance and to compare to the temporal bone measurement from the case of genetically confirmed *NOG*-SSD. The R Commander package of R was used for statistical analysis[71].

3.4 - RESULTS

Clinical Presentation

For both families, pedigrees are shown in Figure 1 and clinical features in Table 3.1. In family 1 (Fig. 3.1A), affected individuals exhibited congenital conductive hearing loss and hyperopia (Fig. 3.2A). For individuals II-2, II-4, II-5 and III-6, stapes ankylosis was confirmed and repaired surgically. Dysmorphic facial and skeletal features varied among family members (Fig. 3.3A; Table 3.1). None of the individuals in family 1 demonstrated vertebral or lower limb skeletal abnormalities, urogenital malformations, intellectual disability, or attention-deficit hyperactivity disorder.

The proband of family 2 (Fig. 3.1B, III-1) was diagnosed with moderate to severe bilateral conductive hearing loss at age 2.5y and was fitted with bilateral hearing aids at age 3y. The hearing loss progressed (Fig. 3.2B) and he underwent bilateral laser stapedotomies with consequent improvements in his hearing. He also has hyperopia (+8 in both eyes) and has worn eyeglasses since age 2.5y. Strabismus is present and corrected by eyeglasses. His facial features are similar to those of family 1 (Fig 3B; Table 3.1). He has slightly broadened thumbs bilaterally with a decreased range of flexion. He also has limitation of his neck motion due to C2-C3 vertebral fusion (Fig. 3.3B). He has no other joint restriction or laxity, body asymmetry, scoliosis, joint dislocation, or intellectual disability. The proband's mother (II-4) reports unilateral conductive hearing loss. She also has hyperopia, bilateral broad thumbs, fusion of bones within her great toes, stiff hip joints, and is unable to flex her wrists. Her two adult sisters (II-5 and II-6) and parents (I-3 and I-4) have no symptoms of *NOG*-SSD.

Genetics of *NOG*-SSD

Family 1 relatives II-2, II-5, and III-6 had no mutations in any gene on the custom panel but shared a deletion at chromosome 17q22 detectable in whole exome sequence using our CNV analysis

pipeline[72]. This deletion included both *NOG* and *ANKFN1* and was confirmed by qPCR analysis to co-segregate perfectly with the phenotype in the family. Whole genome sequence of III-1 confirmed the breakpoints of the deletion as chr17:54,290,100-54,844,894 (GRCh37/hg19; SCV001448202.1).

For the proband of family 2, clinical suspicion for a diagnosis of SYNS1 led to gene-specific sequencing of *NOG* (Prevention Genetics, Marshfield, WI), yielding a single variant, *NOG* c.41T>C p.L14P at chr17:54,671,625 (GRCh37/hg19; NM_005450.6; SCV001451939). This mutation occurs at a residue (Fig. 3.1C) which is conserved as leucine in all vertebrates with high quality sequence (more than 100 species) with the exception of three bird species for which this residue is valine, and appears private to this family (not present on gnomAD). The variant was also present in the proband's affected mother (II-4) but not in his maternal grandfather or grandmother or maternal aunts (Fig. 3.1B), suggesting it occurred *de novo* in the mother.

Consequences of the mutations to protein secretion

We investigated the effects of the *NOG* p.L14P mutation on protein secretion using an *in vitro* secretion assay (Fig. 3.4A-B). *NOG* p.L14P resulted in complete absence of noggin from both cell lysates (mean 0.0 AU; $p<0.0001$) and supernatant (mean 0.0 AU; $p<0.0001$). Another *NOG* variant known to abolish noggin secretion, *NOG* p.P170L[73], was included in the assay as well. It also led to significantly reduced protein in lysate (mean 0.47 AU; $p<0.001$) and supernatant (mean 0.14 AU; $p<0.0001$), although in contrast to the previous report[73], some protein was still observed in the supernatant. *NOG* transcript levels were measured by RT-qPCR and confirmed to be high across all conditions (Fig. 3.4C).

To investigate the role of proteasomal degradation in the absence of cellular *NOG* p.L14P protein, the secretion assay was repeated with the addition of lactacystin, a proteasome inhibitor (Fig.

3.4D-E). In the presence of lactacystin, *NOG* p.L14P noggin appeared in the lysate fraction at detectable levels (mean 0.12 AU; $p<0.05$ compared to empty condition), but remained absent from the supernatant (mean 0.0 AU; $p<0.0001$ compared to *NOG* wild-type). *NOG* p.P170L protein was reduced compared to wild-type in both lysate (mean 0.26 AU; $p<0.01$) and supernatant (mean 0.08 AU; $p<0.001$) fractions in the presence of lactacystin.

Incus-stapes footplate distance

To evaluate the possibility of increased incus-stapes footplate distance as a feature of *NOG*-SSD, this measurement was compared in the temporal bone of a previously described *NOG*-SSD patient[74] versus 40 patients with otosclerosis (Fig. 3.5). In patients with otosclerosis, the mean incus-stapes footplate distance was 3.72mm with standard deviation $\pm$0.38mm (range 3.01mm-4.53mm). Distances were normally distributed among otosclerosis cases ($W=0.975$; $p=0.5$, Shapiro Wilk test; Fig. 3.5C). The incus-stapes footplate distance of the *NOG*-SSD case was 4.62mm, more than 2.4 standard deviations above the mean for the otosclerosis controls, indicating that the *NOG*-SSD case is an outlier with an extremely long incus-footplate distance.

Treatment outcomes

For family 1, surgical reports of stapedectomies of II-2 at age 23y and III-6 at age 21y indicated that long prostheses were required for II-2 (4.5mm at initial surgery, 5.0mm at revision surgery) and for III-6 (5.0mm).

The proband of family 2 underwent laser-assisted stapedotomy of his left ear at age 7y. During the procedure the ossicular chain demonstrated good mobility at the level of the malleus, and incus, but there was rigid stapes fixation at the level of the footplate. A 4.75mm piston was noted to be too short and therefore a 5.5mm re-shaped malleus attachment piston was used. Following the operation, the patient demonstrated markedly improved audiologic testing in the treated ear

(Fig. 3.2B). At age 8y, an identical surgery was performed on the proband's right ear. Once again, the length between the footplate and the incus was measured and it was noted that the 4.75 length piston would be far too short, and so a 5.5mm malleus piston prosthesis was used. Following placement, the prosthesis moved well but the malleus and/or incus were also noted to be fixed. The malleus/incus complex was partly mobilized by repeated pressure on the incus and malleus until mobility was improved but was unfortunately still not normal. Despite this finding, his post-operative audiogram showed notable improvement (Fig. 3.2B).

3.5 - DISCUSSION

Noggin acts as an antagonist of bone morphogenetic proteins (BMPs)[75,76]. BMPs are key regulators of skeletal development[77], responsible for recruiting mesenchymal cells into future skeletal anlagen, for promoting mesenchymal cell proliferation and differentiation into chondroblasts and osteoblasts, and for osteogenic transformation of stem cells[78–80]. The interaction between BMPs and noggin affects body patterning[76,77], apoptosis induction in digital and interdigital regions[81–83], and middle ear formation[81,84]. The role of noggin in mammalian skeletal development was confirmed by experiments in transgenic mice. *Nog*$^{-/-}$ mice do not survive past birth and display developmental abnormalities such as shorter bones, absence of multiple joints, and bony fusion of the appendicular skeleton[82,85]. These mice also display excess bone morphogenetic protein activity and cartilage formation[82].

More than 60 mutations of *NOG*, including both missense and nonsense mutations, have been associated with autosomal dominant *NOG*-SSD[61]. Most pathogenic *NOG* point mutations lead to reduced secretion and/or altered dimerization of noggin[86]. Other *NOG* mutations alter binding of noggin to BMPs and to differentiation factor 5 and are associated with BDB2[87]. Additionally, several microdeletions at chromosome 17q22 lead to phenotypes that include signs of *NOG*-SSD along with more severe developmental defects. The published deletions vary in size from 1.34Mb

to 8.18Mb and encompass between 5 and 60 genes[62–68]. While deletion of *NOG* is present in the majority of cases, several microdeletions do not include *NOG* while still leading to severe syndromes. Because isolated deletion of *NOG* has not previously been observed in humans, the disorders and clinical characteristics that are attributable specifically to its loss have not been definitively determined.

In family 1, the 555kb deletion includes only *NOG* and *ANKFN1* and is the smallest 17q22 deletion reported to date. It results in a mild phenotype of characteristic *NOG*-SSD features. Family 1 lacks the more severe features of other microdeletion cases, such as widespread skeletal dysmorphisms, urogenital malformations, and intellectual disability. The phenotypes of family 1 are similar to those resulting from point mutations of *NOG*, in particular those diagnosed with SABTT. The phenotypes of two published cases with *NOG* frameshift mutations leading to SABTT (*NOG* c.252insC p.E85fs*96 and c.304delG p.A102fs)[57,88,89] are particularly similar to family 1, as expected given the consequences of the mutations to protein function. In all of these cases, affected individuals exhibit bilateral conductive hearing loss, hyperopia, distinct facial features, and bilateral broad thumbs. In contrast, the phenotype of family 1 differs from cases of chromosome 17q22 microdeletions that exclude *NOG*[63,68]. Neither of these latter cases exhibited conductive hearing loss, and both presented with severe syndromic features in organ systems other than skeletal and joint development such as neurological abnormalities and intellectual disability. These other features are likely due to the involvement of other genes. These findings suggest that nearly isolated deletion of *NOG* results in a more typical *NOG*-SSD phenotype, while microdeletions excluding *NOG* cause more severe and different syndromes.

Missense mutation *NOG* p.L14P of family 2 is located in the N-terminal signal peptide of the protein, a domain required for endoplasmic reticulum targeting and secretion. This location suggested that *NOG* p.L14P would lead to intracellular entrapment of noggin, but it instead served

to eliminate the protein from the cell entirely. Transcriptional analysis confirmed high levels of message expression. Addition of the proteasome inhibitor lactacystin did lead to an increase in intracellular *NOG* p.L14P noggin, but not to match wild-type levels. Notably, the protein that was produced was still not secreted. It is likely that this mutation's effect is multifactorial, possibly leading to severe protein misfolding and/or to rapid degradation while also interfering with secretion. Regardless of the precise mechanism, *NOG* p.L14P decreases noggin secretion and consequently leads to the *NOG*-SSD phenotype.

The most common sign in *NOG*-SSD is conductive hearing loss related to congenital stapes fixation. This phenotype is of particular interest in otology, because *NOG* mutations represent one of the few established genetic causes for conductive hearing loss despite clear familial clustering of both conductive hearing loss and otosclerosis[90]. Increased risk of otosclerosis has been associated with variants in *COL1A1* and in several genes of the TGF-ß superfamily[91]. Otosclerosis loci (OTSC1-10) have been identified by linkage analysis but the critical genes are not yet known[92–101]. We hypothesize that critical mutations for conductive hearing loss will be hypomorphic alleles of genes in which loss of function variants cause severe skeletal phenotypes. Mutations in *NOG* are consistent with this prediction, as conductive hearing loss is one of the most common symptoms of *NOG*-SSD, and possibly the only feature in the mildest cases, despite the fact that *NOG* is heavily involved in skeletal and joint development.

Malleus and/or incus fixation, as was seen in the right ear of the proband of Family 2, has not previously been reported in individuals with *NOG*-SSD. Prior histopathologic analysis of stapes fixation in an individual with *NOG*-SSD identified ossified cartilage across the stapedovestibular joints within an otherwise normal middle ear[74]. This report specifically states that no malleus or incus fixation was visible in the individual's unoperated right ear. The possibility of malleus or incus fixation is an important surgical consideration for patients with *NOG*-SSD because the

approach differs: If ankylosis involves ossicles beyond the stapes, then an atticotomy should be considered in order to perform more extensive middle ear repair. In addition, mobility of the malleus/incus complex should be assessed intraoperatively prior to stapedotomy. Future reports of middle ear exploration in *NOG*-SSD patients will be necessary to determine the frequency of malleus or incus fixation.

Fixation of the stapes may be treated by complete or partial stapedectomy which involves removal of all or a portion of the stapes[102], or by stapedotomy which involves the use of a laser to make a small fenestra through the stapes footplate and removal of the stapes suprastructure only[103,104]. This is performed through the ear canal and the stapes is replaced with a prosthetic stapes piston. The length of the prosthetic must be fit properly for each individual, as a long prosthesis can lead to severe vertigo[105] and a short prosthesis may not adequately conduct sound[106,107]. The vast majority of patients fit the same length prosthesis (e.g. either 4.25mm if a conventional prosthesis is selected or 4.5mm if a shape memory alloy prosthesis is used)[108]. It is crucial that the appropriately sized prosthetic be available for use during the surgery, and information about which size(s) may be necessary is critical prior to the operation as many hospitals stock only the common sizes.

We re-examined the genetically confirmed *NOG*-SSD temporal bone mentioned above[74] in order to measure the incus-stapes footplate distance, comparing it to measurements from temporal bones of patients with otosclerosis. The footplate-incus distance is similar to the measurement that surgeons may take intraoperatively to estimate the appropriate prosthesis length. The incus-stapes footplate distance of the *NOG*-SSD case was 4.62mm, more than 2.4 standard deviations above the mean for specimens with otosclerosis and the largest distance out of the 41 measurements made. This distance likely would have required a 5.25mm incus attachment

prosthesis which may not be routinely available in the operating room, as unusual sizes are often not stocked or may not even be manufactured for some prosthesis designs.

Many individuals with *NOG*-SSD, including those described here, have undergone stapedectomy or stapedotomy with improvement of their symptoms[61,81,83,109,110]. Our analysis of the incus-footplate distance for previously published patients, as well as surgical reports from the families in this study, indicate increased incus-stapes footplate distance, and for most cases, need for an unusually long prosthetic. If an extra-long incus-attachment prosthesis cannot be obtained, an alternative solution is to adapt a malleus-attachment prosthesis (which is typically available in longer lengths) for use as an incus-attachment prosthesis. For the proband of family 2, the required 5.5mm prosthetic is longer than the largest size that is available commercially, and a modified malleus attachment prosthesis was successfully used. Further work will be necessary to determine whether an unusually long incus-footplate distance is specific to certain clinical subtypes within *NOG*-SSD or is shared by all patients with *NOG* mutations. Regardless, the need for long or custom prostheses is an important surgical consideration in the treatment of individuals with *NOG*-SSD.

3.6 – FIGURES

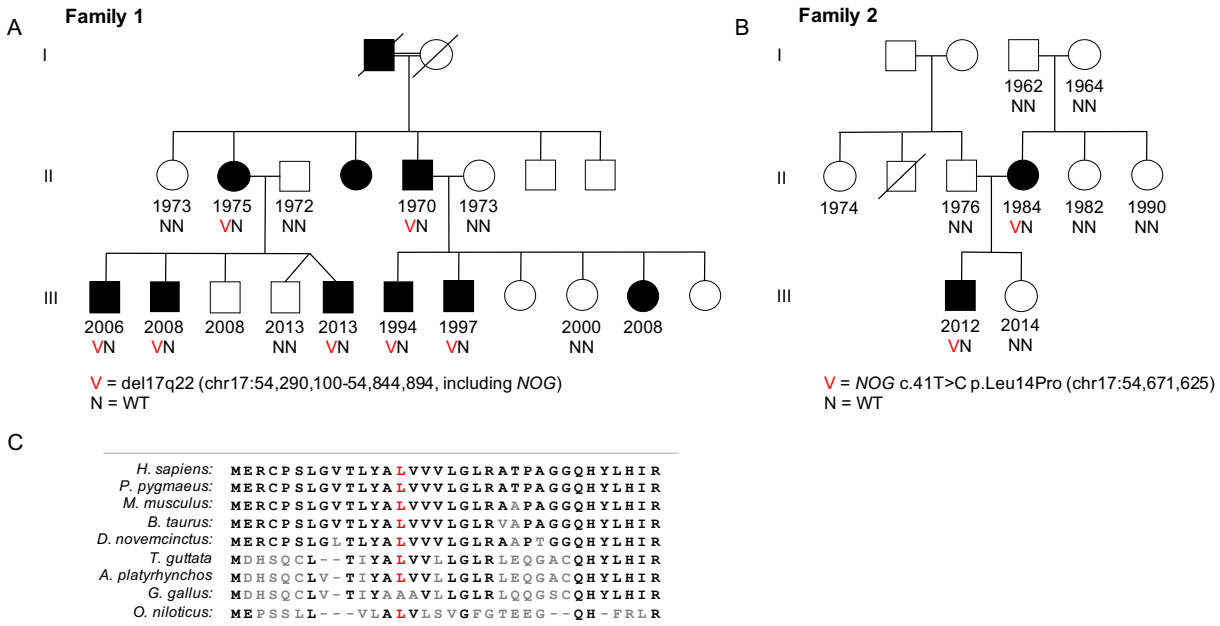

Figure 3.1: Two families with mutations of *NOG*

A. A 3-generation family with deletion of 555kb on chromosome 17q22 that includes *NOG*.

B. Mother and son with point mutation in *NOG*. The mutation is de novo in the affected mother. All affected individuals in both families have conductive hearing loss and hyperopia among other symptoms (Table 3.1).

C. Amino acid sequence at the N-terminus of noggin among selected species shows high conservation at the location of *NOG* p.L14P.

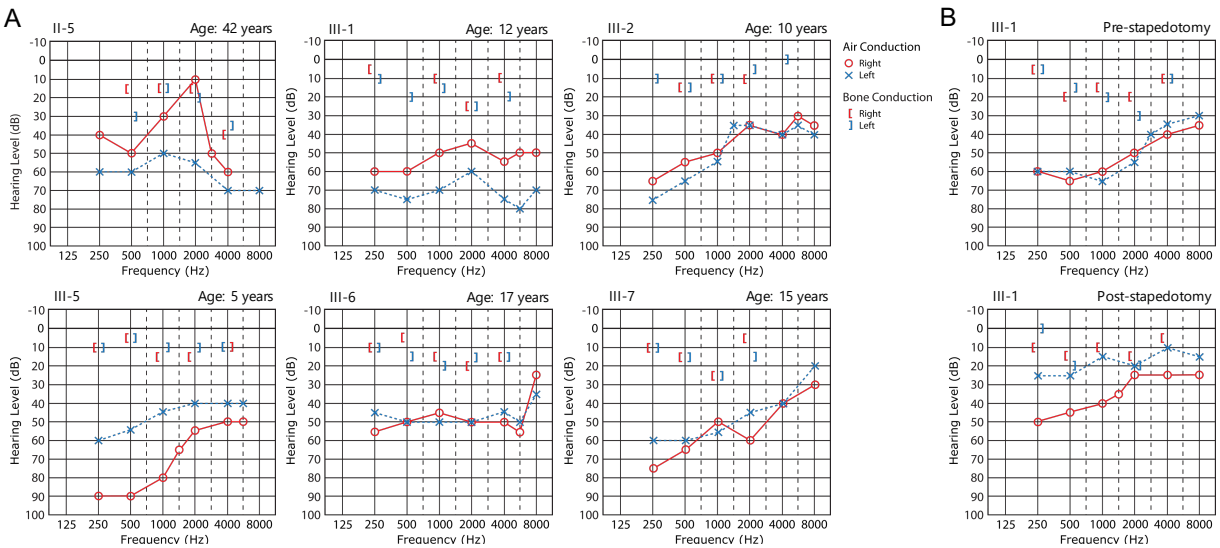

Figure 3.2: Conductive hearing loss in families 1 and 2

A. Audiograms from family 1 relatives aged 5 to 42 years. Individual II-5 was tested post right-sided stapedectomy.

B. Audiograms from family 2 proband III-1 before and after bilateral stapedotomy.

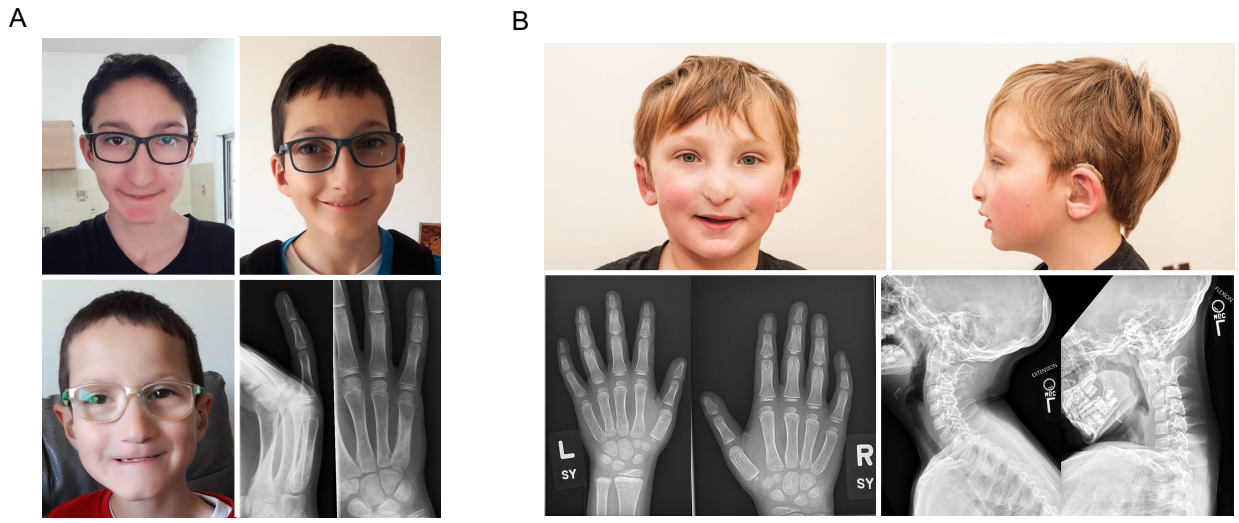

Figure 3.3: Characteristic facial and skeletal features of *NOG*-SSD in families 1 and 2

A. Facial features of family 1 relatives III-1 (top left), III-2 (top right), and III-5 (bottom left) showing characteristic signs of *NOG*-SSD. Radiographs (bottom right) of the right hand of individual III-5 show absence of digital abnormalities. The fracture that is present is the reason for the imaging but is unrelated to the syndrome.

B. Facial features of family 2 individual III-1 (top), and radiographs of his hands (bottom left) without digital abnormalities, and of his spine (bottom right) demonstrating fusion of his C2 and C3 vertebrae.

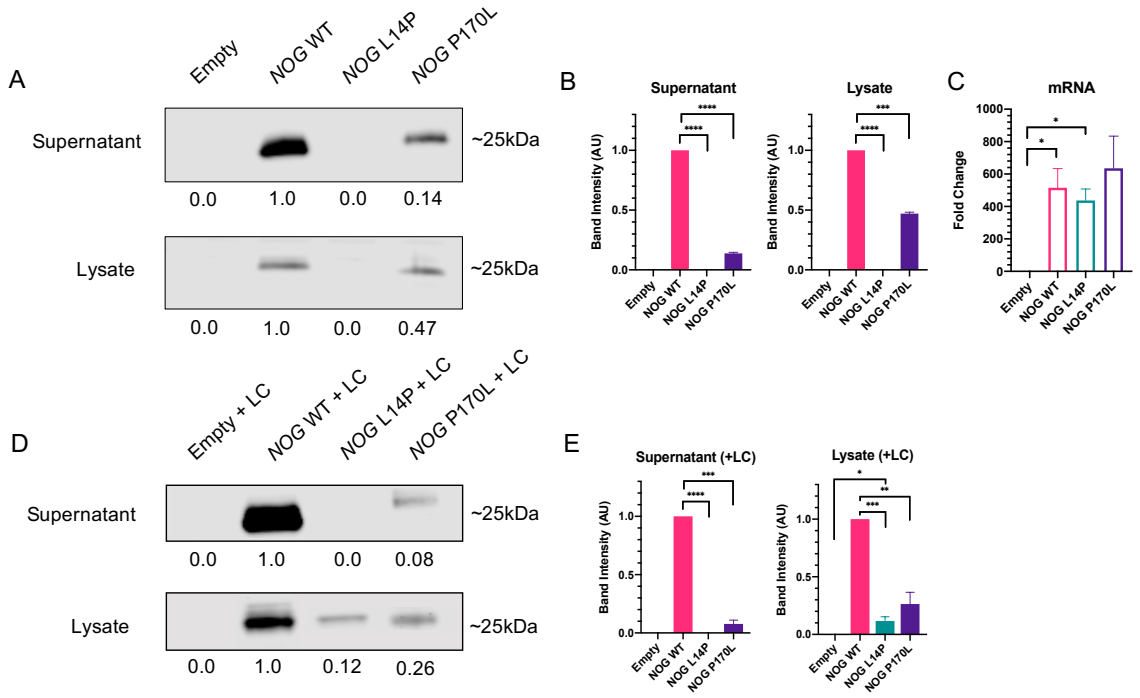

Figure 3.4: *NOG* p.L14P leads to loss of cellular and secreted noggin

A. Western blots showing intracellular (lysate) and extracellular (supernatant) noggin present in HEK 293T cells transfected with various *NOG* ORFs. NOG p.L14P is the missense mutation of family 2. NOG p.P170L was previously reported to cause conductive hearing loss and decrease noggin secretion[73].

B. Quantification of the data from part A shows complete absence of NOG p.L14P and reduced amounts of NOG p.P170L in both supernatant and lysate (*** $p<0.001$, **** $p<0.0001$).

C. qPCR of cDNA from transfected cells shows NOG transcription from all plasmids, despite differences in noggin protein abundance (* $p<0.05$). Expression between transfected plasmids were not significantly different.

D. Western blots as described in part A, but with the addition of 10μM lactacystin 10 hours prior to cell harvest.

E. Quantification of the blots in part E shows an increase in intracellular NOG p.L14P in the presence of lactacystin, but still significantly lower than wild-type (* $p<0.05$, ** $p<0.01$, *** $p<0.001$, **** $p<0.0001$).

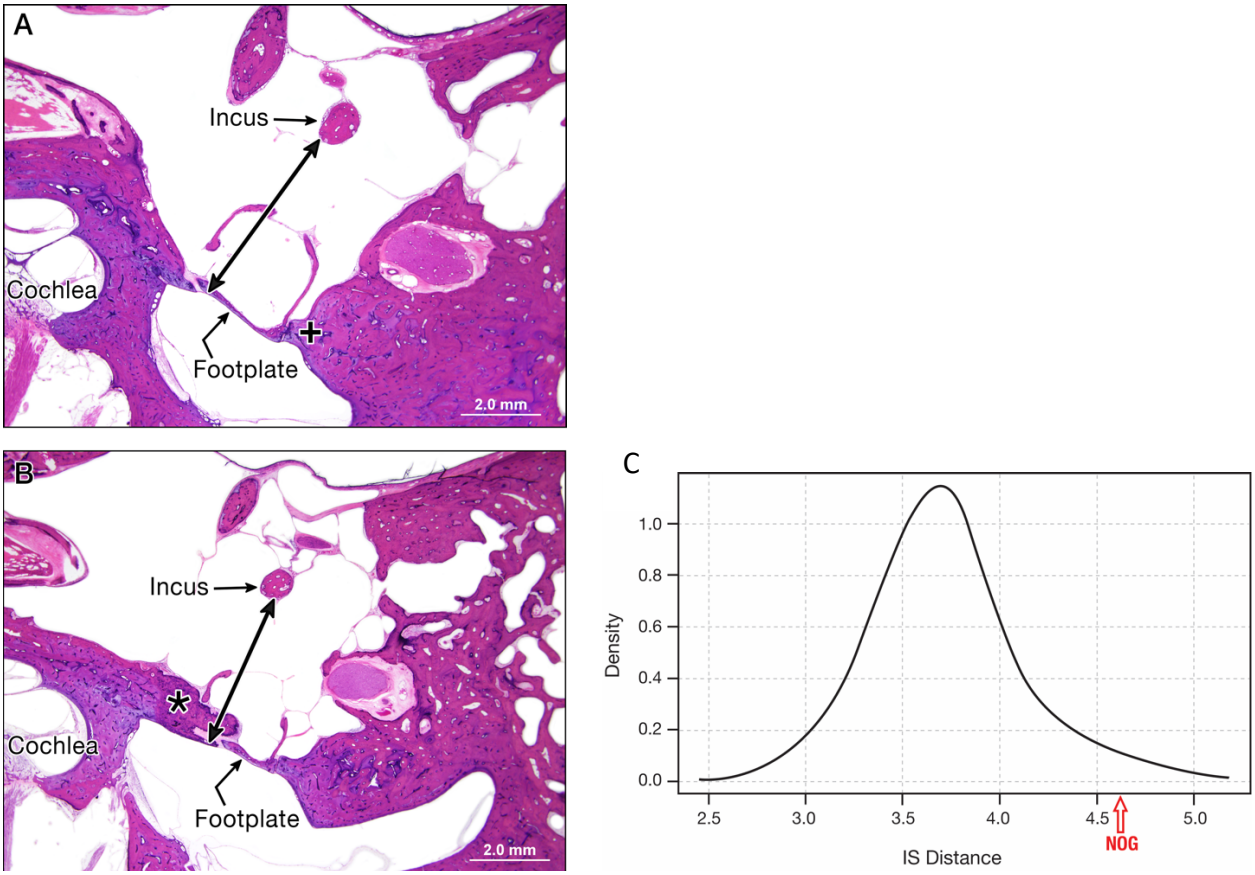

Figure 3.5: Footplate-incus distance of a *NOG*-SSD patient is significantly longer then otosclerosis controls

Light microscopy at 1.25x of human temporal bone sections stained with hematoxylin and eosin. In both images, the double ended arrow indicates the incus-stapes footplate distance, as measured perpendicular to the stapes footplate in the most inferior section containing the footplate.

A. In a patient with *NOG*-SSD, "+" indicates the area of footplate fixation due to ossified cartilage filling the stapedovestibular joint space.

B. In a patient with otosclerosis, "*" indicates a focus of otosclerosis which fixes the stapes at its anterior footplate to the otic capsule.

C. Distribution of incus-stapes (IS) distances in temporal bones of 40 patients with otosclerosis, and in the temporal bone of a patient with *NOG*-SSD (red arrow).

2.7 – TABLES

Table 3.1: Affected members of each family share common features of *NOG*-SSD

Characteristic	II-2	II-5	III-1	III-2	III-5	III-6	II-4	III-1
Face								
Elongated Face			+	+	+		+	+
Maxillary hypoplasia			+	+	+		+	+
Short effaced philtrum			+	+	+		+	+
Thin upper lip			+	+	+		+	+
Micrognathia			+	+	+		+	+
Slightly upslanting palpebral fissures			+	+			+	+
Blepharophimosis							+	+
Nose								
Long bulbous nose			+	+	+		+	+
Broad nasal base			+	+	+		+	+
Hypoplastic alae nasi			+	+	+		+	+
Low columella			+	+	+		+	+
Depressed nasal tip							+	+
Skeletal								
Broadened thumbs							+	+
Broadened halluces								+
Vertebral fusion							+	+
Fusion of bones in great toes							+	
Protruding ribs		+				+		
Unable to flex 5th PIP			+	+		+	+	
Unable to flex thumbs, no flexion creases								+
Unable to flex wrist							+	+
Other								
Conductive hearing loss	+	+	+	+	+	+	+	+
Surgically confirmed stapes ankylosis	+	+				+		+
Hyperopia	+	+	+	+	+	+	+	+
Abnormal outer ears								+

Legend: The left section corresponds to family 1, and the right is for family 2.

CHAPTER 4. Aldolase C (*ALDOC*) as a candidate gene for human hearing loss

4.1 - ABSTRACT

Discovery of genes for inherited hearing loss increases our understanding of the auditory system, improves genetic diagnosis for affected children, informs treatment, and offers options for future pregnancies. Some gene discovery projects also yield unexpected puzzles. In consanguineous Palestinian family BT, including two children with congenital profound bilateral sensorineural hearing loss and three unaffected siblings, whole exome sequencing yielded *ALDOC* c.445C>T p.Arg149Cys as the most promising candidate mutation to explain their phenotype. The mutation alters a residue conserved to *C. elegans*, co-segregates with hearing loss in the family under a recessive model, and is not homozygous in controls from any population. *ALDOC* encodes aldolase C, one of three aldolase enzymes critical to glycolysis and fructose metabolism in vertebrates. We purified recombinant ALDOC p.149C protein and showed that its enzymatic activity was severely reduced compared to ALDOC p.149R. Next, we created a mouse model of the human mutation using CRISPR/Cas9 in an attempt to recreate the hearing phenotype observed in family BT. However, hearing was normal in homozygous mutant, heterozygous, and wild-type mice, as measured by ABR at P21 and P30; and cochlear sensory epithelium of mice of all genotypes appeared normal, as evaluated by SEM. Because human deficiency of aldolase B (which is almost identical in amino acid sequence to aldolase C, but is expressed in different tissues) causes severe fructose intolerance, we hypothesized that hearing loss in the mutant *Aldoc* mice might only appear with exposure to high levels of fructose during development. We therefore exposed offspring of *Aldoc* R149C heterozygous breeding pairs to high fructose under two conditions: from birth and throughout gestation. Fructose had no effect on hearing of mice of any genotype. However, mice born after exposure to high fructose throughout gestation were of

significantly skewed genotypes, with complete absence of wild-type mice (P = 0.0019). We have two speculations based on these observations. First, that humans and mice differ in the role of aldolase C in the ear, and therefore that the best evidence for *ALDOC* as a gene critical to human hearing would be identification of additional human families with hearing loss and different loss-of-function mutations in this gene. Second, that in mouse, high levels of fructose during pregnancy inhibit survival of wild-type embryos, and that paradoxically, reduced levels of aldolase C in the embryo may protect against this effect. We propose future experiments to test these hypotheses.

4.2 - INTRODUCTION

The biology of hearing in mammals has been revealed in large part by the characterization of mutations responsible for its loss. More than 120 genes critical to mammalian hearing have been identified so far[6] through studies based on mouse models and informative human families[111]. Responsible mutations are almost all individually rare with severe effects. Despite identification and characterization of a large number of genes implicated in human hearing loss, some familial cases of hereditary hearing loss remain unexplained by mutations in known hearing loss genes.

Given modern tools, the discovery of novel hearing loss genes involves ascertainment of families with the inherited phenotype, clinical evaluation of both affected and unaffected individuals, genomic analysis by targeted panel or whole exome/genome sequencing, *in vitro* characterization of candidate variants, and *in vivo* replication of the observed phenotype in a model system[11–16]. The *in vitro* assays are necessary to determine a mutation's effect on protein function and must be designed specifically for each candidate gene. For hearing loss, *in vivo* studies evaluating promising candidate mutations have utilized the mouse inner ear as a primary model[111]. Ultimately, the discovery of more genes responsible for hereditary hearing loss will continue to advance our understanding of hearing, improve genetic testing and options for pre-implantation diagnosis, and aid in the development of therapies to treat and prevent hearing impairment.

Here, we propose a new candidate gene for hearing loss that would demonstrate for the first time that proper balance of fructose metabolism is critical to hearing. In consanguineous Palestinian family BT with two children with congenital, profound, nonsyndromic hearing loss and three unaffected siblings, we identified homozygosity for the private allele *ALDOC* p.R149C as the candidate critical gene and mutation. *ALDOC* encodes aldolase C, a metabolic enzyme expressed primarily in the brain and also in the sensory epithelium of the inner ear[112]. Aldolases catalyze the glycolytic conversion of fructose-1,6-bisphosphate to glyceraldehyde-3-phosphate and dihydroxyacetone phosphate, and also the conversion of fructose-1-phosphate to glyceraldehyde and dihydroxyacetone-phosphate. Aldolases A, B, and C are similar in protein sequence, but have dramatically different tissue expression patterns. Aldolase A is widely expressed, most highly in skeletal muscle. Mutations in *ALDOA* cause glycogen storage deficiency 12 (GSD12)[113]. Aldolase B is expressed almost exclusively in the liver, kidney, and small intestine. *ALDOB* mutations lead to hereditary fructose intolerance (HFI)[114], a severe metabolic disorder that causes hepatocyte injury and cellular death due to accumulation of fructose-1-phosphate. HFI is included in routine newborn screening because it is relatively common[115] and can be effectively treated through elimination of dietary fructose. Aldolase C is expressed specifically in the nervous system, including cerebellar Purkinje cells, retinal cells, cartwheel cells of the dorsal cochlear nucleus, and the sensory epithelium of the inner ear[112]. Nerve-growth-factor-induced B factor enhances *Aldoc* expression in rat brain embryos, suggesting a neurodevelopmental role for aldolase C[116]. Mutations in *ALDOC* have not been reported previously in humans.

To test whether *ALDOC* p.R149C has a deleterious effect on protein function, we showed that purified mutant protein has dramatically reduced enzymatic activity. In collaboration with the Weizmann Institute Transgenic and Knockout Facility, we then generated a CRISPR/Cas-9

mouse model of this mutation. However, auditory brainstem response (ABR) testing in homozygous animals, along with their heterozygous and wild-type littermates, demonstrated no difference in hearing among genotypes. This was true across multiple ages and persisted despite dietary fructose supplementation. Follow up whole genome sequencing failed to reveal any other likely causative mutation. We therefore present *ALDOC* as a candidate hearing loss gene with a potentially differential importance to human and mouse hearing. Our hope is that identification of *ALDOC* mutations in other families with hereditary hearing loss will provide additional insight where mouse biology could not.

4.3 - METHODS

Participants

The project was approved by the human subjects' committees of Bethlehem University, the University of Washington, Tel Aviv University, and the Palestinian and Israeli Ministries of Health. Family BT was referred to the study by audiologist Michael Rahil from Bethlehem, Palestine. All audiologic examinations were carried out by Michael Rahil and measured both air and bone pure tone thresholds.

Genomic analysis

DNA was extracted from whole blood by standard procedures[117]. For sequencing using our deafness gene panel[15], protein-coding genes and microRNAs related to hearing loss were captured using the SureSelect Target Enrichment system (Agilent). Molecular barcodes were assigned, and the samples were multiplexed and sequenced in a single flow-cell of the HiSeq 2500 (Illumina) with 100bp paired-end reads. Whole exome sequencing, alignment, and interpretation of variants were performed as previously described[5,118]. Whole genome sequencing was completed through MedGenome (Foster City, CA). Sequencing reads were aligned to hg19 with BWA-MEM (0.7.12-r1039), split-reads and discordant-reads extracted using

SAMBLASTER (0.1.22) and BAM files sorted and indexed using Sambamba (0.6.7). Variant call files were generated including annotations for genomic position, genic location, rarity (gnomAD[29]), and predicted function using our in-house pipeline[5].

Aldolase purification and enzymatic expression assay

The human *ALDOC* ORF was PCR-amplified from a commercially available clone (Origene, CAT#: RC200333) and restriction enzyme sites (Nhe1 and Sal1) were added to each end. Product was ligated to linearized pET-28a(+) (NovaGen) containing a His tag using T4 ligase (Sigma) and verified by Sanger sequencing. The *ALDOC* p.R149C mutation was introduced using the Q5 site-directed-mutagenesis kit (NEB). The resulting plasmids (WT and R149C) were transformed into DE3 cells, allowed to grow at room temperature to OD_{600} of 0.6-0.8, and then stimulated with 200μM IPTG and allowed to grow overnight at 37°C. Cells were then pelleted and lysed using Xtractor buffer (Takara). The resulting supernatant was collected and purified using the His60 Ni gravity column (Takara). Ten 1mL fractions were collected and visualized on acrylamide gel, and fractions with a high purity of aldolase C were pooled to maximize product and minimize dilution. Isolate was dialyzed to Buffer A[119,120] (10mM Tris-HCl, 1mM EDTA, pH = 7.5).

Aldolase enzymatic activity was assessed by spectrophotometry, modified from methods previously described[120,121]. In a 96-well plate, 0.3M fructose-1-6-bisphosphate, 0.15mM NADH, 0.1 mg/mL alpha-glycerophosphate dehydrogenase, and 0.1U aldolase (WT, or equivalent mass of R149C, or empty control) was combined at a total volume of 200uL. Aldolase was added last to begin the reaction. Absorbance at 380nM was measured every 10 seconds over a period of 10 minutes to determine amount of NADH produced over time.

Generation of CRISPR-Cas9 gene edited *Aldoc* R149C/R149C mice

Guide RNAs targeting the *Aldoc* mutation site were created, along with a repair template containing *Aldoc* c.445C>T and synonymous changes in the PAM site to prevent Cas9 cleavage following homology directed repair (HDR). With these constructs, the Weizmann Institute Transgenic and Knockout Facility generated *Aldoc* c.445C>T heterozygous founder mice though embryo microinjection and implantation, as approved by their IACUC protocol (No. 33600117-1). Animals were transferred to the University of Washington (UW) and all following procedures were approved by UW IACUC protocol (No. 4519-01). Potential off-target mutations were excluded by backcross to wild-type C57bl6 mice (Jackson Laboratories). Heterozygous mice were then bred to produce homozygotes. Homozygous mice were analyzed by whole genome sequencing and confirmed to have a region of homozygosity of ~45MB surrounding the *Aldoc* mutation following backcrossing steps. No other potentially damaging SNPs were found.

Fructose supplementation

Fructose supplementation was achieved by dissolving D-Fructose (-) (Sigma) into drinking water at a ratio of 40% (m/m). Supplementation was started at different time points depending on experimental group: none, at birth (P0), or prior to conception (*in utero).*

Auditory brainstem recording

Mice were anesthetized by intraperitoneal injection (ketamine, 100 mg/kg; xylazine, 5 mg/kg) and placed on a heating pad (to maintain body temperature of ~37°C) inside a sound-attenuating chamber. Auditory brainstem responses (ABRs) were measured using standard subcutaneous needle electrodes and placement: the positive electrode was inserted at the left temporal bone above the pinna, the negative electrode at the vertex of the skull, and the ground electrode in the thigh. Pure tone stimuli were generated by a speaker located rostral to the animal and ABRs were digitized using custom software. Tones were 5ms in duration with 1ms rise/fall times and were

presented at a repetition rate of 20/s. Broadband clicks were presented at the beginning and end of each session to assess for any changes in the animal's condition. All stimuli were calibrated online at the beginning of each experiment with a probe microphone placed at the approximate location of the animal's ear. Neural responses were pre-amplified (100x, P55 amplifier; Grass Technologies), sent through an MA3 amplifier with an additional 20dB post-preamp gain (Tucker Davis Technologies), band-pass filtered (100–3000Hz; filter model 3360; Krohn-Hite), and digitized at 24.4kHz. Responses were sampled in a 20ms window (with a 5ms stimulus onset delay). The threshold was defined as the lowest sound pressure level (SPL) in which a recognizable waveform was present and repeatable. Thresholds were determined at 6, 12, 18, 24, 30, 36kHz, and for a broad-band click. Stimuli were presented 500 times from 80 to 20dB SPL in steps of 10dB SPL. To determine the reliability of the waveform at the estimated threshold, testing was repeated at +5, 0, and -5dB SPL from expected threshold.

For each supplementation condition, three to four litters of mice who were offspring of heterozygous x heterozygous matings were evaluated by ABR. The numbers of mice tested with no fructose supplementation were 7 homozygotes, 6 heterozygotes, and 5 wild-type. The numbers of mice tested with fructose supplementation beginning at birth were 2 homozygotes, 10 heterozygotes, and 5 wild-type. The numbers of mice tested with fructose supplementation beginning at conception were 3 homozygotes and 20 heterozygotes. Hearing was tested at ages P21 and P30.

Scanning electron microscopy

Inner ears from homozygous mutant and wild-type mice at P0 were dissected and fixed overnight using 2% glutaraldehyde solution. The samples were fine dissected and incubated with osmium and tetroxide-thiocarbohydrazide alternately according to the OTOTO protocol, described previously[122]. After ethanol dehydration, samples were processed using critical point drying

followed by gold-coating and were scanned using a JSM 840A Scanning Electron Microscope (Jeol).

4.4 - RESULTS

Hearing loss phenotype and genomic analysis

Family BT includes two children with congenital, profound, sensorineural hearing loss and three siblings with normal hearing (Fig. 4.1A, B). The parents are first cousins, both with normal hearing. The affected children have no syndromic features. Pedigree analysis suggests that this hearing loss is autosomal recessive.

Genomic DNA of the affected children was first sequenced using our targeted sequencing panel of 375 genes related to hearing loss in either humans or mice[5,118], but no candidate genes were revealed. We next carried out whole exome sequencing of all seven enrolled members of family BT and identified three rare variants (allele frequency <0.01), all missense substitutions, that co-segregated with hearing loss. Of the three missense variants, only one occurred at a conserved amino acid residue. (Each of the other two variants, *KIAA2012* p.G813A and *SLC47A1* p.L488F, occurred at a residue not conserved in vertebrates, with multiple species having the variant amino acid as the reference allele. *ALDOC* c.445C>T, p.Arg149Cys at chr17:26,901,809 (hg19) is conserved throughout vertebrates, with *in silico* test scores polyphen 1.00 (0.00 to 1.00 scale), gerp 5.8 (-6.0 to +6.0 scale), revel 0.96 (0.0 to 1.00 scale), CADD 32 (0 to 36 scale) (Fig. 4.1A, C). This variant lies in the longest region of homozygosity shared by the two affected children and not by their unaffected siblings: 27.5MB on chromosome 17.

Consequences of *ALDOC* p.R149C on enzymatic function

Several observations suggested that *ALDOC* p.R149C is detrimental to protein function. First, *ALDOC* residue 149 is completely conserved as arginine from humans to *C. elegans* (Fig. 4.1C)

and mutation from arginine to cysteine is predicted to be damaging by all *in silico* tools. Second, mutations in the two adjacent amino acids of aldolase B (W148R and A150P) result in decreased enzyme activity[120] (Fig. 4.1D). Third, *ALDOC* p.R149C is located only two amino acids from K147, a critical residue in the active site of aldolase B[116] (Fig. 4.2D).

To determine the effect of *ALDOC* p.R149C on enzymatic activity, we isolated purified human wild-type and mutant aldolase C from transformed *E. coli*. We then utilized an assay system in which production of dihydroxyacetone-phosphate catalyzed by aldolase C is coupled to the oxidation of NADH in a subsequent reaction catalyzed by α-glycerophosphate dehydrogenase[120,121] (Fig. 4.3A). Consumption of NADH was measured by spectrophotometry and reflects the catalytic rate (reaction velocity) of aldolase C. The reaction was allowed to run for ten minutes, and the velocity was measured as the rate of NADH consumption (slope of the line). Based on these data, aldolase C p.R149C has greatly diminished catalytic activity compared to wild-type aldolase C (Fig. 4.3B) with fructose-1,6-bisphosphate as a substrate.

Hearing evaluation in *Aldoc* R149C/R149C mice

Animals heterozygous for *Aldoc* p.R149C were bred to yield litters including homozygotes, heterozygous, and wild-type genotypes. Animals were evaluated by ABR at ages P21 and P30 with stimuli including a broad-band click and pure tones at 6, 12, 18, 24, 30, and 36kHz. To determine if fructose exposure had an effect on hearing, their diet was supplemented with 40% (m/m) fructose water in three regimens: no fructose water, fructose water from birth, and fructose water prior to conception (*in utero).* Normal hearing was observed in all groups of animals regardless of genotype, fructose exposure, or age at testing (Fig. 4.4).

Scanning electron microscopy

Cochleae of wild-type and *Aldoc* R149C/R149C P0 animals were dissected and the cochlear sensory epithelium was imaged by scanning electron microscopy (SEM). Images (900x) were taken of cochlear regions located in the apex, middle, and base of the cochlea (Fig. 4.5). Hair cell morphology and survival appeared consistent between genotypes across the length of the cochlea, in agreement with their observed hearing thresholds.

Whole genome sequencing

When confronted with the inability to recreate this hearing loss in mice, we carried out whole genome sequencing of five members of family BT to identify possible candidate non-coding mutations. The region of homozygosity shared by the affected children and not by their hearing sibs spanned 27.5 MB on chromosome 17p13-q12. This region is very gene rich, including more than 100 genes, but no other mutations in coding sequence or ENCODE-predicted regulatory regions were promising candidates with respect to allele frequency or conservation. Because *MYO15A* lies in this genomic region and is a frequent cause of congenital severe to profound hearing loss, we identified all variation in *MYO15A* co-segregating with hearing loss in family BT, and evaluated each variant using *in silico* tools for possible transcriptional effect (*MYO15A* is not expressed in blood so experimental tests in family BT were not possible). Two non-coding variants (in *cis*) in the *MYO15A* locus were homozygous in the affected children: *MYO15A* c.7888-60C>T in intron 40, and *MYO15A* c.9076+35G>A in intron 51. Neither variant was predicted to alter splicing. While the possibility of damaging non-coding mutations cannot be definitively ruled out, we did not identify any candidates more promising than the *ALDOC* mutation.

Mouse genotypes with fructose supplementation

High fructose diet during gestation leads to increased fetal loss and lower litter size in mice[123]. Fructose both impairs the process of uterine decidualization, which prepares endometrial tissue

for implantation of fertilized embryos[124], and increases the potential for mid-pregnancy fetal loss by resorption[123]. Paradoxically, high levels of fructose supplementation in our *Aldoc* R149C heterozygote x heterozygote breeding pairs resulted in slightly increased litter size overall, to an average of 7.5 pups (Table 4.1). Most importantly, these litters failed to produce any wild-type pups, a significant deviation from expected genotypes (P = 0.0019). We therefore must consider the possibility that the *Aldoc* mutation is protective in the developing embryo, and confers a selective advantage to embryos with the mutation. While previous work has focused on the effects of high fructose on the uterus during gestation, the absence of wild-type pups after fructose exposure suggests that fructose also affects the developing fetus directly.

4.5 - DISCUSSION

For many genes that cause human hearing loss, similar genetic lesions in the mouse have recreated the phenotype nearly perfectly[111]. However, exceptions to this rule do exist. For example, mutations in *GJB2* account for most human inherited hearing loss, yet homozygous knockout mutations in mice are embryonic lethal due to the crucial role of *Gjb2* in glucose uptake in murine placenta[125]. Conditional knockouts only in the inner ear of *Gjb2* in mice demonstrate a similar phenotype to humans with *GJB2* mutation[126], but the phenotypic difference exists nonetheless. The complex interplay between tissue expression of the three aldolase enzymes and the relative enzymatic activity for their two attributed reactions presents ample opportunity for differences between mice and humans.

We propose that the likely mechanism of cellular injury in *ALDOC*–related hearing loss is similar to that of hereditary fructose intolerance (HFI), which is due to mutations in *ALDOB*; namely, accumulation of fructose-1-phosphate leads to death of cells reliant on aldolase C for fructose metabolism. This accumulation would occur with loss of aldolase C activity because ketohexokinase, the enzyme that produces fructose-1-phosphate (Fig. 4.2A), lacks a negative

feedback mechanism[127]. Of the three aldolases, *ALDOA* has an enzymatic preference for the glycolytic reaction, *ALDOB* for the fructose metabolism reaction, and the specificity of *ALDOC* is intermediate[128]. Since expression of *ALDOB* is highly restricted, *ALDOC* may be required for fructose metabolism in the tissues in which it is expressed. If cells in a crucial auditory sensorineural pathway rely primarily on aldolase C for fructose metabolism, its loss could lead to hearing loss without syndromic effects. That is, aldolase A expression would not compensate because it is much less active in catalyzing the fructose-1-phosphate reaction[128].

This process naturally depends on the amount of fructose metabolism occurring in these cells. Much as the liver is affected by dietary fructose in HFI, fructose metabolism in the brain depends on dietary fructose intake[127]. Dietary supplementation with high levels of fructose leads to increased fructose metabolism in multiple areas of the brain including the cerebellum, hippocampus, cortex, and olfactory bulb in mice[127]. Since the hearing loss of family BT is congenital, it is likely that any cellular damage occurred prior to birth. Fructose is a primary energy source for developing human fetuses, and is the most abundant hexose in fetal blood[129]. Because mice have a shorter gestation time than humans, and because their hearing is not fully developed at birth, they may not normally experience a prenatal level of fructose exposure that leads to toxicity. This would also explain why the *Aldoc*$^{-/-}$ double-knockout mouse created by the International Mouse Phenotyping Consortium (IMPC; mousephenotype.org) did not have hearing loss.

We attempted to address this experimentally through dietary fructose supplementation, with paradoxical results that not only did not resolve the hearing loss but raised additional questions. In contrast to prior published findings, high levels of fructose supplementation (40% m/m) in pregnant heterozygous females did not result in decreased overall litter size, but did result in a complete absence of wild-type pups. Previous work has robustly quantified the effects of fructose

on uterine decidualization as a potential cause of mid-pregnancy fetal resorption[123]. Our results also suggest that the *Aldoc* R149C mutation confers an ability to escape fetal resorption to a degree that is not possible for wild-type embryos. Because fetal genotype therefore appears to influence resorption, it suggests that this process is not wholly caused by impaired uterine decidualization. To further explore this possibility, we propose the following experiments. First, we will confirm that our method of fructose supplementation (40% m/m in water) can recreate the decrease in litter size observed in previous studies in wild-type breeding pairs[123]. Second, in high fructose *Aldoc* het x het breeding pairs, we will genotype litters at both early (dpc5.5) and middle (dpc18.5) stages of pregnancy to determine if wild-type pups are preferentially lost by fetal resorption. If wild-type embryos are in fact implanted and later resorbed, this provides evidence that *Aldoc* plays a role during development beyond that observed in adult animals. Lastly, subcutaneous injection of exogenous progesterone (P4) can rescue uterine decidualization in the setting of high fructose diet[123]. We will test if progesterone administration can rescue normal genotype ratios. This will determine if wild-type embryos are still preferentially resorbed despite intact decidualization.

To return to the hearing loss, given the data and rationale explained above, we believe that the human genomics, tissue expression pattern, and *in vitro* findings are strong enough to warrant consideration of *ALDOC* as a likely hearing loss gene in humans. The phenotypic differences between the humans and mice could be due to differential expression of aldolases, variable substrate specificity among aldolases, or species differences in fructose exposure during development. Further experimentation is necessary to differentiate these possibilities. Regardless of the cause, we present these findings in the hope that awareness of the possible implication of *ALDOC* in human hearing loss will lead to the discovery of more families with hearing loss due to this gene, or to a better understanding of metabolic differences between these two species.

4.6 – FIGURES

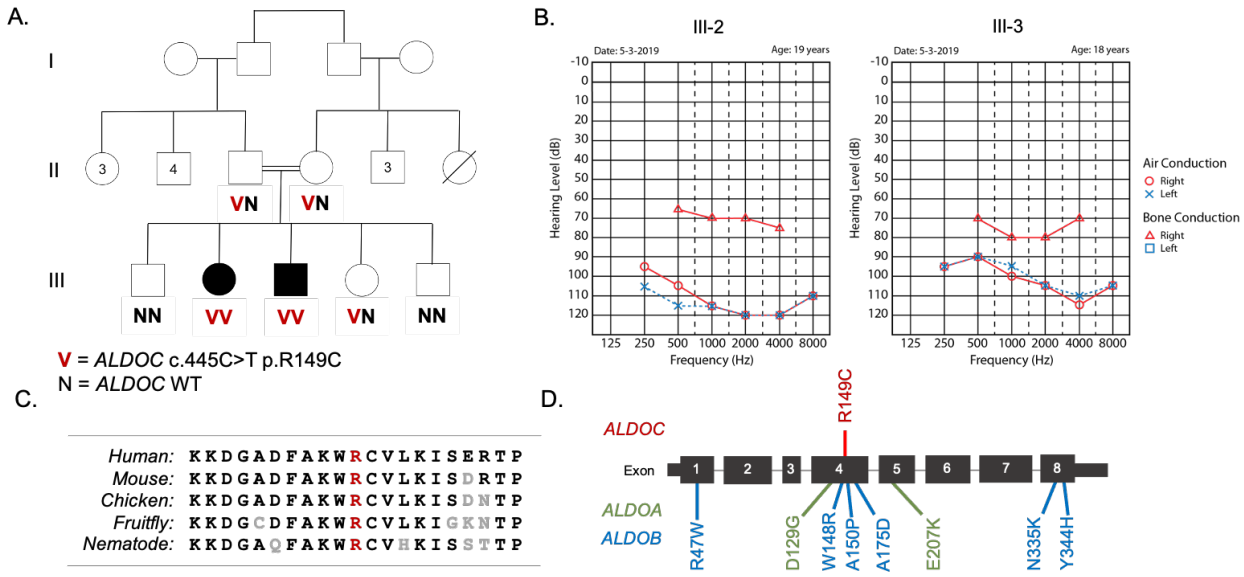

Figure 4.1: Genomic and phenotypic findings in Family BT

A. Pedigree of family with congenital nonsyndromic sensorineural hearing loss in two children (filled symbols), with genotypes at *ALDOC* c.445C>T, p.R149C.

B. Audiograms of affected individuals, III-2 and III-3.

C. Alignment of amino acid sequence at *ALDOC* p.R149C (red) across multiple species.

D. Missense mutations in other aldolases that cause clinical phenotypes. Not all *ALDOB* mutations are listed.

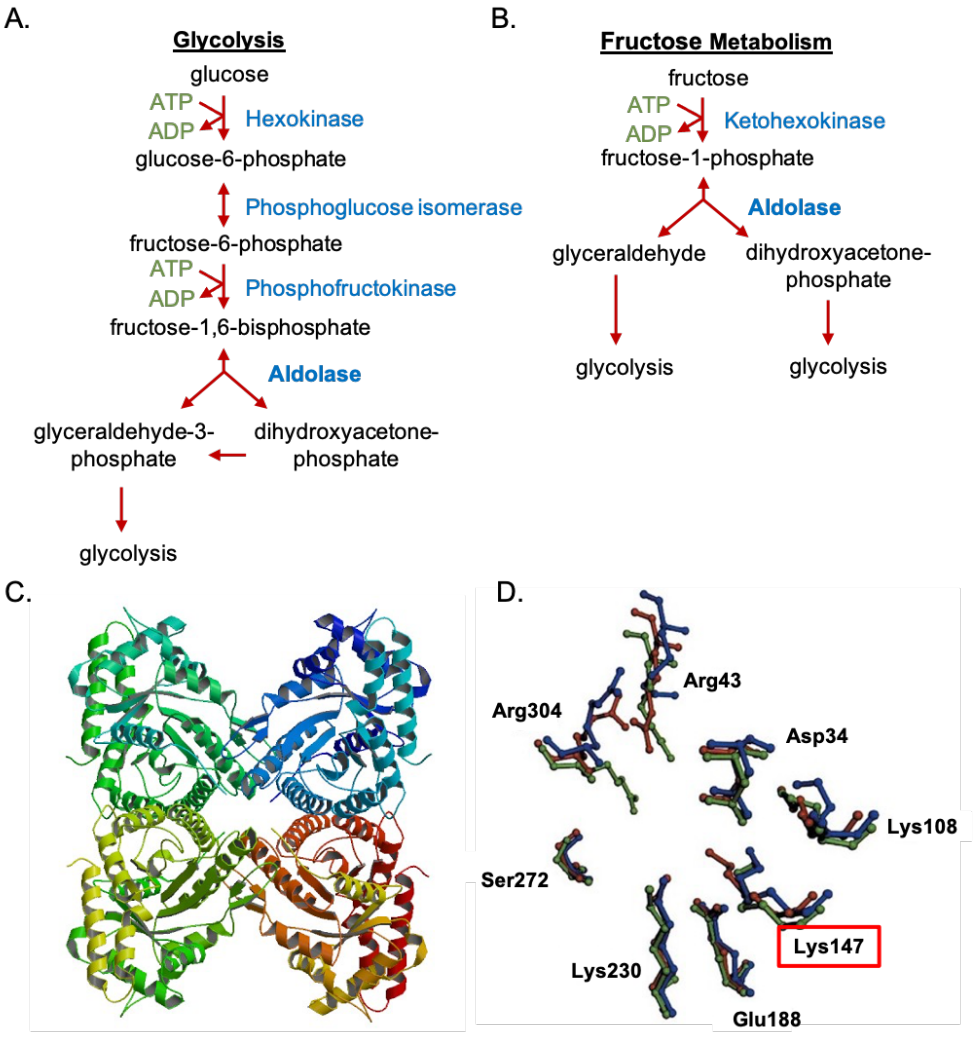

Figure 4.2: Biochemical rationale for pathogenicity

A. Aldolases catalyze a reaction in the glycolytic pathway.

B. Aldolases are integral to fructose metabolism.

C. Protein structure of the aldolase C tetramer.

D. Amino acid residues integral to the active site of aldolase B. Lys147 (red box) is two residues from Arg149 (adapted from publication)[116].

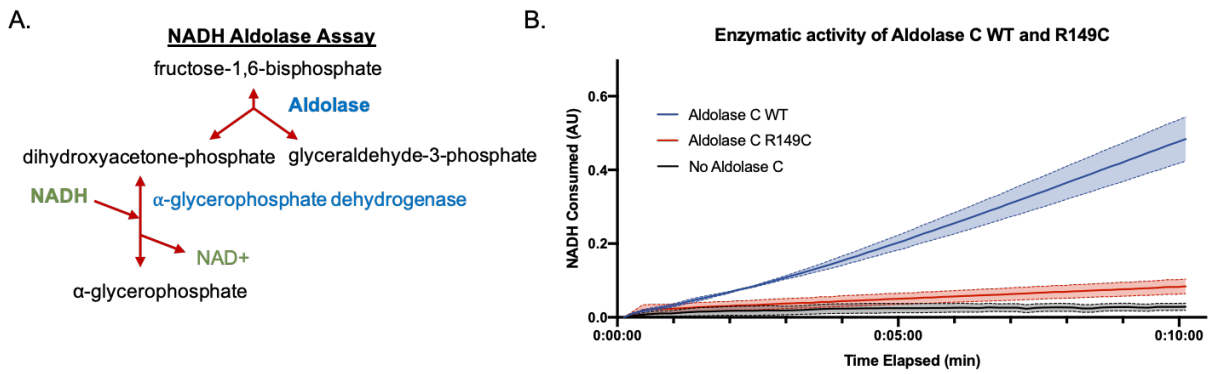

Figure 4.3: Effects of *ALDOC* p.R149C on enzymatic activity

A. Assay design such that aldolase C activity consumes NADH via a coupled reaction with faster rate.

B. NADH consumption increases linearly over time when WT aldolase C is used in the reaction. However, consumption increases only slightly with *ALDOC* p.R149C. Error bars represent SEM over 3 separate experiments.

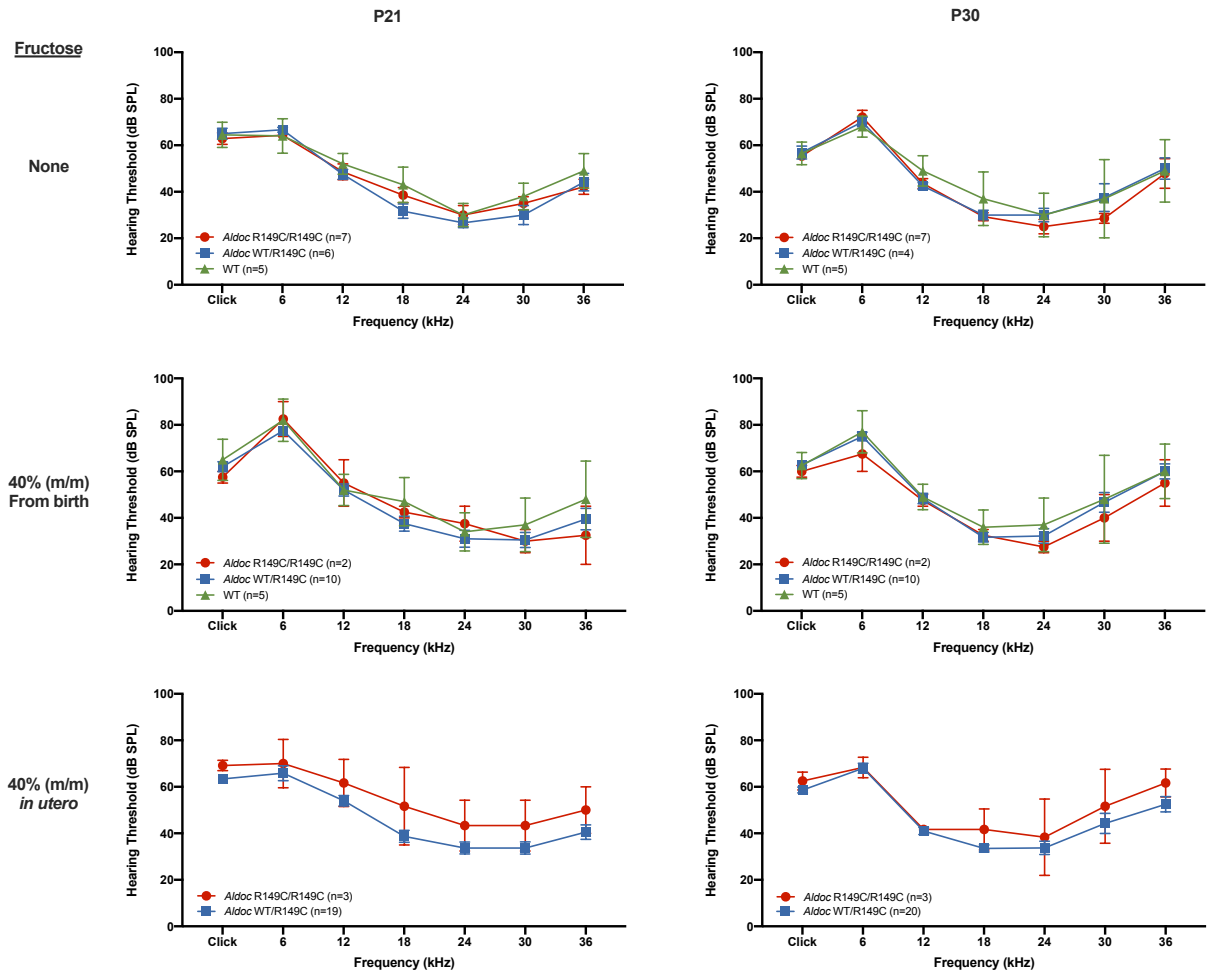

Figure 4.4: Evaluation of hearing in *Aldoc* R149C/R149C mice

Auditory brainstem recording of CRISPR/Cas9 edited mice with *Aldoc* R149C. Homozygotes were tested along with heterozygous and wild-type (WT) litter mates. Columns represent different testing ages: P21 and P30. Rows depict different levels of fructose supplementation: none, 40% (m/m) from birth, and 40% (m/m) *in utero* (prior to conception). No significant differences are seen between genotypes in any condition. Error bars depict SD.

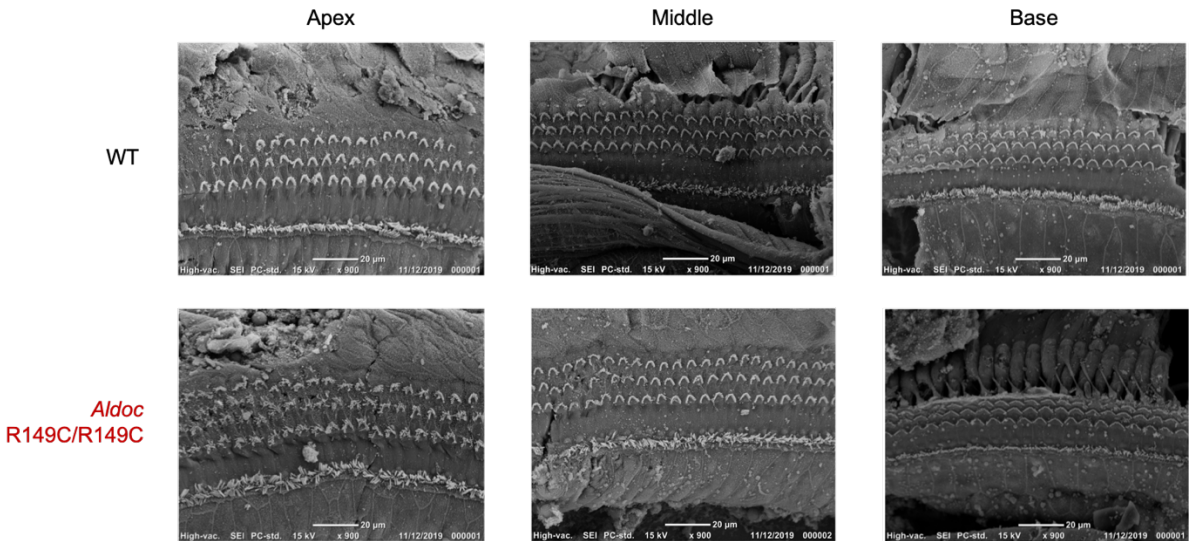

Figure 4.5: Scanning electron microscopy (SEM) of cochlear sensory epithelium in *Aldoc* R149C/R149C and wild-type P0 mice

Amplification is x900 and images were taken at the apical, middle, and basal cochlear locations. No difference in hair cell morphology or survival is apparent between the two genotypes.

4.7 – TABLES

Table 4.1: Mouse genotypes under different fructose conditions

		Aldoc genotypes			
Fructose exposure	**Litter sizes**	**Homoz mutant**	**Hetero-zygous**	**Homoz Wild-type**	**P-value for deviation of genotypes from expected ratios**
None	6, 6, 6	7	6	5	ns
After birth	6, 5, 6	2	10	5	ns
Prior to conception	7, 8, 8, 7	6	24	0	**0.0019**

CHAPTER 5. Translation from a *GOSR2* non-AUG start codon mutation is sufficient to prevent progressive myoclonic epilepsy

5.1 - ABSTRACT

Translation initiation in eukaryotic cells typically begins at an *AUG* start codon within a Kozak sequence. However, translation from non-*AUG* start codons may also occur, with varying efficiency depending on the specific Kozak sequence. We describe family CJ of Middle Eastern ancestry, ascertained for recessive congenital severe-to-profound hearing loss, for which the sole co-segregating candidate allele was *GOSR2* c.1A>C p.M1L. *GOSR2* encodes a member of the ER-Golgi SNARE complex and mutations of *GOSR2* are known to cause a severe form of recessive progressive myoclonic epilepsy (PME) in humans. No signs of epilepsy or ataxia were present in any of the family members homozygous for the mutation, despite dramatically reduced levels (to ~5%) of GOSR2 protein in their B-lymphocytes. Using a custom *in vitro* assay, we confirmed that this reduction was due to decreased translation of the mutant protein (25% of wild-type). Next, we used CRISPR/Cas9 gene editing to create a knock-in model of this genotype in mouse, which shares a nearly identical *GOSR2* Kozak sequence with humans. Western blot of brain tissue from the homozygous mutant mice confirmed reduced GOSR2 protein level (8% of wild-type). However, homozygous mutant mice appeared phenotypically normal, with neither hearing loss nor early-onset epilepsy. Despite severely reduced GOSR2 protein levels in key tissues, residual GOSR2 protein appears sufficient to preclude the epilepsy phenotype in both humans and mice. We cannot yet explain the absence in mice of any hearing loss. These results indicate that translation from novel non-*AUG* start codons may be adequate for some biochemical processes, and provide insight into evaluation of mutations in the start codon and 5'UTR.

5.2 - INTRODUCTION

Eukaryotic translation initiation is accomplished via a scanning mechanism in which the 40S ribosomal subunit moves across an mRNA molecule in a 5' -> 3' direction[130]. Generally, initiation occurs when the translational complex identifies a methionine (*AUG*) start codon, surrounded by an initiation (Kozak) sequence[131]. This Kozak sequence comprises 9 bases preceding the translation start and the first 4 translated bases. The consensus translation initiation sequence is GCCGCCACC|AUGG, with variations leading to increased or decreased translation efficiency[131,132]. Ribosomal profiling studies have identified many cases of translation initiation from start codons that differ from *AUG* by a single nucleotide[133]. Such translation events have functional relevance in the stress response of mammalian cells[134,135]. For example, translation from the alternate start codon *CUG* is implicated in cancer progression, as *c-myc* translation from an upstream *CUG* is increased in the setting of high cell density[136,137]. Start codon mutations are very frequently identified in human disease, generally leading to complete loss of translation (e.g. of *GJB1* in Charcot-Marie-Tooth disease[138]), but occasionally to partial translational loss and a milder phenotype (e.g. of *HBA1* and *HBA2* in alpha thalassemia)[139]. *In vitro* motif analysis of all possible translation initiation sequences has provided predictions of efficiency that can be used to better understand start codon mutations[140].

In consanguineous family CJ from the Middle East, with four affected children in two sibships with bilateral congenital profound sensorineural hearing loss, we discovered homozygosity for *GOSR2* c.1A>C p.M1L by whole exome sequencing. *GOSR2* encodes a member of the soluble-NSF-attachment-protein-receptor (SNARE) family of vesicle locking proteins. The Golgi SNARE proteins mediate membrane fusion during transit of proteins to and from the endoplasmic reticulum[141]. *GOSR2* is known to be essential to this process as its knockdown leads to a loss in ER – Golgi transport and interferes with Golgi maintenance[142]. Homozygosity or compound heterozygosity for loss-of-function mutations in *GOSR2* cause a severe form of progressive

myoclonic epilepsy (PME)[143,144]. Family CJ has no signs of epilepsy other than an isolated febrile seizure during infancy in one individual.

The *GOSR2* mutation of family CJ converts the starting methionine to leucine, and the specific mutation, to *CTG*, is predicted to retain partial translation: 45.8% compared to *ATG*[140]. A different start codon mutation, *GOSR2* p.M1R, has been reported in a patient with dystroglycanopathy who was compound heterozygous for *GOSR2* p.M1R and the known pathogenic mutation *GOSR2* p.G144W[145]. Mutation of codon 1 from methionine to arginine via *ATG* to *AGG* was predicted to nearly abolish translation: 0.6% compared to *ATG*[140]. We showed that *GOSR2* p.M1L leads to decreased, but not absent, translation of *GOSR2* in patient lymphocytes and in a custom cellular assay. Mice homozygous for this mutation had decreased GOSR2 concentration in brain tissue but normal hearing. These findings suggest that even depleted cellular GOSR2 protein concentration is sufficient to avoid the severe epilepsy phenotype, and that start codon mutations with severe translation effects can lead to relatively benign phenotypes.

5.3 - METHODS

Participants

The project was approved by the human subjects' committees of Bethlehem University, the University of Washington, Tel Aviv University, and the Palestinian and Israeli Ministries of Health. Family CJ was referred for genetic evaluation of hereditary hearing loss, identified via hearing screening at Qalqilya School for Children with Hearing Loss in the Palestinian West Bank. Audiologic examinations were carried out at the school and included measurement of both air and bone pure tone thresholds.

Genomic analysis

DNA was extracted from whole blood by standard procedures[117]. For sequencing using our deafness gene panel[5], protein-coding genes and microRNAs related to hearing loss were captured using the SureSelect Target Enrichment system (Agilent). Molecular barcodes were assigned, and the samples were multiplexed and sequenced in a single flow-cell of the HiSeq 2500 (Illumina) with 100bp paired-end reads. Whole exome sequencing, alignment, and interpretation of variants were performed as previously described[5]. Whole genome sequencing was completed through MedGenome (Foster City, CA). Sequencing reads were aligned to hg19 with BWA-MEM (0.7.12-r1039), split-reads and discordant-reads extracted using SAMBLASTER (0.1.22) and BAM files sorted and indexed using Sambamba (0.6.7). Variant call format (VCF) files included annotations for genomic position, genic location, rarity (gnomAD[29]), and predicted function using in-silico tools.

Generation of CRISPR-Cas9 gene edited *Gosr2* M1L/M1L mice

CRISPR/Cas9 mice were generated in the Transgenic and Knockout Facility at the Weizmann Institute of Science. Experiments were approved by the Weizmann Institute's IACUC committee (No. 33600117-1) and were carried out in accordance with their approved guidelines.

Mouse lines were generated by CRISPR/Cas9 gene targeting technology as previously described[146]. Two single stranded guide RNAs (sgRNA) were designed using the MIT (http://crispr.mit.edu/) and CHOPCHOP (https://chopchop.cbu.uib.no/) algorithms to minimize potential off-target effects. sgRNAs were designed to target exon 1 of *Gosr2* and purchased from IDT as chemically modified Alt-R to increase resistance to degradation by nucleases and avoid stimulating innate immunity responses in some cells. Then, to obtain optimal HDR efficiency, homology arms of at least 40 nucleotides on either arm flanking the desired point mutations were manually designed (donor template). These single-stranded donor oligonucleotides (ssODN)

spanning the region were designed to contain the variants of interest and an extra silent mutation at the PAM sites to avoid destruction of the donor by the Cas9 enzyme.

In vitro transcribed Cas9 RNA (100ng/µl), and sgRNA (EnGen® sgRNA Synthesis Kit, 50ng/µl), were injected into the cytoplasm of one-cell fertilized embryos isolated from superovulated CB6F1 hybrid mice mated with CB6F1 males Harlan Biotech Israel Ltd. (Rehovot, Israel). Injected embryos were transferred into the oviducts of pseudo-pregnant ICR females. Genomic DNA from resulting pups was analyzed at weaning for the point mutations by PCR and Sanger sequencing. Positive founders were tested by direct sequencing at all potential off-target sites with fewer than 3bp mismatches.

Western blot of patient B-lymphocyte lysates and mouse brain tissue

B-lymphocytes were extracted from whole blood of human patients and mouse brain tissue was dissected from sacrificed animals. Lysis was performed using RIPA buffer (Sigma) containing cOmplete™, Mini, EDTA-free protease inhibitor cocktail (Roche). Protein concentration was measured using the Bradford Assay reagent (Bio-Rad). B-cell lysates were analyzed by western blot with polyclonal mouse anti-GOSR2 antibody (H00009570-B01P: Abnova) and normalized to mouse anti-actin. Band intensities were quantified using ImageJ software.

***in vitro* GOSR2 translation assay**

A plasmid containing the human *GOSR2* ORF fused to mGFP, followed by an internal ribosome entry site (IRES) and mCherry (Fig. 5.2B) was synthesized (Genscript). The human *GOSR2* Kozak sequence was included to best represent natural translational effects. Mutant plasmids (*GOSR2* p.M1L and p.M1R) were created using the Q5 site-directed mutagenesis kit (NEB) and verified by Sanger sequencing. HEK 293T cells were transfected with each plasmid, or pGFP/empty pCMV6 as control, using the Lipofectamine 2000 transfection kit (Invitrogen). After

24 hours, cells were harvested and separated for flow cytometry and western blot analysis. For western blots, cells were lysed and protein concentrations were determined by Pierce BCA assay (Thermo). Identical quantities of protein for each sample (25µg) were analyzed by western blot using a polyclonal mouse anti-GOSR2 antibody (H00009570-B01P: Abnova). Band intensities were normalized to mouse monoclonal anti-actin antibody (Sigma; A2228) and then to the wild-type condition.

For flow assays, cells were resuspended in FACS buffer and strained into flow cytometry tubes to ensure single cell suspension. Dead cells were visualized by addition of SYTOX blue dead cell stain (Invitrogen). Cells were assessed using a BD LSR II flow cytometer. A total of 100,000 live single cells were recorded for each condition over four different experimental replicates. Data was analyzed using FlowJo software (BD), and cells were gated for appropriate cell size, single cell status, lack of SYTOX staining, and linear relationship of expression between mGFP and mCherry (Fig. 5.3A). A derived parameter calculated as the ratio of mGFP fluorescence to mCherry (mGFP:mCherry) was used to determine relative translation for each condition.

Auditory brainstem response testing

Auditory brainstem responses (ABRs) were measured using the Tucker-Davis Technologies System (TDT, USA) workstation. Mice were anesthetized using a combination of ketamine (100 mg/kg) and xylazine (10 mg/kg) and placed on a heated surface inside a MAC-1 acoustic attenuation chamber (Industrial Acoustic Company). Three sub-dermal electrodes were connected to each mouse, behind the left ear (ground), right ear (reference) and on the forehead (active). RZ and MF1 speakers (TDT) were calibrated using an ACO Pacific 7017 microphone and placed 10 cm away from the mouse head. Hearing thresholds were determined as the lowest four distinctive peaks identified in at least three repeated sounds levels.

Two protocols were used to measure hearing, including a click and frequency-specific pure tones. In the click protocol, broad-frequency noise was delivered beginning at a volume 10dB and increasing to 90dB in 10dB increments. For pure tones, testing began at 36 kHz at 10 dB and increased in 5 dB steps up to 90 dB. This 10-90 dB range was tested for 30, 24,18, 12 and 6 kHz. Hearing threshold measurements were performed on 3- to 8-week-old mice. All genotypes were tested for hearing, with at least six mutant mice and thirteen littermate wild-type controls.

5.4 - RESULTS

Phenotypic and genomic analysis

Family CJ includes four children in two sibships, ages 12 – 15 years at enrollment, with congenital profound sensorineural hearing loss, and seven additional children in these sibships with normal hearing (Fig. 5.1A, B). Both sets of parents are first cousins with normal hearing. Pedigree analysis suggests that this hearing loss is autosomal recessive. The children with hearing loss had no overt syndromic features. The family reported an isolated febrile seizure in infancy for one affected child. Complete workup for signs of epilepsy was not feasible given the family's location and absence of local resources, but severe epilepsy could be excluded.

Genomic DNA from the family was first sequenced using our targeted sequencing panel of 375 genes related to hearing loss in either humans or mice[5,118] but no candidate genes were revealed. Next, we carried out whole exome sequencing of all enrolled individuals and filtered the resulting variants by co-segregation, rarity, and predicted damaging effect. The most likely candidate was *GOSR2* c.1A>C p.M1L at chr17:45,000,559 (hg19). This mutation is not present on any public database of human variation, is the only exonic variant of predicted functional effect anywhere in the human genome that co-segregates with the phenotype, and has a likelihood of co-segregation with hearing loss in family CJ by chance of P = 0.0012. *GOSR2* is widely expressed, including in the inner ear[147].

Whole genome sequencing of all affected informative members of family CJ was also carried out to search for other mutations, either in unannotated exons or in non-coding regions, that might cause hearing loss. Family CJ is highly informative for genetic analysis, and the only genomic region co-segregating with hearing loss in the family was a 4.37 MB region of chromosome 17q21.3 which includes *GOSR2*. This region included 25 other rare variants (allele frequency <0.001) co-segregating with hearing loss in the family, but none were in coding sequence of any gene, or had features identified by ENCODE as likely to regulate any gene related to hearing loss. We also considered the possibility that more than one mutation could be responsible for hearing loss in family CJ, so evaluated from whole genome sequence all variation in each affected child, individually and in subsets, in all known hearing loss genes genome-wide. No candidate variants other than GOSR2 p.M1L were identified by either strategy.

GOSR2 concentration in affected individuals

Mutation of *GOSR2* codon 1 from *ATG* to *CTG* would be expected to affect *GOSR2* translation (Fig. 5.1C). Previous work on the efficiency of translation from non-*AUG* start codons predicts translation efficiency of 46% for the specific combination of mutant *CTG* at codon 1 and the adjacent strong (non-mutant) Kozak sequence of family CJ[140]. (This specific mutation yielded the highest predicted efficiency of any codon 1 or Kozak sequence mutation.) Western blot of human B-lymphocyte cell lysates from individuals in family CJ revealed that GOSR2 protein was detectable, but significantly reduced, in a homozygote compared to a control (III-7, 8.5% of control, P = 0.0007; III-8, 3.4% of control, P = 0.0002) and slightly reduced in a heterozygous carrier (II-4, 62% of control, P = 0.0228; Fig. 5.1D, E).

In vitro quantification of *GOSR2* translation

To test whether lower levels of GOSR2 protein were due to decreased translation or to protein instability, we designed a custom flow cytometry assay based on previously published methods[140]. A plasmid was created containing the human Kozak sequence and the *GOSR2* ORF fused to mGFP, followed by an IRES driving mCherry (Fig. 5.2A). This plasmid design allowed for measurement of translation by mGFP fluorescence and for measurement of plasmid copy number by mCherry fluorescence. Therefore, the ratio mGFP:mCherry is an accurate representation of *GOSR2* translation (Fig. 5.2B). Versions of this plasmid containing GOSR2 p.M1L and GOSR2 p.M1R were created by site-directed mutagenesis. These plasmids were transfected into HEK 293T cells which were analyzed by flow cytometry and western blot (Fig. 5.3A, B). Flow cytometry results indicated that the *GOSR2* p.M1L plasmid had 64% of the signal of wild-type plasmid (P = 0.004 Fig. 5.3C) and 26% of wild-type when the intensity of the GOSR2 p.M1R plasmid was used as a negative control (P = 0.005; Fig. 5.3D). Western blot analysis of HEK 293T lysates following transfection of *GOSR2* WT, p.M1L, and p.M1R plasmids showed a similar translation profile (Fig. 5.3E, F). *GOSR2* p.M1L transfection led to 23% of wild-type protein concentration, while p.M1R transfection led to 0.8% of wild-type protein concentration. (The very low concentration of GOSR2 p.M1R by western blot motivated its use as a negative control in the above flow experiment.)

Evaluation of *Gosr2* p.M1L homozygous mice

First, we thoroughly evaluated the mouse model by whole genome sequencing to ensure that it carries the human mutation with no off-target CRISPR/Cas9 effects. Animals heterozygous for *GOSR2* p.M1L were bred to yield litters including homozygous, heterozygous, and wild-type animals. Littermates were tested by auditory brainstem response (ABR) with a click and pure tones at 6, 12, 18, 24, 30, and 36kHz at ages P21, P30 and P60 (Fig. 5.4A). Normal hearing was observed for all genotypes at all ages.

Brain tissue was dissected from 3 animals of each genotype and lysates were evaluated by western blot (Fig. 5.4B, C). GOSR2 translation was significantly reduced for both heterozygous animals (47% of wild-type, P = 0.045) and homozygous animals (7.7% of wild-type, P = 0.001). These were more dramatic deficits than the predicted translation efficiency of this mutant mouse Kozak sequence (38% of wild-type)[140].

5.5 - DISCUSSION

Partial loss-of-function mutations, including many missense mutations, lead to reduced protein function by affecting protein stability, enzymatic activity, or structure. The amount of residual protein function required to prevent a clinical phenotype varies by gene and condition, with compensatory mechanisms frequently offsetting for partial loss due to only a single wild-type allele. The *GOSR2* mutation of family CJ yields 20-30% of normal protein translation by *in vitro* assays and <10% of expected protein concentration in primary cells from homozygous individuals and in brain tissue from homozygous animals. Despite this extremely low level of GOSR2 protein, homozygous individuals in family CJ do not display any of the features of progressive myoclonic epilepsy described in individuals with other known pathogenic *GOSR2* mutations[143,144]. This finding provides interesting insight into the resiliency of the Golgi-ER SNARE system to a severe reduction in one of its key components. Vesicular transport is a highly regulated process, with each protein having a required topological expression and specific binding partners[148]. One possibility is that the topological organization and binding specificity are more essential to this process than the precise amount of protein present. Previously described pathogenic mutations, *GOSR2* p.G144W and p.K164del, both change the primary structure of the SNARE binding motif and have effects on binding that are likely not present in GOSR2 p.M1L protein[143,144,149,150].

Analysis of the *GOSR2* mutation from family CJ partially answers one question and frustratingly fails to answer another. The partially answered question is that low levels of GOSR2 are

apparently adequate to preclude the severe progressive myoclonic epilepsy known to be caused by loss of function of *GOSR2*[143,144]. The children in family CJ homozygous for *GOSR2* p.M1L are older than the ages at onset (generally 1-3 years) of the progressive myoclonus epilepsy described in multiple children homozygous for *GOSR2* p.G144W, none of whom were reported to have hearing loss[143]. Given the absence of full neurological evaluation of family CJ, we cannot preclude the possibility of subtle signs that might lead to a later-onset phenotype, but by the mid-second decade, none of the family CJ children homozygous for their family's allele express any epilepsy, ataxia, or any other neurological signs unrelated to their hearing loss. However, it is possible to test neurological features in the mouse model of *GOSR2* p.M1L, including behavioral monitoring for spontaneous convulsive seizures with age and also seizure induction by thermal modulation[151]. We propose to carry out these studies in the mouse over the next several months.

The unanswered question of family CJ and *GOSR2* p.M1L is whether this mutation causes the hearing loss of family CJ, and if not, what does. Because the *GOSR2* p.M1L mutation failed to recreate hearing loss in the mouse model, the observed hearing loss in the family remains unexplained. We thoroughly evaluated family CJ by whole genome sequencing, including evaluation of structural variants, in an attempt to identify any other potentially causal mutation, coding or non-coding, that co-segregated with hearing loss in the family. We also evaluated each family member separately in case a mutation might explain hearing loss in a subset of the affected family CJ children, with the others being possible phenocopies. No candidate variants were identified. The mechanism by which mutation of *GOSR2* could lead to non-syndromic hearing loss is not clear, and the reason that the mechanism would differ in development of human and mouse hearing is even more mysterious. The most convincing evidence for the involvement of *GOSR2* in hearing loss would be identification of another human family with hearing loss and a partial-loss-of-function mutation in *GOSR2*. Alternatively, variation in family CJ not recognized as

functional could nonetheless be causing the hearing loss. With current technology and information, we cannot distinguish these possibilities.

In the world of human genomics, mechanisms of translation are often overlooked or assumed to be inconsequential. The case of family CJ revealed a non-canonical start codon that allowed for a level of *GOSR2* translation sufficient to avoid a severe epileptic phenotype. This escape was possible due to the overall strength of the Kozak sequence and the apparent ability of the Golgi – ER transport system to adapt to the reduced translation. This finding is relevant both to the study of *GOSR2* and progressive myoclonic epilepsy and to the consideration of the translational effects of other first-codon and 5'UTR mutations.

5.6 – FIGURES

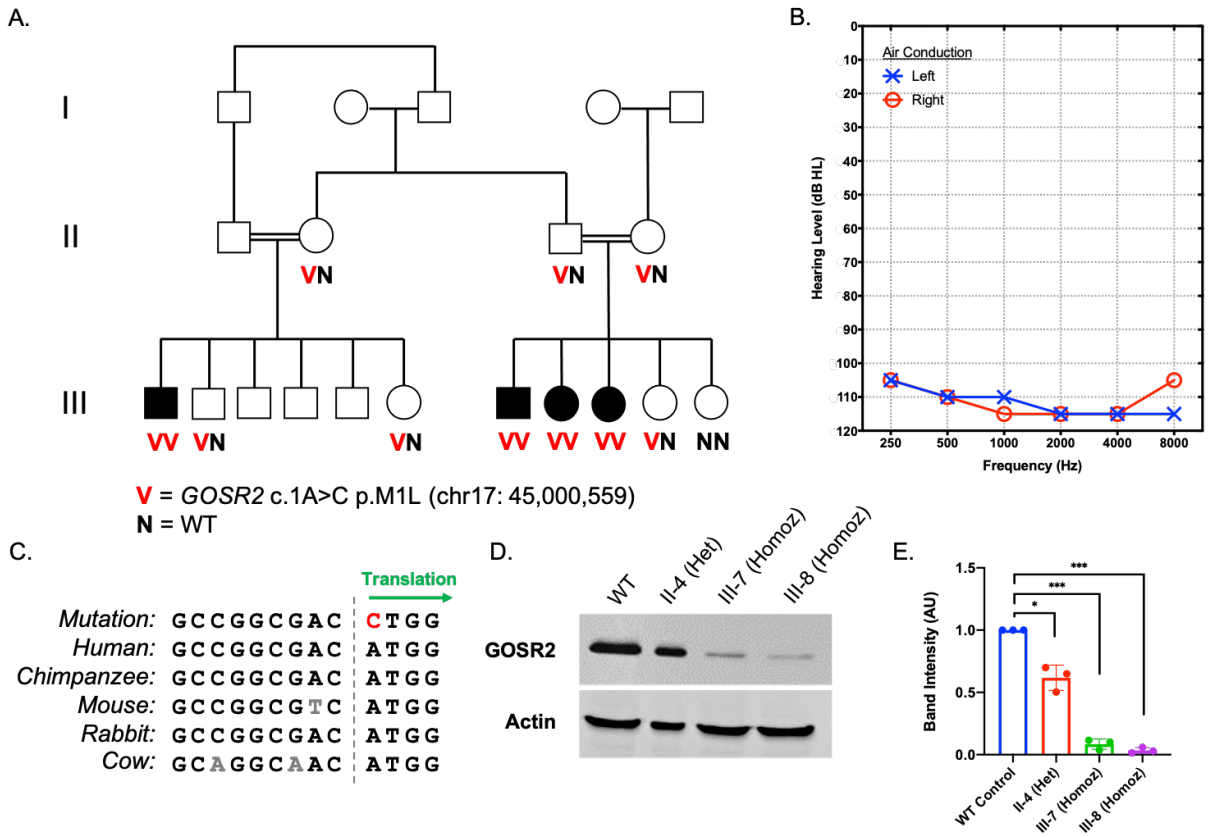

Figure 5.1: *GOSR2* mutation in Family CJ leads to decreased protein concentration

A. Family CJ with congenital nonsyndromic sensorineural hearing loss in four children (filled symbols), with genotypes at *GOSR2* c.1A>C p.M1L depicted.

B. Representative audiogram of affected individuals (III-1).

C. Alignment of nucleotide sequence of the *GOSR2* Kozak sequence across multiple species.

D. Western blot of GOSR2 concentration in patient primary B-lymphocyte lysates.

E. Quantification of band intensities in blot shown in part D, normalized to actin and WT condition. Error bars depict SEM (* $P < 0.05$, *** $P < 0.001$).

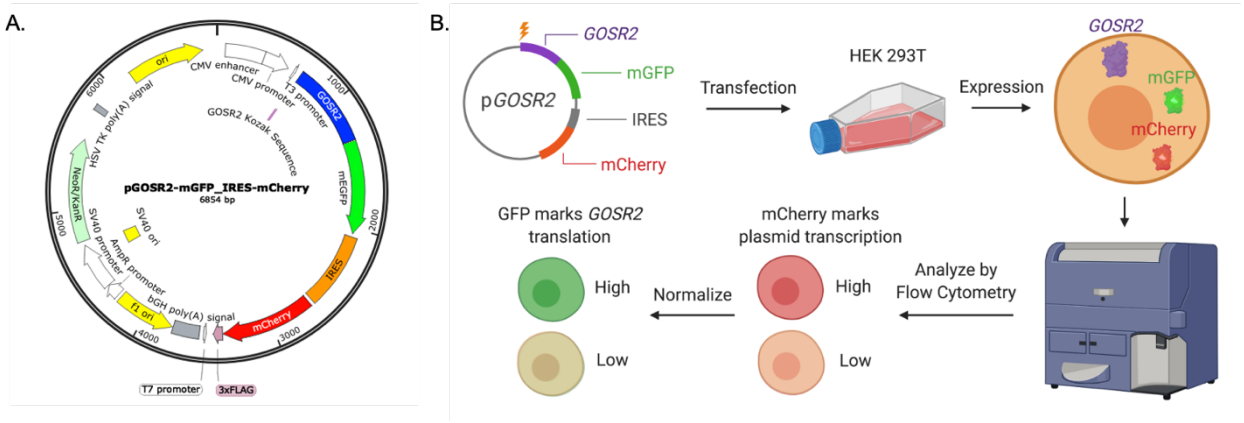

Figure 5.2: Experimental design

A. Plasmid design for in vitro experiments.

B. Experimental design for flow assay.

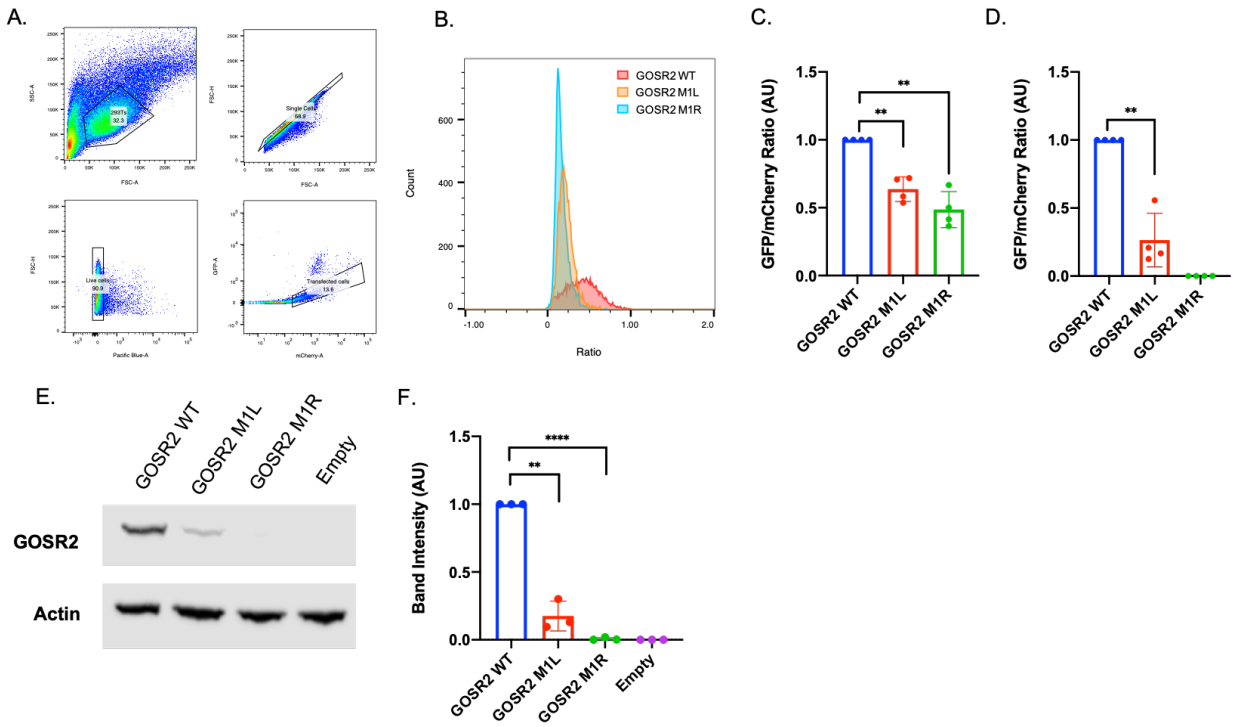

Figure 5.3: *in vitro* quantification of *GOSR2* p.M1L translation

A. Gating strategy for flow data, including gating on expected cell size, single cell status, lack of dead cell staining, and linear relationship between mGFP and mCherry.

B. Histograms of mGFP:mCherry Ratio (x-axis) across cell populations.

C. Comparison of geometric mean mGFP:mCherry in different transfected conditions across four replicates.

D. Data in part C rescaled with the GOSR2 p.M1R condition treated as a negative control (set to 0).

E. Representative western blot of *GOSR2* translation in transfected cells used in flow experiments.

F. Quantification of GOSR2 band intensity among three replicate western blots, normalized to actin and WT condition. All error bars depict SEM (* P < 0.05, ** P < 0.01, *** P < 0.001, **** P < 0.0001).

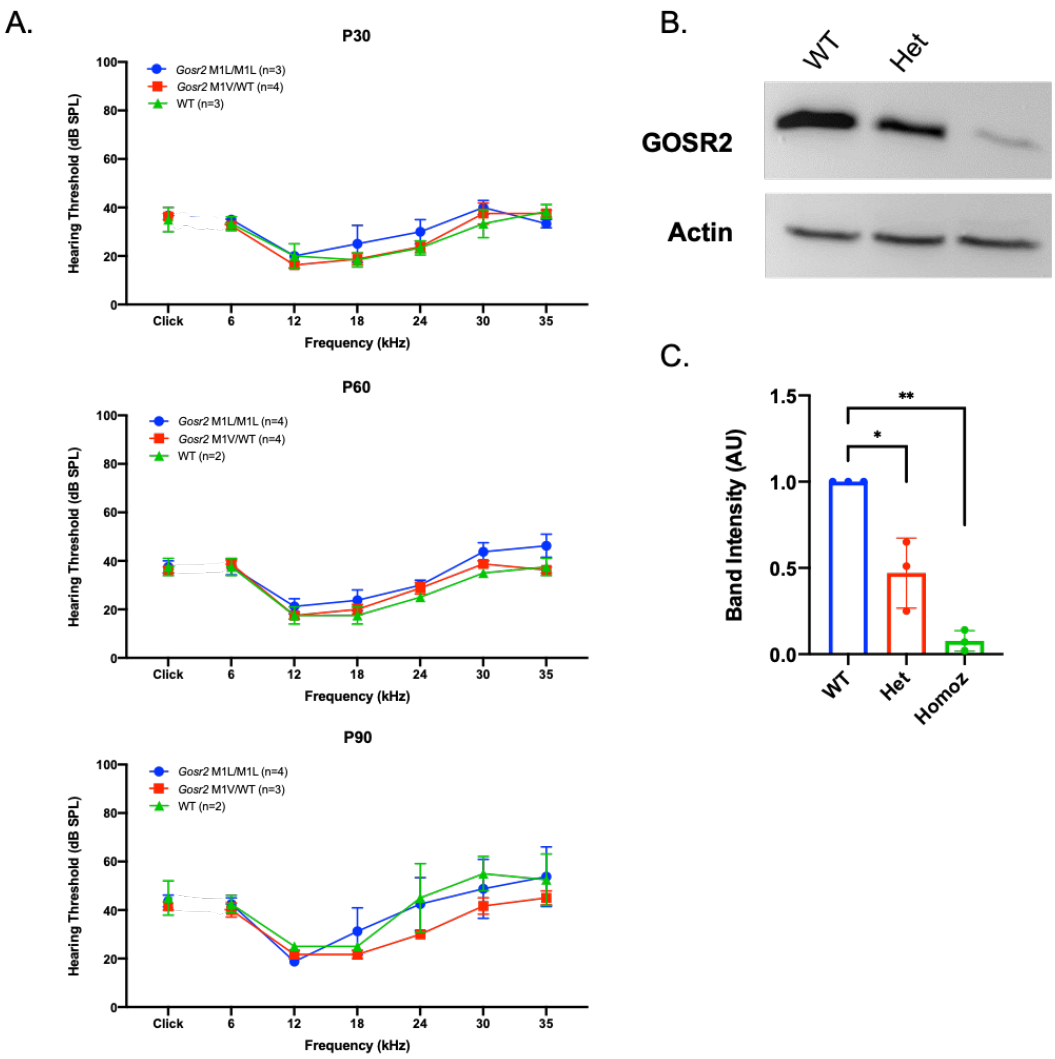

Figure 5.4: Outcomes of *Gosr2* p.M1L in CRISPR/Cas9 edited mice

A. Auditory Brainstem Response (ABR) thresholds for *Gosr2* p.M1L/M1L homozygous animals, along with WT and heterozygous littermates. Error bars depict SD.

B. Representative western blot of GOSR2 translation in lysates from brain tissue of animals with varying genotype.

C. Quantification of three replicate western blots of GOSR2 translation, normalized to actin and WT condition. Error bars depict SEM (* $P < 0.05$, ** $P < 0.01$).

Chapter 6. Discussion

6.1 – SUMMARY OF RESEARCH

This dissertation focuses on the ways in which genomic sequencing technologies can improve our understanding of hereditary hearing loss and guide its clinical care. Although many genetic causes of human hearing loss have already been identified, the accumulation of accurate phenotypic information is essential for the translation of this knowledge to patient care. By sequencing more than 400 pediatric patients with hearing impairment and assessing their audiological tests, I was able to clearly describe the diversity of phenotypes amidst the marked genetic heterogeneity of hearing loss. Likewise, the identification of novel genes and mutations that lead to hearing loss is crucial to expanding the scope of genetic testing and better understanding the fundamental mechanisms of auditory transduction. Above, I outline my work to identify and characterize novel mutations in four different families with hereditary hearing loss due to the genes *NOG, ALDOC,* and *GOSR2.*

6.2 – IMPLICATIONS FOR CLINICAL CARE

Despite the rapid advancement of hearing loss genomics and the ever-increasing number of identified hearing loss genes, clinical genetic testing for hearing loss is underutilized. This is due in part to an impending shift in the fundamental understanding of genetics in the clinical world. As sequencing technologies become faster, cheaper, and easier to analyze, a growing number of individuals are receiving genetic testing as part of their clinical care. This is leading to a newfound understanding of the causes of various different phenotypes and their underlying genetic heterogeneity: Researchers and clinicians are beginning to see that established clinical diagnoses are actually groupings of similar (but not identical) phenotypes with varied genetic causes. This is especially apparent in hearing loss. For example, syndromes that were classically diagnosed based on clinical presentation, such as Usher Syndrome[152] and Waardenburg Syndrome[153], are

ultimately caused by multiple different genes, each with a different severity and distinct sequelae. As sequencing continues to become more common, a fundamental shift in the understanding of genetic syndromes is inevitable. Namely, that the underlying genetic cause of a syndrome is a more apt description than the classical clinical diagnoses that preceded it. Just like in the field of cancer, where specific somatic mutations are used to accurately describe disease status, other fields can benefit from an increased understanding of the genetic basis of their diagnosed phenotypes.

My hope is that the research described in Chapter 2 of this dissertation serves as a step toward that reality. In clearly depicting the link between a specific genetic basis of hearing loss and its resulting phenotype, I hope to increase the resolution at which clinicians can understand their patients' prognosis and optimal route of treatment. This work takes that resolution even one step further, by confirming phenotypic differences among individuals with hearing loss due to the same gene but with different specific genotypes. The clinical language of the future must expand to include genomic findings, and it is my hope to one day read a clinic note of patient described as having "*TMPRSS3* fs/fs hearing loss."

Another primary reason for the lack of implementation of genetic testing is the fact that results often have little impact on treatment course. Currently, hearing loss is treated by hearing aid amplification or by cochlear implantation. The choice of correct treatment is based primarily on the severity of the phenotype[7]. While the genotype-specific prognostic information that our study (and others) provides will surely guide the implementation of the above treatments, I believe that it will become increasingly important to understanding a patient's genotype for future targeted therapies. Recent advances in gene therapy methods for hearing loss have had promising success in mouse models[154,155]. Despite the fact that fundamental hurdles to the application of this technique in humans still exist[156], I suspect that they will be overcome in time. Any gene

therapy, in its current form, will ultimately address hearing loss due to mutations in only a single gene, and so optimal genomic sequencing methods will be necessary to identify eligible patients.

6.3 – MODERN GENE DISCOVERY EFFORTS

The number of known hearing loss genes has grown from zero to more than 120 over the last 30 years[6]. These critical genes were identified primarily through the study of mouse models and of informative human families[11–17,111]. As would be expected, the genes most commonly associated with hearing loss were discovered first, including *GJB2*[157]*, MYO7A*[158]*, and MYO15A*[159], and their link to hearing loss was readily apparent. As research progressed, remaining hearing loss genes were increasingly rare causes of hearing loss and therefore required different methods of identification and characterization to determine causality. The burden of proof to show that a mutation led to hearing loss shifted from human genetics to *in vitro* methods showing that a mutation was damaging to protein function, and *in vivo* recreation of hearing loss showing that it was sufficient to cause the phenotype.

Genes critical to human hearing remain undiscovered: Families with clearly inherited forms of hearing loss remain unsolved by sequencing of known hearing loss genes. Hearing loss in these families is surely due to a genetic cause that escapes our current abilities to characterize it. Possibilities include mutations in noncoding regions that are unannotated or of unknown importance based on our current tools for predicting functional effects. Other mutations are surely missed by the applied sequencing technologies, such as structural or highly-repetitive mutations that may be identified by modern long-read sequencing approaches[36]. Certainly, some cases are also caused by coding mutations in novel hearing loss genes whose evaluation is complicated in some way experimentally.

My belief is that my characterization of *ALDOC* as a candidate hearing loss gene (Chapter 4) falls in that final category. The complication in this case is that species-specific differences in fructose metabolism or aldolase expression make recreation of the observed human phenotype impossible (or highly difficult) in a mouse model. Publication of our results, despite this missing piece, may be a necessary step in the evaluation of this gene. If work that falls short of the entire burden of proof required by modern genomics is not published, then it could be years before enough families with *ALDOC*-hearing loss are accumulated by one group to prove causation themselves.

In contrast, the hearing loss in the family described in Chapter 5 is still unclear. Without the biochemical rationale to justify species-specific differences, I instead highlight the fundamentally interesting effects of their first codon mutation on translation and its protection against the PME phenotype. Hopefully this example will lend insight into the evaluation of first codon mutations elsewhere in the genome. Application of long-read sequencing in this family, the improvement in analysis of noncoding variants from whole genome sequencing data, or additional information on the biochemical processes involving *GOSR2* may provide the answer to their hearing loss in the future.

6.4 – FINAL THOUGHTS

The underlying genetic basis of hearing loss is complex. My doctoral research, and this dissertation, is just a small sample of the breadth of work and knowledge that will be required to ultimately understand it. However, I believe that the work described in this text represents a significant and meaningful contribution to that effort. The results outlined above improve our understanding of the correlations between genotype, phenotype, and treatment outcome for known hearing loss genes, and present several novel genes and mutations that appear implicated in hearing loss. All of these findings serve to increase the diagnostic benefit of genetic testing for

hearing loss and thereby improve prognostic information, guide clinical treatment, and also expand family planning options in genetic counseling. Discovery of novel genes and mutations will also lead to a greater understanding of the molecular and cellular mechanisms of hearing and potentially guide the development of future targeted therapies for hearing impairment.

APPENDIX A. GENE LIST FOR OUR CUSTOM PANEL

Genes					
ACTG1	*COL2A1*	*GAB1*	*MARVELD2*	*PDZD7*	*STRC*
ADCY1	*COL4A3*	*GATA3*	*MCM2*	*PEX1*	*STRCP1*
ADGRV1	*COL4A4*	*GIPC3*	*MET*	*PEX6*	*SYNE4*
AIFM1	*COL4A5*	*GJB2*	*METTL13*	*PJVK*	*TBC1D24*
ALDOC	*COL4A6*	*GJB3*	*MIRN96*	*PLS1*	*TBX1*
ALMS1	*COL9A1*	*GJB6*	*MITF*	*PNPT1*	*TCOF1*
ATP2B2	*COL9A2*	*GPSM2*	*MPZL2*	*POLR1C*	*TECTA*
ATP6B1	*CRYL1*	*GRAP*	*MSRB3*	*POLR1D*	*TECTB*
ATP6V1B2	*CRYM*	*GREB1L*	*MTRNR1*	*POU3F4*	*TIMM8A*
BCS1L	*DCDC2*	*GRHL2*	*MTTE*	*POU4F3*	*TJP2*
BDP1	*DFNA5*	*GRXCR1*	*MTTK*	*PRPS1*	*TMC1*
BSND	*DIAPH1*	*GRXCR2*	*MTTL1*	*PTPRQ*	*TMEM132E*
CABP2	*DIAPH3*	*GZF1*	*MTTS1*	*PTRH2*	*TMIE*
CACNA1D	*DMXL2*	*HARS*	*MYH14*	*RDX*	*TMPRSS3*
CATSPER2	*DNMT1*	*HARS2*	*MYH9*	*REST*	*TNC*
CCDC50	*DSPP*	*HGF*	*MYO15A*	*ROR1*	*TPRN*
CD151	*EDN3*	*HOMER2*	*MYO1A*	*S1PR2*	*TRIOBP*
CD164	*EDNRB*	*HSD17B4*	*MYO3A*	*SCD5*	*TRRAP*
CDC14A	*ELMOD3*	*ILDR1*	*MYO6*	*SEMA3E*	*TSPEAR*
CDH23	*EPS8*	*KARS*	*MYO7A*	*SERPINB6*	*TWNK*
CDKL3	*EPS8L2*	*KCNE1*	*NARS2*	*SIX1*	*USH1C*
CEACAM16	*ERAL1*	*KCNJ10*	*NDP*	*SIX5*	*USH1G*
CHD7	*ERCC2*	*KCNQ1*	*NLRP3*	*SLC12A2*	*USH2A*
CIB2	*ESPN*	*KCNQ4*	*OPA1*	*SLC17A8*	*WBP2*
CISD2	*ESRP1*	*KITLG*	*OSBPL2*	*SLC22A4*	*WFS1*
CLDN14	*ESRRB*	*LARS2*	*OTOA*	*SLC26A4*	*WHRN*
CLDN9	*EYA1*	*LHFPL5*	*OTOF*	*SLC26A5*	
CLIC5	*EYA4*	*LMX1A*	*OTOG*	*SLITRK6*	
CLPP	*FAM65B*	*LOC653786*	*OTOGL*	*SMAC/DIABLO*	
CLRN1	*FGF3*	*LOXHD1*	*P2RX2*	*SMPX*	
COCH	*FGFR1*	*LOXL3*	*PAX3*	*SNAI2*	
COL11A1	*FGFR2*	*LRTOMT/COMT2*	*PCDH15*	*SOX10*	
COL11A2	*FOXI1*	*MAP1B*	*PDE1C*	*SPNS2*	

REFERENCES

1. Vohr, B. Overview: Infants and Children With Hearing Loss- Part I. *Ment. Retard. Dev. Disabil. Res. Rev.* **64**, 62–64 (2003).
2. Blackwell, D.L., Lucas, J.W., & Clarke, T. Summary Health Statistics for U.S. Adults: National Health Interview Survey 2012. *Vital Health Stat* **260**, 1-161 (2014).
3. Petit, C., Levilliers, J. & Hardelin, J. Molecular Genetics of Hearing Loss. *Annu. Rev. Genet.* **35**, 589–646 (2001).
4. Sloan-Heggen, C.M., Bierer, A.O., Shearer A.E. *et al.* Comprehensive genetic testing in the clinical evaluation of 1119 patients with hearing loss. *Hum. Genet.* **135**, 441–450 (2016).
5. Abu Rayyan, A., Kamal, L., Casadei, S. *et al.* Genomic Analysis of Inherited Hearing Loss in the Palestinian Population. *Proc. Natl. Acad. Sci.* **117**, 20070-20076 (2020).
6. Van Camp, G. & Smith, R. Hereditary Hearing Loss Homepage. Available at: https://hereditaryhearingloss.org.
7. Liu, C. C., Anne, S. & Horn, D. L. Advances in Management of Pediatric Sensorineural Hearing Loss. *Otolaryngol. Clin. North Am.* **52**, 847–861 (2019).
8. Raine, C. H., Summerfield, Q., Strachan, D. R *et al.* The cost and analysis of nonuse of cochlear implants. *Otol. Neurotol.* **29**, 221–224 (2008).
9. Miyagawa, M., Nishio, S.-Y. & Usami, S.-I. A Comprehensive Study on the Etiology of Patients Receiving Cochlear Implantation With Special Emphasis on Genetic Epidemiology. *Otol. Neurotol*. **37**, 1–9 (2016).
10. Carlson, R. J., Quesnel, A., Wells, D. *et al.* Genetic Heterogeneity and Core Clinical Features of *NOG*-Related-Symphalangism Spectrum Disorder. *Otol. Neurotol.* **42**, e1143–e1151 (2021).
11. Vahava, O., Morell, R., Lynch, E.D. *et al.* Mutation in Transcription Factor *POU4F3*

Associated with Inherited Progressive Hearing Loss in Humans. *Science* **279**, 1950-4 (1998).

12. Walsh, T., Walsh, V., Vreugde, S. *et al.* From flies' eyes to our ears : Mutations in a human class III myosin cause progressive nonsyndromic hearing loss DFNB30. *Proc. Natl. Acad. Sci.* **99**, 7518-23 (2002).
13. Shahin, H. Walsh, T., Sobe, T. *et al.* Mutations in a novel isoform of *TRIOBP* that encodes a filamentous-actin binding protein are responsible for DFNB28 recessive nonsyndromic hearing loss. *Am. J. Hum. Genet.* **78**, 144–152 (2006).
14. Shahin, H., Rahil, M., Abu Rayyan, A. *et al.* Nonsense mutation of the stereociliar membrane protein gene *PTPRQ* in human hearing loss DFNB84. *J. Med. Genet.* **47**, 643-5 (2010).
15. Walsh, T., Shahin, H., Elkan-Miller, T. *et al.* Whole exome sequencing and homozygosity mapping identify mutation in the cell polarity protein *GPSM2* as the cause of nonsyndromic hearing loss DFNB82. *Am. J. Hum. Genet.* **87**, 90–94 (2010).
16. Walsh, T., Pierce, S.B., Lenz, D. *et al.* Genomic duplication and overexpression of *TJP2/ZO-2* leads to altered expression of apoptosis genes in progressive nonsyndromic hearing loss DFNA51. *Am. J. Hum. Genet.* **87**, 101–109 (2010).
17. Lynch, E. D., Lee, M.K., Morrow, J.E. *et al.* Nonsyndromic deafness DFNA1 associated with mutation of a human homolog of the Drosophila gene diaphanous. *Science.* **278**, 1315–1318 (1997).
18. Shearer, E. A., Hildebrand, M. S. & Cmith, R. J. Gene Reviews. in *Gene Reviews* (eds. Adam, M., Ardinger, H. & Pagon, R.) [Online] (2017).
19. Mo, B., Lindbæk, M. & Harris, S. Cochlear implants and quality of life: A prospective study. *Ear Hear.* **26**, 186–194 (2005).
20. Moberly, A. C., Bates, C., Harris, M. S. *et al*. The enigma of poor performance by adults with cochlear implants. *Otol. Neurotol.* **37**, 1522–1528 (2016).

21. Lazard, D. S. *et al.* Pre-, Per- and Postoperative Factors Affecting Performance of Postlinguistically Deaf Adults Using Cochlear Implants: A New Conceptual Model over Time. *PLoS One* **7**, 1–11 (2012).
22. Kileny, P. R., Zwolan, T. A. & Ashbaugh, C. The influence of age at implantation on performance with a cochlear implant in children. *Otol. Neurotol.* **22**, 42–46 (2001).
23. Fryauf-Bertschy, H., Tyler, R. S., Kelsay, D. M. R., *et al*. Cochlear implant use by prelingually deafened children: The influences of age at implant and length of device use. *J. Speech, Lang. Hear. Res.* **40**, 183–199 (1997).
24. Eppsteiner, R. W., Shearer, A.E., Hildebrand, M.S. *et al.* Prediction of cochlear implant performance by genetic mutation : The spiral ganglion hypothesis. *Hear. Res.* **292**, 51–58 (2012).
25. Shearer, A. E., Eppsteiner, R. W., Frees, K. *et al.* Genetic variants in the peripheral auditory system significantly affect adult cochlear implant performance. *Hear. Res.* **348**, 138–142 (2017).
26. Seligman, K. L., Shearer, A. E., Frees, K. *et al.* Genetic Causes of Hearing Loss in a Large Cohort of Cochlear Implant Recipients. *Otolaryngol. - Head Neck Surg.* Online ahead of print (2021).
27. Brownstein, Z., Friedman, L., Shahin, H. *et al.* Targeted genomic capture and massively parallel sequencing to identify genes for hereditary hearing loss in middle eastern families. *Genome Biol.* **12**, R89 (2011).
28. Ito, T., Kawashima, Y., Fujikawa, T. *et al.* Rapid screening of copy number variations in *STRC* by droplet digital PCR in patients with mild-to-moderate hearing loss. *Hum. Genome Var.* **6**, 1-6 (2019).
29. Karczewski, K. J., Francioli, L., Tiao, G. *et al.* The mutational constraint spectrum quantified from variation in 141,456 humans. *Nature* **581**, 434–443 (2020).
30. Richards, S., Aziz, N., Bale, S. *et al.* Standards and guidelines for the interpretation of

sequence variants. *Genet Med* **17**, 405–424 (2015).

31. Spahr, A. J., Dorman, M. F., Litvak, L. M. *et al.* Development and Validation of the AzBio Sentence Lists. *Ear Hear.* **33**, 112–117 (2012).
32. Spahr, A. J., Dorman, M. F., Litvak, L. M. *et al.* Development and validation of the Pediatric AzBio sentence lists. *Ear Hear.* **34**, 418–422 (2014).
33. Nilsson, M., Soli, S. D. & Sullivan, J. A. Development of the Hearing In Noise Test for the measurement of speech reception thresholds in quiet and in noise. *J. Acoust. Soc. Am.* **95**, 1085–1099 (1994).
34. Haskins, H. A phonetically balanced test of speech discrimination for children. (Northwestern University, 1949).
35. Peterson, G. E. & Lehiste, I. Revised CNC lists for auditory tests. *J Speech Hear Discord* **27**, 62–70 (1962).
36. Shearer, A. E., Kolbe, D. L, Azaiez, H. *et al.* Copy number variants are a common cause of non-syndromic hearing loss. *Genome Med.* **6**, 1–10 (2014).
37. Snoeckx, R. L., Huygen, P. L. M., Feldmann, D. *et al. GJB2* mutations and degree of hearing loss: A multicenter study. *Am. J. Hum. Genet.* **77**, 945–957 (2005).
38. Kenna, M. A., Feldman, H. A., Neault, M. W. *et al.* Audiologic phenotype and progression in *GJB2* (connexin 26) hearing loss. *Arch. Otolaryngol. - Head Neck Surg.* **136**, 81–87 (2010).
39. Pryor, S. P., Madeo, A. C., Reynolds, J. C. *et al. SLC26A4*/PDS genotype-phenotype correlation in hearing loss with enlargement of the vestibular aqueduct (EVA): Evidence that Pendred syndrome and non-syndromic EVA are distinct clinical and genetic entities. *J. Med. Genet.* **42**, 159–165 (2005).
40. Chao, J. R., Chattaraj, P., Munjal, T. *et al. SLC26A4*-linked CEVA haplotype correlates with phenotype in patients with enlargement of the vestibular aqueduct. *BMC Med. Genet.* **20**, 1–6 (2019).

41. Elmaleh-Bergès, M., Baumann, C., Noël-Pétroff, N. *et al.* Spectrum of temporal bone abnormalities in patients with waardenburg syndrome and *SOX10* mutations. *Am. J. Neuroradiol.* **34**, 1257–1263 (2013).

42. Wineland, A., Menezes, M. D., Shimony, J. S. *et al.* Prevalence of semicircular canal hypoplasia in patients with CHARGE syndrome: 3C syndrome. *JAMA Otolaryngol. - Head Neck Surg.* **143**, 168–177 (2017).

43. Oonk, A. M. M., Leijendeckers, J. M., Lammers, E. M. *et al.* Progressive hereditary hearing impairment caused by a *MYO6* mutation resembles presbyacusis. *Hear. Res.* **299**, 88–98 (2013).

44. Sugiyama, K., Moteki, H., Kitajiri, S. *et al*. Mid-Frequency Hearing Loss Is Characteristic Clinical Feature of *OTOA*-Associated Hearing Loss. *Genes* **16**, 715 (2019).

45. Miyagawa, M., Nishio, S.-Y., Usami, S.-I. *et al.* Mutation spectrum and genotype-phenotype correlation of hearing loss patients caused by *SLC26A4* mutations in the Japanese: A large cohort study. *J. Hum. Genet.* **59**, 262–268 (2014).

46. Miyagawa, M., Nishio, S.-Y., Sakurai, Y. *et al.* The patients associated with *TMPRSS3* mutations are good candidates for electric acoustic stimulation. *Ann Otol Rhinol Laryngol* **124**, 193S-204S (2015).

47. Scott, H. S., Kudoh, J., Wattenhofer, M. *et al.* Insertion of β-satellite repeats identifies a transmembrane protease causing both congenital and childhood onset autosomal recessive deafness. *Nat. Genet.* **27**, 59–63 (2001).

48. Weegerink, N. J. D., Schraders, M., Oostrik, J. *et al.* Genotype-phenotype correlation in DFNB8/10 families with *TMPRSS3* mutations. *JARO - J. Assoc. Res. Otolaryngol.* **12**, 753–766 (2011).

49. Holder, J. T., Morrel, W., Rivas, A. *et al.* Cochlear Implantation and Electric Acoustic Stimulation in Children With *TMPRSS3* Genetic Mutation. *Otol. Neurotol.* **42**, 396–401 (2021).

50. Mehta, D., Noon, S. E., Schwartz, E. *et al.* Outcomes of evaluation and testing of 660 individuals with hearing loss in a pediatric genetics of hearing loss clinic. *Am. J. Med. Genet. Part A* **170**, 2523–2530 (2016).

51. Shearer, A. E., Shen, J., Amr, S., *et al*. A proposal for comprehensive newborn hearing screening to improve identification of deaf and hard-of-hearing children. *Genet. Med.* **21**, 2614–2630 (2019).

52. Ivarsdottir, E. V., Holm, H., Benonisdottir, S. *et al.* The genetic architecture of age-related hearing impairment revealed by genome-wide association analysis. *Commun. Biol.* **4**, 1-13 (2021).

53. Tropitzsch, A., Knoblich, N. & Muller, M. Cochlear implant performance in patients with *TMPRSS3* mutations. *Laryngorhinootologie* **97**, S272 (2018).

54. Shearer, A. E., Tejani, V. D., Brown, C. J. *et al.* In Vivo Electrocochleography in Hybrid Cochlear Implant Users Implicates *TMPRSS3* in Spiral Ganglion Function. *Sci. Rep.* **8**, 1–9 (2018).

55. Gong, Y., Krakow, D., Marcelino, J. *et al.* Heterozygous mutations in the gene encoding noggin affect human joint morphogenesis. *Nat. Genet.* **21**, 302–304 (1999).

56. Teunissen, B. & Cremer, W. R. An autosomal dominant inherited syndrome with congential stapes ankylosis. *Laryngoscope* **100**, 380–384 (1990).

57. Brown, D. J., Kim, T. B., Petty, E. M. *et al.* Autosomal Dominant Stapes Ankylosis with Broad Thumbs and Toes, Hyperopia, and Skeletal Anomalies Is Caused by Heterozygous Nonsense and Frameshift Mutations in NOG, the Gene Encoding Noggin. *Am. J. Hum. Genet.* **71**, 618–624 (2002).

58. Gregersen, H. N. & Petersen, G. Congenital malformation of the feet with low body height: A new syndrome, caused by an autosomal dominant gene. *Clin. Genet.* **12**, 255–262 (1977).

59. Drawbert, H. P., Stevens, D. B., Cadle, R. G. *et al*. Tarsal and carpal coalition and

symphlangism of the Fuhmann type: Report of a family. *J. Bone Jt. Surg.* **67**, 884–889 (1985).

60. Kjaer, K. W., Tiner, M., Cingoz, S. *et al.* A Novel Subtype of Distal Symphalangism Affecting Only the 4th Finger. *Am. J. Med. Genet. Part A* **149A**, 1571–1573 (2009).
61. Potti, T. A., Petty, E. M. & Lesperance, M. M. A Comprehensive Review of Reported Heritable Noggin-Associated Syndromes and Proposed Clinical Utility of One Broadly Inclusive Diagnostic Term: NOG-Related-Symphalangism Spectrum Disorder (*NOG*-SSD). *Hum. Mutat.* **32**, 877–886 (2011).
62. Laurell, T., Lundin, J., Britt-Marie, A. *et al.* Molecular and clinical delineation of the 17q22 microdeletion phenotype. *Eur. J. Med. Genet.* **21**, 1085–1092 (2013).
63. Khattab, M., Xu, F., Li, P. *et al*. A De Novo 3.54 Mb Deletion of 17q22-q23.1 Associated With Hydrocephalus: A Case Report and Review of Literature. *Am. J. Med. Genet. Part A* **155**, 3082–3086 (2011).
64. Martinez-Fernandez, L., Fernandez-Toral, J., Llano-Rivas, I. *et al.* Delineation of the clinically recognizable 17q22 contiguous gene deletion syndrome in a patient carrying the smallest microdeletion known to date. *Am. J. Med. Genet. Part A* **167**, 2034–2041 (2015).
65. Shimizu, R., Mitsui, N., Mori, Y. *et al.* Cryptic 17q22 deletion in a boy with a t(10;17)(p15.3;q22) translocation, multiple synostosis syndrome 1, and hypogonadotropic hypogonadism. *Am. J. Med. Genet. Part A* **146A**, 1458–1461 (2008).
66. Pang, X., Luo, H., Chai, Y. *et al*. A 1.6-Mb Microdeletion in Chromosome 17q22 Leads to NOG-Related Symphalangism Spectrum Disorder without Intellectual Disability. *PLoS One* **10**, 1–8 (2015).
67. Puusepp, H., Zilina, O., Teek, R. *et al.* 5.9 Mb microdeletion in chromosome band 17q22-q23.2 associated with tracheo-esophageal fistula and conductive hearing loss. *Eur. J. Med. Genet.* **52**, 71–74 (2009).
68. Nimmakayalu, M., Major, H., Sheffield, V. *et al.* Microdeletion of 17q22q23.2

encompassing TBX2 and TBX4 in a patient with congenital microcephaly, thyroid duct cyst, sensorineural hearing loss, and pulmonary hypertension. *Am. J. Med. Genet.* **155A**, 418–423 (2011).

69. Gulsuner, S., Walsh, T., Watts, A. C. *et al.* Spatial and temporal mapping of de novo mutations in schizophrenia to a fetal prefrontal cortical network. *Cell* **154**, 518-29 (2013).
70. Schindelin, J., Arganda-Carreras, I., Frise, E. *et al.* Fiji: An open-source platform for biological-image analysis. *Nat. Methods* **9**, 676–682 (2012).
71. Fox, J. & Bouchet-Valat, M. R Commander. (2018).
72. Nord, A. S., Lee, M., King, M. C. *et al*. Accurate and exact CNV identification from targeted high-throughput sequence data. *BMC Genomics* **12**, 1-10 (2011).
73. Shu, Y., Wang, L., Cheng, X. *et al.* The p.(Pro170Leu) variant in NOG impairs noggin secretion and causes autosomal dominant congenital conductive hearing loss due to stapes ankylosis. *J. Genet. Genomics* **46**, 445–449 (2019).
74. Quesnel, A. M., Nadol Jr, J. B., Nielsen, G. P. *et al*. Temporal Bone Histopathology in NOG-Symphalangism Spectrum Disorder. *Otol. Neurotol.* **36**, 1651–1656 (2015).
75. Smith, W. C. & Harland, R. M. Expression Cloning of noggin, a New Dorsalizing Factor Localized to the Spemann Organizer in Xenopus Embryos. *Cell* **70**, 829–840 (1992).
76. Zimmerman, L. B., Jesu, M. D. *& Harland, R. M*. The Spemann Organizer Signal noggin Binds and Inactivates Bone Morphogenetic Protein 4. *Cell* **86**, 599–606 (1996).
77. Hogan, B. L. M. Bone morphogenetic proteins in development. *Curr. Opin. Genet. Dev.* **6**, 432–438 (1996).
78. Groeneveld, E. H. J. & Burger, E. H. Bone morphogenetic proteins in human bone regeneration. *Eur. J. Endocrinol.* **142**, 9–21 (2000).
79. Zou, H. & Niswander, L. Requirement for BMP signaling in interdigital apoptosis and scale formation. *Science* **272**, 1–7 (1996).
80. Cheng, H., Jiang, W., Philips, F. M. *et al.* Osteogenic Activity of the Fourteen Types of

Human Bone Morphogenetic Proteins (BMPs). *J. Bone Jt. Surg.* **85-A**, 1544–1552 (2003).

81. Declau, F., Van Den Ende, J., Baten, E. *et al*. Stapes ankylosis in a family with a novel *NOG* mutation: Otologic features of the facioaudiosymphalangism syndrome. *Otol. Neurotol.* **26**, 934–940 (2005).
82. Brunet, L. J., Mcmahon, J. A., Mcmahon, A. P. *et al*. Noggin, cartilage morphogenesis, and joint formation in the mammalian skeleton. *Science.* **280**, 1455–1458 (1998).
83. Weekamp, H. H., Kremer, H., Hoefsloot, L. H., *et al*. Teunissen-Cremers Syndrome: A Clinical, Surgical, and Genetic Report. *Otol. Neurotol.* **26**, 38–51 (2005).
84. Hwang, C. & Wu, D. K. Noggin heterozygous mice: an animal model for congenital conductive hearing loss in humans. *Hum. Mol. Genet.* **17**, 844–853 (2008).
85. Mcmahon, J. A., Takada, S., Zimmerman, L. B. *et al.* Noggin-mediated antagonism of BMP signaling is required for growth and patterning of the neural tube and somite. *Genes Dev.* **12**, 1438–1452 (1997).
86. Marcelino, J., Sciortino, C. M., Romero, M. F. *et al.* Human disease-causing *NOG* missense mutations: Effects on noggin secretion, dimer formation, and bone morphogenetic protein binding. *Proc. Natl. Acad. Sci.* **98**, 11353–11358 (2001).
87. Lehmann, K., Seemann, P., Silan, F. *et al.* A New Subtype of Brachydactyly Type B Caused by Point Mutations in the Bone Morphogenetic Protein Antagonist NOGGIN. *Am. J. Hum. Genet.* **81**, 388–396 (2007).
88. Milunsky, J., Suntra, C. & Macdonald, C. B. Congenital Stapes Ankylosis, Broad Thumbs, and Hyperopia: Report of a Family and Refinement of a Syndrome. *Am. J. Med. Genet. Part A* **82**, 404–408 (1999).
89. Thomeer, H. G. X. M., Admiraal, R. J. C., Hoefsloot, L. *et al*. R. J. Proximal symphalangism, hyperopia, conductive hearing impairment, and the *NOG* gene: 2 new mutations. *Otol. Neurotol.* **32**, 632–638 (2011).
90. Babcock, T. A. Otosclerosis From Genetics to Molecular Biology. **51**, 305–318 (2019).

91. Mckenna, M. J., Nguyen-huynh, A. T. & Kristiansen, A. G. Association of Otosclerosis With Sp1 Binding Site Polymorphism in *COL1A1* Gene: Evidence for a Shared Genetic Etiology With Osteoporosis. *Otol. Neurotol.* **25**, 447–450 (2004).

92. Tomek, M. S., Brown, M. R., Mani, S. R. *et al.* Localization of a gene for otosclerosis to chromosome 15q25–q26. *Hum. Mol. Genet.* **7**, 285–290 (1998).

93. Van Den Bogaert, K., Govaerts, P. J., Chatteman, I. *et al.* A Second Gene for Otosclerosis, OTSC2, Maps to Chromosome 7q34-36. *Am. J. Hum. Genet.* **68**, 495–500 (2001).

94. Chen, W., Campbell, C. A., Green, C. E. *et al.* Linkage of otosclerosis to a third locus (OTSC3) on human chromosome 6p21.3-22.3. *J. Med. Genet.* **39**, 473–477 (2002).

95. Bel Hadj Ali, I., Thys, M., Beltaief, N. *et al.* Clinical and Genetic Analysis of Two Tunisian Otosclerosis Families. **1660**, 1653–1660 (2007).

96. Brownstein, Z., Goldfarb, A., Levi, H. *et al*. Chromosomal Mapping and Phenotypic Characterization of Hereditary Otosclerosis Linked to the OTSC4 Locus. *Arch Otolaryngol. Head Neck Surg* **132**, 416–424 (2019).

97. Van Den Bogaert, K., De Leenheer, E. M. R., Chen, W. *et al.* A fifth locus for otosclerosis, OTSC5, maps to chromosome 3q22-24. *J. Med. Genet.* **41**, 450–453 (2004).

98. Iliadou, V., Van Den Bogaert, K., Eleftheriades, N. *et al.* Monogenic nonsyndromic otosclerosis: Audiological and linkage analysis in a large Greek pedigree. *Int. J. Pediatr. Otorhinolaryngol.* **70**, 631–637 (2006).

99. Pauw, R. J., Huygen, P. L. M., Thys, M. *et al.* Phenotype Description of a Dutch Otosclerosis Family With Suggestive Linkage to OTSC7. **1622**, 1613–1622 (2007).

100. Bel Hadj Ali, I., Thys, M., Beltaief, N. *et al.* A new locus for otosclerosis, OTSC8, maps to the pericentromeric region of chromosome 9. *Hum. Genet.* **123**, 267–272 (2008).

101. Shrauwen, I., Weegerink, N., Fransen, E. *et al*. A new locus for otosclerosis, OTSC10, maps to chromosome 1q41–44. *Clin. Genet.* **79**, 495–497 (2011).

102. Ishiyama, A. & Glasscock, M. E. Total stapedectomy. *Oper. Tech. Otolaryngol. - Head Neck Surg.* **9**, 3–7 (1998).

103. De La Cruz, A. & Chandrasekhar, S. S. Mechanical small fenestra stapedotomy. *Oper. Tech. Otolaryngol. - Head Neck Surg.* **9**, 33–37 (1998).

104. Young, E., Mitchell-Innes, A. & Jindal, M. Lasers in stapes surgery: A review. *J. Laryngol. Otol.* **129**, 627–633 (2015).

105. Spandow, O., Soderberg, O. & Bohlin, L. Long-term results in otosclerotic patients operated by stapedectomy or stapedotomy. *Scand. Audiol.* **29**, 186–190 (2000).

106. Scierski, W., Namyslowski, G., Czerwinska, G. *et al.* Postoperative vertigo caused by too long stapes prosthesis-radiological diagnostics. *Otolaryngol. Pol.* **66**, 363—367 (2012).

107. Portmann, D., Alcantara, M. & Vianna, M. The length of the piston in otosclerosis surgery. *Rev. Laryngol. Otol. Rhinol. (Bord).* **128**, 55—58 (2007).

108. Husain, Q., Lin, K. F. & Selesnick, S. H. Stapes prosthesis length and hearing outcomes. *Laryngoscope* **128**, 722–726 (2018).

109. Massey, B. L., Hillman, T. A. & Shelton, C. Stapedectomy in congenital stapes fixation: Are hearing outcomes poorer? *Otolaryngol. Neck Surg.* **134**, 816–818 (2006).

110. Ensink, R. J. H., Sleeckx, J.-P. & Cremers, C. W. R. J. Proximal Symphalagism and Congenital Conductive Hearing Loss: Otologic Aspects. *Am. J. Otol.* **20**, 344–349 (1999).

111. Dror, A. A. & Avraham, K. B. Hearing Loss : Mechanisms Revealed by Genetics and Cell Biology. *Annu. Rev. Genet.* **43**, 411-37 (2009).

112. Fujita, H., Aokji, H., Aijoka, I. *et al.* Detailed Expression Pattern of Aldolase C (*Aldoc*) in the Cerebellum , Retina and Other Areas of the CNS Studied in Aldoc-Venus Knock-In Mice. *PLoS One* **9**, 22–27 (2014).

113. Kishi, H. *et al.* Human aldolase A deficiency associated with a hemolytic anemia: thermolabile aldolase due to a single base mutation. *Proc. Natl. Acad. Sci.* **84**, 8623–8627 (1987).

114. Ali, M., Rellos, P., & Cox, T. M. Hereditary fructose intolerance. *J. Med. Genet.* **35**, 353–365 (1998).

115. Santer, R., Rischewski, J., Weihe, *et al*. The Spectrum of Aldolase B (*ALDOB*) Mutations and the Prevalence of Hereditary Fructose Intolerance in Central Europe. *Hum. Mutat.* **814**, 594–603 (2005).

116. Arakaki, T. L., Pezza, J. A., Cronin, M. A. *et al.* Structure of human brain fructose 1,6-(bis)phosphate aldolase: Linking isozyme structure with function. *Protein Sci*. **13**, 3077–3084 (2004).

117. Miller, S. A., Dykes, D. D. & Polesky, H. F. A simple salting out procedure for extracting DNA from human nucleated cells. *Nucleic Acids Res.* **16**, 1215 (1988).

118. Danial-Farran, N., Brownstein, Z., Gulsuner, S. *et al.* Genetics of hearing loss in the Arab population of Northern Israel. *Eur. J. Hum. Genet.* **26**, 1840–1847 (2018).

119. Kusakabe, T., Motoki, K., & Hori, K. Human aldolase C: Characterization of the recombinant enzyme exprressed in Escherichia coli. *J. Biochem.* **115**, 1172–1177 (1994).

120. Rellos, P., Sygusch, J. & Cox, T. M. Expression, Purification, and Characterization of Natural Mutants of Human Aldolase B. *J. Biol. Chem.* **275**, 1145–1151 (2000).

121. Racker, E. Spectrophotometric measurement of hexokinase and phosphohexokinase activity. *J. Biol. Chem.* **167**, 843–854 (1947).

122. Horn, H. F., Brownstein, Z., Lena, D. R. *et al.* The LINC complex is essential for hearing. *J. Clin. Invest.* **123**, 740–750 (2013).

123. Saben, J. L., Ashgar, Z., Rhee, J. S. *et al.* Excess maternal fructose consumption increases fetal loss and impairs endometrial decidualization in mice. *Endocrinology* **157**, 956–968 (2016).

124. Ramathal, C. Y., Bagchi, I. C., Taylor, R. N. *et al*. Endometrial decidualization: Of mice and men. *Semin. Reprod. Med.* **28**, 17–26 (2010).

125. Gabriel, H. D., Jung, D., Bützler, C. *et al.* Transplacental uptake of glucose is decreased in

embryonic lethal connexin26-deficient mice. *J. Cell Biol.* **140**, 1453–1461 (1998).

126. Cohen-Salmon, M., Ott, T., Michel, V. *et al.* Targeted ablation of connexin26 in the inner ear epithelial gap junction network causes hearing impairment and cell death. *Curr. Biol.* **12**, 1106–1111 (2002).
127. Oppelt, S. A., Zhang, W. & Tolan, D. R. Specific regions of the brain are capable of fructose metabolism. *Brain Res.* **1657**, 312–322 (2017).
128. Penhoet, E. E. & Rutter, W. J. Catalytic and immunochemical properties of homomeric and heteromeric combinations of aldolase subunits. *J. Biol. Chem.* **246**, 318–323 (1971).
129. Kim, J., Song, G., Wu, G. *et al*. Functional roles of fructose. *Proc. Natl. Acad. Sci. U. S. A.* **109**, 1619–1628 (2012).
130. Kozak, M. How do eucaryotic ribosomes select initiation regions in messenger RNA? *Cell* **15**, 1109–1123 (1978).
131. Kozak, M. At least six nucleotides preceding the AUG initiator codon enhance translation in mammalian cells. *J. Mol. Biol.* **196**, 947–950 (1987).
132. Kozak, M. An analysis of 5'-noncoding sequences from 699 vertebrate messenger RNAs. *Nucleic Acids Res.* **15**, 8125–8148 (1987).
133. Fritsch, C., Herrmann, A., Nothnagel, M. *et al.* Genome-wide search for novel human uORFs and N-terminal protein extensions using ribosomal footprinting. *Genome Res.* **22**, 2208–2218 (2012).
134. Starck, S. R., Tsai, J. C., Chen, K. *et al.* Translation from the 5' untranslated region shapes the integrated stress response. *Science* **351**, 465 (2016).
135. Zhang, X., Gai, X., Coots, R. A. *et al.* Translational control of the cytosolic stress response by mitochondrial ribosomal protein L18. *Nat. Struct. Mol. Biol.* **22**, 404–410 (2015).
136. Hann, S. R., Sloan-Brown, K. & Spotts, G. D. Translational activation of the non-AUG-initiated *c-myc* 1 protein at high cell densities due to methionine deprivation. *Genes Dev.* **6**, 1229–1240 (1992).

137. Hann, S. R., King, M. W., Bentley, D. L. *et al.* A non-AUG translational initiation in *c-myc* exon 1 generates an N-terminally distinct protein whose synthesis is disrupted in Burkitt's lymphomas. *Cell* **52**, 185–195 (1988).

138. Sargiannidou, I., Kim, G.-H., Kyriakoudi, S. *et al*. A start codon *CMT1X* mutation associated with transient encephalomyelitis causes complete loss of Cx32. *Neurogenetics* **16**, 193–200 (2015).

139. Moi, P., Cash, F. E., Liebhaber, S. *et al*. An initiation codon mutation (AUG → GUG) of the human α1-globin gene: Structural characterization and evidence for a mild thalassemic phenotype. *J. Clin. Invest.* **80**, 1416–1421 (1987).

140. De Arce, A. J. D., Noderer, W. L. & Wang, C. L. Complete motif analysis of sequence requirements for translation initiation at non-AUG start codons. *Nucleic Acids Res.* **46**, 985–994 (2018).

141. Hay, J. C., Chao, D. S., Kuo, C. S. *et al*. Protein interactions regulating vesicle transport between the endoplasmic reticulum and Golgi apparatus in mammalian cells. *Cell* **89**, 149–158 (1997).

142. Gordon, D. E., Bond, L. M., Sahlender, D. A. *et al*. A targeted siRNA screen to identify SNAREs required for constitutive secretion in mammalian cells. *Traffic* **11**, 1191–1204 (2010).

143. Corbett, M. A., Schwake, M., Bahlo, M. *et al.* A mutation in the Golgi Qb-SNARE gene *GOSR2* causes progressive myoclonus epilepsy with early ataxia. *Am. J. Hum. Genet.* **88**, 657–663 (2011).

144. Praschberger, R., Balint, B., Mencacci, N. E. *et al.* Expanding the Phenotype and Genetic Defects Associated with the *GOSR2* Gene. *Mov. Disord. Clin. Pract.* **2**, 271–273 (2015).

145. Larson, A. A., Baker, P. R., Milev, M. P. *et al. TRAPPC11* and *GOSR2* mutations associate with hypoglycosylation of α-dystroglycan and muscular dystrophy. *Skelet. Muscle* **8**, 1–10 (2018).

146. Wang, H., Yang, H., Shivalila, C. S. *et al.* One-step generation of mice carrying mutations in multiple genes by CRISPR/cas-mediated genome engineering. *Cell* **153**, 910–918 (2013).

147. Kolla, L., Kelly, M. C., Mann, Z. F. *et al.* Characterization of the development of the mouse cochlear epithelium at the single cell level. *Nat. Commun.* **11**, 1-16 (2020).

148. Malsam, J. & Söllner, T. H. Organization of SNAREs within the Golgi stack. *Cold Spring Harb. Perspect. Biol.* **3**, 1–17 (2011).

149. Praschberger, R., Lowe, S. A., Malintan, N. T. *et al.* Mutations in Membrin/*GOSR2* Reveal Stringent Secretory Pathway Demands of Dendritic Growth and Synaptic Integrity. *Cell Rep.* **21**, 97–109 (2017).

150. Völker, J. M., Dergai, M., Abriata, L. A. *et al.* Functional assays for the assessment of the pathogenicity of variants of *GOSR2*, an ER-to-Golgi SNARE involved in progressive myoclonus epilepsies. *DMM Dis. Model. Mech.* **10**, 1391–1398 (2017).

151. Almog, Y., Fadila, S., Brusel, M. *et al.* Developmental alterations in firing properties of hippocampal CA1 inhibitory and excitatory neurons in a mouse model of Dravet syndrome. *Neurobiol. Dis.* **148**, 105209 (2021).

152. Mathur, P. & Yang, J. Usher syndrome: Hearing loss, retinal degeneration and associated abnormalities. *Biochim. Biophys. Acta - Mol. Basis Dis.* **1852**, 406–420 (2015).

153. Pingault, V., Ente, S., Dastot-Le Moal, F. *et al.* Review and update of mutations causing Waardenburg syndrome. *Hum. Mutat.* **31**, 391–406 (2010).

154. Taiber, S., Cohen, R., Yizhar-Barnea, O. *et al.* Neonatal AAV gene therapy rescues hearing in a mouse model of SYNE4 deafness. *EMBO Mol. Med.* **13**, 1–15 (2021).

155. Shubina-Oleinik, O., Nist-Lund, C., French, C. *et al.* Dual-vector gene therapy restores cochlear amplification and auditory sensitivity in a mouse model of DFNB16 hearing loss. *Sci. Adv.* **7**, 1–10 (2021).

156. Ahmed, H., Shubina-Oleinik, O. & Holt, J. R. Emerging Gene Therapies for Genetic

Hearing Loss. *JARO - J. Assoc. Res. Otolaryngol.* **18**, 649–670 (2017).

157. Kelsell, D. P., Dunlop, J., Stevens, H.P. *et al.* Connexin 26 mutations in hereditary non-syndromic sensorineural deafness. *Nature* **387**, 80–83 (1997).

158. Well, D., Blanchard, S., Kaplan, J. *et al.* Defective myosin VIIA gene responsible for Usher syndrome type IB. *Nature* **374**, 60–61 (1995).

159. Wang, A., Liang, Y., Fridell, R. A. *et al.* Association of unconventional myosin *MYO15* mutations with human nonsyndromic deafness DFNB3. *Science* **280**, 1447–1451 (1998).

CURRICULUM VITAE

Ryan Carlson
Department of Genome Sciences
University of Washington School of Medicine
Seattle, WA 98195
Work: (206) 616-9662

2424 E Madison St
Seattle, WA 98112
rjc630@uw.edu

EDUCATION

University of Washington — Seattle, WA
Medical Scientist Training Program (MD/PhD) trainee — 2016-Present
Graduate student in the lab of Dr. Mary-Claire King

University of Washington — Seattle, WA
B.S. in Neurobiology, B.S. in Biochemistry — 2011-2015
Graduated with honors, *cum laude*

GRANTS AND AWARDS

NIH/NIDCD 1F30 DC018702 – Kirschstein Pre-doctoral Fellowship — 2021-Present
National Institute of Deafness and Communication Disorders (NIDCD)

Auditory Neuroscience Training Grant (T32) — 2019, 2020
University of Washington Department of Neurobiology and Behavior

Achievement Rewards for College Scientists (ARCS) Fellowship — 2018, 2019
Seattle Chapter ARCS Foundation

Otolaryngology Training Grant (T32) — 2018
University of Washington Department of Otolaryngology

Turner Society Endowed Fellowship — 2016
University of Washington School of Medicine

Phi Beta Kappa Inductee — 2014
University of Washington chapter

Mary Gates Undergraduate Research Scholarship — 2014
University of Washington undergraduate research program

RESEARCH EXPERIENCE

University of Washington — Seattle, WA
Graduate student; Advisor: Dr. Mary-Claire King — 2018-Present
Department of Genome Sciences
Discovery and characterization of genes responsible for hereditary hearing loss

National Institute of Allergy and Infectious Disease — Bethesda, MD
Post-baccalaureate fellow; Advisor: Dr. Jon Lyons — 2015-2016
Investigation of the genetic basis of glycosylation disorders as they pertain to immunodeficiency syndromes.

- Developed a lectin-based flow cytometry assay to detect PGM3 deficiency, a rare hyper IgE syndrome.
- Used flow cytometry techniques to analyze variations in cell signaling in lymphoblasts from patients with glycosylation disorders.

University of Washington Seattle, WA
Undergraduate student; Advisor: Dr. Chet Moritz 2012-2015

- Developed a brain-machine-spinal-interface (BMSI) for limb reanimation following spinal cord injury
- Analyzed muscle fiber type changes and variation in rat triceps following unilateral spinal cord contusion.
- Quantified the effect of chondroitinase-based therapies in the facilitation of recovery following spinal cord injury.

TEACHING EXPERIENCE

University of Washington Seattle, WA
Department of Genome Sciences 2020
Teaching Assistant- *Advanced Human Genetics*

University of Washington Seattle, WA
University of Washington School of Medicine 2018-2020
Medical student tutor

PEER-REVIEWED ARTICLES

Carlson RJ, Quesnel A, Wells D, Brownstein Z, Gilony D, Gulsuner S, Avraham KB, King MC, Walsh T, Rubinstein J. Genetic heterogeneity and core clinical features of *NOG*-related-symphalangism spectrum disorder. *Otol Neurotol* **42(8)**, e1143-51 (2021).

Abu Rayyan A, Kamal L, Casadei S, Browstein Z, Zahdeh F, Shahin H, Canavati C, Dweik D, Jaraysa T, Rabie G, **Carlson RJ**, Gulsuner S, Lee MK, Avraham KB, Walsh T, King MC, Kanaan MK. Genomic analysis of inherited hearing loss in the Palestinian population. *Proc Natl Acad Sci* **117(33)**, 20070-76 (2020)

Brownstein Z, Gulsuner S, Walsh T… **Carlson RJ**… King MC, Avraham KB. Spectrum of genes for inherited hearing loss in the Israeli Jewish population, including the novel human deafness gene *ATOH1*. *Clin Genet* **98**, 353-64 (2020)

Carlson RJ, Bond MR, Hutchins S, Brown Y, Wolfe LA, Lam C, Nelson C, DiMaggio T, Jones N, Rosenzweig SD, Stone KD. Detection of phosphoglucomutase-3 deficiency by lectin-based flow cytometry. *Journal of Allergy and Clinical Immunology*. **140(1)**, 291-4 (2017).

Lyons JJ, Yu X, Hughes JD, Le QT, Jamil A, Bai Y, Ho N, Zhao M, Liu Y, O'Connell MP, Trivedi NN… **Carlson RJ**. Elevated basal serum tryptase identifies a multisystem disorder associated with increased TPSAB1 copy number. *Nature genetics*. **48(12)**, 1564 (2016).

REVIEW ARTICLES

Carlson RJ, Nghiem P. Ch. 4- Merkel Cell Carcinoma. *Tumors and Cancers: Skin-Soft Tissue-Bone-Urogenitals*, CRC Press, Taylor & Francis Group (2018).

ABSTRACTS AND PRESENTATIONS

Carlson RJ. Genetic causes of hearing loss: *Inheritance, testing technologies, and clinical impact.* WA EHDDI Learning Community Seminar, oral presentation, October 22, 2021.

Carlson RJ, Walsh T, Mandell J, Ou H, Sie K, Mancl L, Horn D, King MC, Rubinstein J. Genomic Analysis of Hearing Loss and Cochlear Implant Outcomes. Medical Scientist Training Program annual retreat, poster presentation, Jul 24, 2021. *[Best poster award]*

Carlson RJ. Genomic Analysis of Hearing Loss and Cochlear Implant Outcomes. Auditory Neuroscience Training Grant Annual Retreat, oral presentation, May 26, 2021.

Carlson RJ. Projects in gene discovery for hereditary hearing loss. Department of Genome Sciences Research Reports, oral presentation, May 18, 2021.

Carlson RJ. Genomic Analysis of Hearing Loss and Cochlear Implant Outcomes. Auditory Neuroscience Training Grant Annual Retreat, oral presentation, May 28, 2020.

Carlson RJ, Walsh T, Horn D, King MC, Rubinstein J. Genomic Analysis of Hearing Loss and Cochlear Implant Outcomes. Association for Research in Otolaryngology, Mid-Winter Meeting, poster presentation, January 25, 2020.

Carlson RJ. Gene Discovery for Inherited Hearing Loss: Koch's Postulates in the 21st Century. Department of Genome Sciences Research Reports, oral presentation, September 27, 2019.

Carlson RJ, Abu-Rayyan A, Walsh T, Avraham K, King MC, Kanaan M. A new candidate gene for hereditary hearing loss: *ALDOC*. Department of Genome Sciences annual retreat, poster presentation, September 18, 2019. *[Best poster award]*

Carlson RJ, Abu-Rayyan A, Walsh T, Avraham K, King MC, Kanaan M. A new candidate gene for hereditary hearing loss: *ALDOC*. Medical Scientist Training Program annual retreat, poster presentation, August 2, 2019.

Carlson RJ. Gene Discovery for Inherited Hearing Loss: Koch's Postulates in the 21st Century. Otolaryngology Graduation Symposium, oral presentation, June 21, 2019

Carlson RJ. Gene discovery and characterization for inherited hearing loss in Middle Eastern families. Karen Avraham Lab Meeting, Tel Aviv University, oral presentation, April 8, 2019.

Carlson RJ. Genomic analysis of inherited hearing loss. Otolaryngology/HNS T32 Progress Report, oral presentation, February 20, 2019

Carlson RJ. Genomic analysis of inherited hearing loss. Department of Genome Sciences Research Reports, oral presentation, October 12, 2019.